THE DEVELOPMENT OF A CORRELATION LOG

BY

ADRIAN MILES HORWITZ

SUBMITTED IN PARTIAL FULFILMENT OF THE
REQUIREMENTS FOR THE DEGREE OF
MASTER OF SCIENCE IN ENGINEERING

UNIVERSITY OF CAPE TOWN

APRIL 1985

ACKNOWLEDGEMENTS

I would like to take this opportunity to thank my supervisor, Professor P.N. Denbigh for the unfailing encouragement and inspiration he has extended to me over the last two years.

Thanks are also extended to the Institute for Maritime Technology, Simonstown, for the use of the research vessel the 'Shirley T' and the test facilities at the Simonstown Reservoir.

Finally I would like to thank all the members of the Central Acoustics Laboratory, for their assistance in this project.

ABSTRACT

A measure of ship speed is needed for dead reckoning navigation, docking, and as an input to satellite navigation systems. Ship speed is also used as an input to fire control systems on Naval vessels. The need for an accurate speed measuring device, that measures ship speed relative to the sea bed is thus apparent.

All non acoustic logs measure ship speed relative to the water, and absolute ship speed can only be estimated if a knowledge of water currents is available. An acoustic log that provides an absolute measure of ship speed at limited operating depths is the Doppler log. For deep water the Doppler log measures speed relative to the water and it is thus affected by currents.

A new development in acoustic logs is the correlation log. The correlation log can measure absolute speed at much greater depths than can the Doppler log. This is because it utilises a wide beam pointing vertically at the sea bed. The wide beam permits a low operating frequency to be used which implies low attenuation. The high back-scattering strength at normal angles of incidence combined with the low attenuation, means that relative to the Doppler log, the correlation log can measure absolute speed at much greater depths.

The correlation log consists of a transmitter, which utilises tone burst transmission, and two or more receivers in line with the direction of motion. The signals received by two transducers will be similar except for a time shift 'T', which is given by the equation $T = d/2V$, where V is the speed and d the transducer separation. A device based on these principles has been built and tested. Results have shown that the system concepts are viable and will lead to an absolute speed measuring device that can operate at great depth.

TABLE OF CONTENTS

LIST OF DIAGRAMS

CHAPTER 1

1.1 INTRODUCTION

During 1984 alone, over 80 000 merchant ships grossing more than 500 million tons steamed along the world's trade routes. This trading ship density has increased by 100% in the last 20 years. With the increase in congestion of the world's waterways, the demand for extremely accurate navigational aids has increased.[1]

The position of a ship is usually determined by the use of visual bearings, or by using cellestial or electronic navigation techniques. Between position fixes, however, ships are navigated by the dead reckoning process: a method which establishes a ship's position from knowledge of the course sailed, the distance traversed and the known or estimated drift. The distance travelled is measured by integrating ship speed. This process is complicated by the presence of unknown and variable currents. A means of measuring ship speed relative to the sea bed is thus most desirable.

A further requirement for accurate speed measurement at low speeds exists when large ships, for example tankers, with stopping distances of several kilometers are piloted to dock. Small errors in speed estimation on these ships can have serious consequences.

It is therefore evident that a requirement exists for an instrument which can accurately measure ship speed relative to the sea bed. Such an instrument, the Doppler log, exists. However, it has a limited operating depth and is inaccurate at low speeds. The correlation log developed in this study can operate at much greater depths and has a good accuracy at slow speeds.

1.2 DEVELOPMENT OF LOGS

The earliest recorded attempt to measure ship speed has been attributed to the Romans. Vitruvius, a Roman historian described Roman sailors using a paddlewheel-type rotor with a revolution-counting device to measure distances travelled at sea. This primitive "hodometer" was developed from a similar apparatus used on chariot wheels to measure the distance travelled on land journeys. The hodometer eventually gave way to the first legitimate speed "log".[1]

During the industrial revolution, the classical "chip" log was used to measure ship speed. This system consisted of a wooden chip attached to a line. The line had knots tied at regular intervals (fraction of a nautical mile) and was wound on a reel.
The log was operated by lowering the chip over the ship's stern and into the water where, by virtue of its shape, it remained relatively stationary. Speed could then be calculated by counting the number of knots to pass overboard during the time it took sand to run through a 28 second hourglass. The "chip" log was unreliable

because overused chips would often sink or the line would become entangled and snap.[2]

A successor to the "chip" log was the "taffrail" log, so called because of the position of the display on the stern rail of the ship. This log is still used today and is marketed by such companies as Thomas Walker and Seafarer International Ltd.[2] In this log the chip is replaced by a propeller that is towed astern by a braided cable. The revolutions of the propeller are transferred by the cable to a clockwork recording device, the display of which reads nautical miles. The "taffrail" log is found to be inaccurate at speeds in excess of 15 knots and, like the "chip" log, the propeller and cable are likely to be snared and fouled by floating objects.

The Pitot-tube evolved to replace the classical chip log. The Pitot log which consists of a tube having a short, right-angled bend, is placed vertically in the water with the mouth of the bent tube directed towards the water flow. Used in conjunction with a manometer (pressure guage), the Pitot log measures the fluid flow velocity, or ship speed through the water, by comparing the differences between recorded water pressures.

The Pitot log relies on the assumption that the pressure measured is only due to ship velocity. This is not so as the ship disturbs the water in two ways. Firstly, the velocity and the pressure in its vicinity vary because of streamline action of the hull. Secondly, the friction of the surface produces a turbulent layer

adjacent to the ship where the motion is confused. The nett result is a wake whose forward velocity, very close to the hull, is as great as 50% of the ship speed. Due to the inherent inaccuracy of the Pitot log, the electromagnetic log was developed.

The electromagnetic or EM log operates on the electromagnetic principle whereby a linear voltage proportional to speed is generated within an underwater sensor assembly and electronically converted to speed. Typical EM logs consist of a sensor and a signal processing unit (Indicator/Transmitter). The sensor is a rod meter, or sword, that protrudes from the ship's hull. Within the sword is a coil of wire which sets up a magnetic field in the nearby water. The ship's motion through this magnetic field induces currents in the conductive sea water. As the water moves past the sensor, the magnetic field induces a voltage in the water which is picked up by two electrodes on the sensor. The voltage is linearly proportional to the ship's speed through the water. The EM log has been produced commercially by such companies as Chernekeff, Aquatronic Systems and Seafarer International Ltd.

Like the Pitot log the EM log's speed measurement is not accurate because of water motion near the sensor that is not related to ship speed. Compensation for these hydrodynamic effects requires complex calibration procedures since the flow characteristics at the sensor vary with the sensor location, hullshape, speed, depth and manoeuvres. The sensor sword of the EM log can be broken or fouled by marine life because it protrudes into the water. These

inadequacies of the EM log led to the development of the Doppler log.

Doppler logs consist of keel mounted transducers which send down pulsed sonic beams, inclined at an angle to the vertical. The return signals are converted into displays of ship speed in the forward and transverse directions. The Doppler log operates on the principle of projecting a narrow acoustical beam of known frequency into the water and measuring the frequency of the scattered return signal.

The frequency shift, caused by the Doppler effect, is directly proportional to ship speed. A typical Doppler log system consists of a single transducer to transmit the acoustic signal and receive the scattered reflection. This transducer is mounted flush with the hull, and is not subject to sensor damage associated with other speed log systems.

The Doppler log has been produced commercially by such companies as Sperry, Rosemont Inc. and Sal Jungner Marine. Doppler logs are especially effective in determining ship's speed relative to the bottom in shallow water (less than 250 metres). This limited depth range is because of the Doppler log's use of a narrow beam to reduce the effect of frequency spreading of the return signal. A narrow beam is produced by high operating frequencies for a given transducer size. The higher the operating frequency the greater the attenuation of the acoustic signal and the less the range.

At greater depths, a signal can be reflected off such targets as particles, bubbles, plankton, schools of fish or other marine life. These targets could be moving due to deep water currents and so the Doppler log is inherently inaccurate in deep water.[3]

From the different types of logs described, it is evident that there exists a need for a log that can operate at great depth and measure ship speed accurately relative to the sea bed. The correlation log has this capability. This is because of its use of broadbeam transducers that point vertically at the sea bed. They can operate at much lower frequencies and hence have a much greater operating depth.

1.3 CORRELATION LOG

The correlation log performs a cross correlation funtion on signals measured at spatially separated receivers. These signals comprise the resultant backscattered return that arises when a normal incident, low frequency broadbeam acoustic wave is transmitted at the sea bed.

The amplitude of the return signal will fluctuate as the ship moves. This is because the return signal is made up of a complex interference pattern. The interference pattern will change with ship position, but it is possible that as the ship moves forward, first one then the second receiver of a receiver pair will move over the same interference pattern. This is provided that the transmitter position changes with ship movement so that the two receivers move over the same insonified backscattering area.

If the receivers move over the same interference pattern they will measure the same return signals, except the forward receiver will receive the signal earlier in time than the aftward receiver. It is possible then that with a single projector and two displaced receivers on a moving ship, the signals received by the two receivers will be identical except for a time shift T. If the time shift T and the receiver separation is known, the velocity can be determined. This is discussed in detail in Chapter 2.

Not much literature exists on correlation logs. Correlation logs were first developed for measuring aircraft velocity. These systems use downward pointing radars and receive the ground clutter on two closely spaced receivers. The received signals are crosscorrelated and the delay T between the identical received signals is related to ground speed via the receiver separation. Such systems have been described by Dickey[4], Snyder[5], Koschmeder[6] and Miller[7].

Sonar correlation logs have been described by Dickey and Edward in 1978[8] and Volovov **et al** in 1977[9]. Dickey and Edward's work was performed at the General Electric Company. Spatial correlation techniques similar to those described in this thesis were used. They reported that speed was successfully measured during sea trials. This work resulted in a production model trademarked Quo Vadis[10] produced by the General Electric Company. It is not yet, however, commercially available.

Volovov's work, which involved using two receivers and cross-

correlating the receive signals to determine the time delay, does not address the problem of shallow water operation. He uses very deep water tests (that approximate continuous-wave transmission) which produced impressive results.

Denbigh[11] in 1982, published a design feasibility study in which many aspects of the correlation log were discussed. His M.Sc. student Tucker[12] published a thesis in 1983 in which results pertaining to the temporal and spatial correlation log were presented. In 1984 Denbigh[13] published a further paper superceding his system design study of 1982. In this paper he showed that the temporal correlation log would be unable to function for all possible velocity and depth situations. He also showed that interpolation to find the peak position of the spatial correlation function resulted in unacceptable inaccuracies of measured velocity. Denbigh proposed a new correlation log based on a combination of the temporal and spatial correlation logs. This thesis gives the details of this log, called the inter-intrapulse correlation log and presents the results obtained and the conclusions drawn.

REFERENCES

1. Keyes D., "Submarine Speed Measurement with Doppler Sonar", Sea Technology, pp 26-30, (February 1984).

2. Saunders H.E., "Hydrodynamics in Ship Design", Volume One, The Society of Naval Architects and Marine Engineers, New York (1957) pp 561-563.

3. Taylor E.G.R., and Richey M.W., "The Geometrical Seaman", Hollis and Carter, Great Britain (1962), pp 34-36.

4. Dickey F.R. Jr., "The Correlation Aircraft Navigator, a vertically beamed Doppler radar", Proceedings of National Conference on Aeronautical Electronics, (May 1958).

5. Snyder F.B., "Correlation Velocity Sensor", Bicentennial National Aerospace Symposium on New Frontiers in Aerospace Navigation, Warminster, Pennysylvania, (27-28 April 1976), pp 97-101.

6. Koschmeder R.F., "Coran (A Correlation Velocity Sensor)", Proc. I.E.E.E., National Aerospace and Electronics Conference, Dayton, Ohio, (18-20 May 1976), pp 2-5.

7. Miller R.J., "Air and Space Navigation System uses Cross-correlation Techniques", Electronics, pp 55-59, (December 1961).

8. Dickey F.R. Jr, and Edward J.A., "Velocity measurement using correlation sonar", I.E.E.E. Position Location and Navigation Symposium, San Diego, (6-9 November 1978), pp 255-264.

9. Volovov V.I., Krasnoborod'ko V.V., Lysanov Yu.p., and Sechkin V.A., "A New Acoustical Method for Determining the Speed of a Ship", Oceanology, (1977), 17, pp 101-104.

10. Quo Vadis™ Correlation Sonor Velocity Log, General Electric Company publication, EHM 12, 739(IM) 8/79.

11. Denbigh P.N., "A design study for a correlation log to measure speed at sea", J. Navigation, (1982), 35, pp 160-184.

12. Tucker A.D., "Speed measurement at sea and sea bed characterization using correlation techniques", M.Sc. thesis, University of Cape Town (1983).

13. Denbigh P.N., "Ship velocity determination by Doppler and correlation techniques", I.E.E. Proceedings, Volume 131, Part F, No. 3 (June 1984), pp 315-326.

CHAPTER 2

2. THEORY

2.1 GENERAL PRINCIPLE

The principle upon which the correlation log is based can be described as follows:

Consider a transducer assembly consisting of a projector and two receivers, moving through the water at a velocity V metres/second. Let the fore receiver be F and at a distance d behind F, the aft receiver A. Broadbeam transducers are used that point vertically downwards at the sea bed.

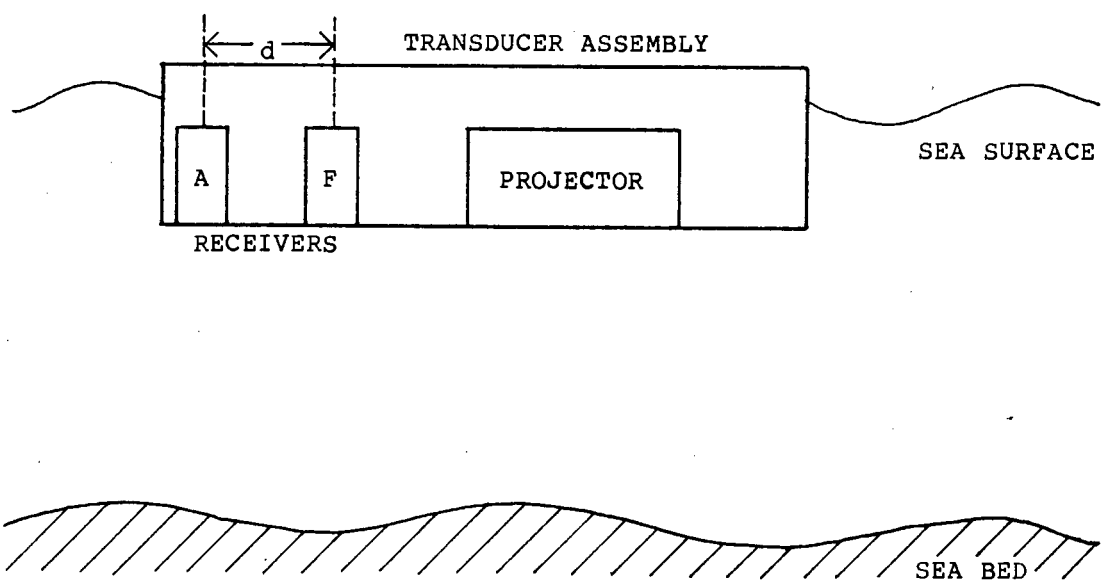

Transducer Assembly

FIGURE 1

Let the projector transmit CW at the sea bed and the two receivers receive the resultant return echoes. If certain conditions relating to transducer separation hold, then the signals from the fore and aft receivers will be identical except for a time shift T. This is depicted in Figure 2.

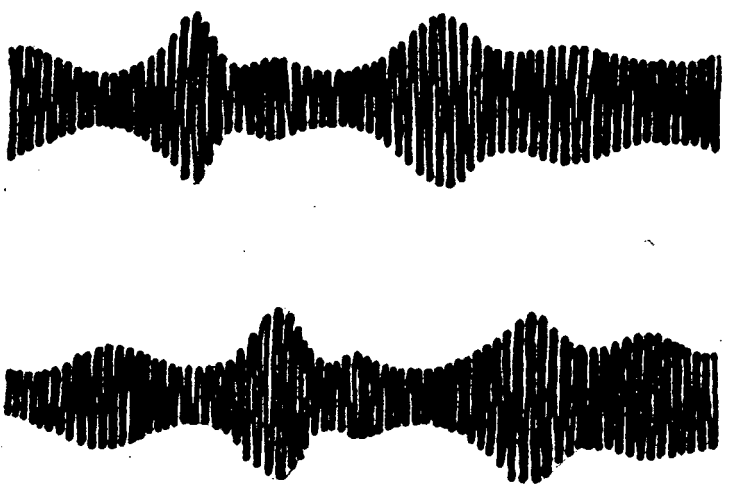

Fore and Aft Receiver Signals

FIGURE 2

The time shift T is related to the transducer separation d and the transducer assembly's velocity V, by the equation:

$$V = \frac{d}{2T} \qquad \text{Equation 1}$$

For a derivation of this equation the reader is referred to a paper by Denbigh[1].

The principle of the correlation log is that if d and T are known, the velocity V may be calculated from equation 1.

2.2 SYSTEM PROPOSALS

The V = d/2T equation suggests a number of ways of determining the velocity V. These suggestions can be explored in the form of system proposals and are as follows:

(a) Fix the value of d by having two receivers and search for the time shift between the two received signals which results in the maximum correlation.
This search can be implemented in one of two ways:

(i) The crosscorrelation function can be evaluated and the time shift T of the peak determined.

(ii) A delay can be applied to the fore receiver signal and this delayed signal can be correlated with the aft receiver signal to form a correlation coefficient. The delay can be varied until the correlation coefficient is maximum. This value of delay corresponds to the time shift T.

(b) Have a large number of receivers and, for a fixed time shift T, search for that receiver spacing d which gives maximum correlation. The search is implemented by forming a spatial correlation function and determining the position of the peak which corresponds to the separation d.

(c) Have two receivers at spacings X_1 and X_2 from a reference receiver and search for the time shift T that gives the same correlation between the reference and receiver 1 and between the reference and receiver 2. It can then be assumed that the peak of the spatial correlation function is midway between receivers 1 and 2 at a distance $(X_1 + X_2)/2$ from the reference receiver.

The above system proposals have only been stated; they will, however, be fully discussed in the next chapter.

2.3 CONTINUOUS-WAVE AND PULSED TRANSMISSION SYSTEMS

The signals received back from the sea bed emanating from a continuous-wave transmitter may vary both in amplitude and phase (see Figure 2). Correlation is best achieved on low frequency signals, so the carrier of the received signal should be removed. This is achieved by envelope detection. Figure 3(a) shows a CW transmission and Figures 3(b) and 3(c) show the envelope detected returns that would be expected on

two receive transducers a distance d apart and moving through the water at a velocity V.

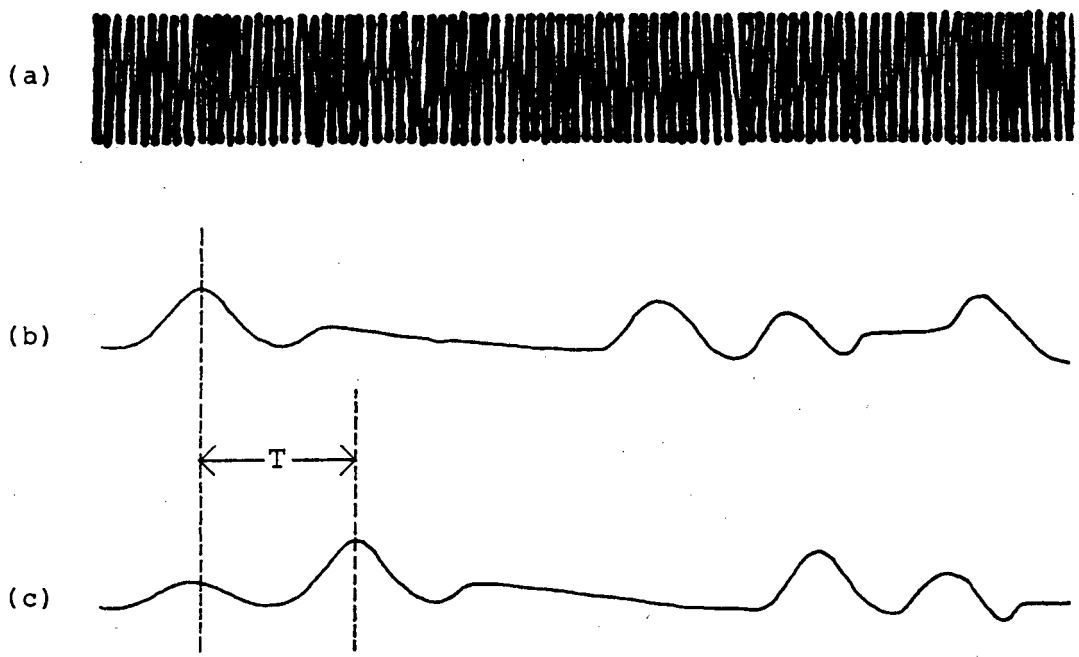

CW Transmission and Received Signal Envelopes

FIGURE 3

The use of continuous-wave transmission for the correlation log is unsatisfactory. This is because transmitter breakthrough, volume reverberation and other short-range backscatter effects contaminate the signal from the sea bed. The signals used for correlation must emanate from the sea bed, so pulsed transmission must be used and the return signals must be range gated.

Pulsed transmission gives rise to many of the practical difficulties encountered in correlation log design. A pulse cannot be transmitted when a return pulse from the sea bed is being received. Range gating and pulsed transmissions both rely upon the knowledge of when the return pulse will be received. This information can only be gained by knowing the water depth Z and the speed of sound in water C. The need for a depth sounder as part of the correlation log system now becomes apparent.

The two-way propagation time for sound to travel from the sea surface to the sea bed and back again is:

$$\text{Two-way propogation time } T_{TWP} = \frac{2Z}{c} \quad \text{Equation 2}$$

Figure 4(a) shows a transmitted pulsed signal and Figures 4(b) and 4(c) show possible receive signals that are to be expected on two transducers a distance d apart and moving through the water at a velocity V.

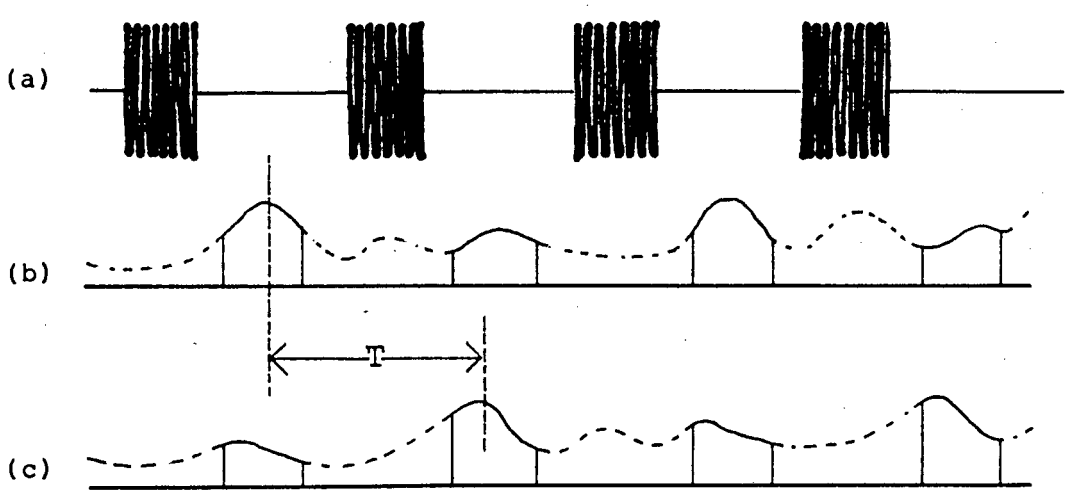

Pulsed Transmission and Received Signal Envelopes

FIGURE 4

2.4 SHAPE OF THE CORRELATION FUNCTIONS

The system proposals are based either on the time or the spatial correlation function. It is important to establish the characteristics of these two functions. It is simplest first to consider the situation where continuous-wave transmission could be used and where there is no unwanted back scatter. In later sections the effect of pulsed transmission on the correlation functions are examined. The analysis of the correlation functions has been performed by Denbigh[1].

2.4.1 TIME CORRELATION FUNCTION

The time displacement of the peak of the time correlation function has already been shown to equal d/2 V (Equation 1). The signal received on the fore receiver will be identical to the signal received on the aft receiver, except for a time shift T. It follows that the shape of the time correlation function of these two signals is the same as the autocorrelation function of one of the receive signals, apart from a time shift T.

Making use of the Wiener-Khintchine theorem the autocorrelation function is found by taking the Fourier transform of the power spectrum.

Denbigh[1] estimated the shape and the width of the power spectrum of the envelope detected return as follows:

A reasonable approximation is to assume that the insonifying beam pattern is Gaussian and that therefore the shape of the spectrum of the envelope detected return signal is also Gaussian centred around zero frequency.

The width of spectrum is estimated by considering how much frequency spreading the envelope detected return signal has undergone due to Doppler frequency shift of the insonifying beam. The -3dB half bandwidth of the spectrum corresponds to the Doppler shift which occurs at the -3dB half beamwidth. If the -3dB points of the projector beam pattern occur at angles $\pm\ \theta/2$ to the vertical, and $\theta/2$ is small, then it can be shown that the Doppler frequency shifts at the -3dB points are $\pm\ Vf\theta/c$, where V is the ship velocity and f the transmit frequency.

The Fourier transform of the one sided Gaussian power spectrum of bandwidth B corresponds to the auto-correlation function which is also Gaussian of width $1/\pi B$. The bandwidth $B = Vf\theta/c$ and hence the halfwidth at 61% of the autocorrelation function is $c/(2\pi Vf\theta)$.

The beamwidth θ of the project whose length is D is

$\theta = \lambda/D = c/Df$.

Replacing for θ in the halfwidth formula it follows that the width of the correlation function to the 61% points is $D/2\pi V$. The shape of the correlation function is as shown in Figure 5.

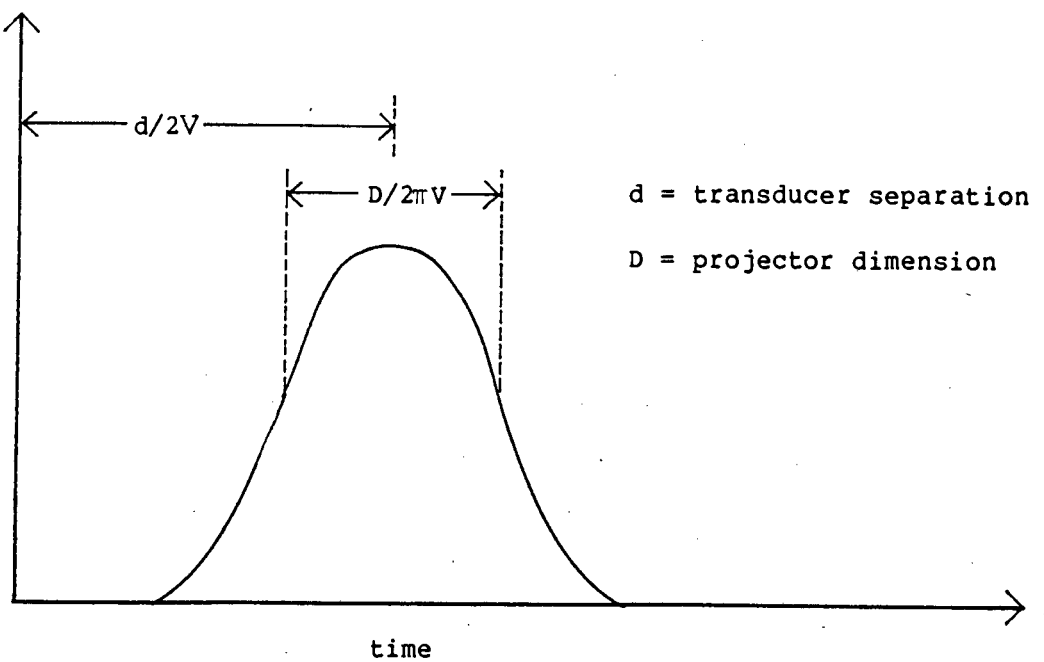

Time correlation function

FIGURE 5

2.4.2 SPATIAL CORRELATION FUNCTION

Consider a number of receivers. The spatial correlation function is obtained by multiplying the signal on one receiver called the reference (which is delayed by a time T) by the signal on a second receiver and averaging

the product. Normalisation of these correlation coefficients is usually performed.

This process is repeated for all possible receiver combinations and the displacement d which gives the maximum correlation coefficient is given by Equation 1 as d = 2VT.

With each receiver in turn being used as the reference, a large number of correlation coefficients can be calculated. Half of these will be for negative displacement which means the second receiver is ahead of the reference with respect to the direction of motion. A typical spatial correlation function is shown in Figure 6.

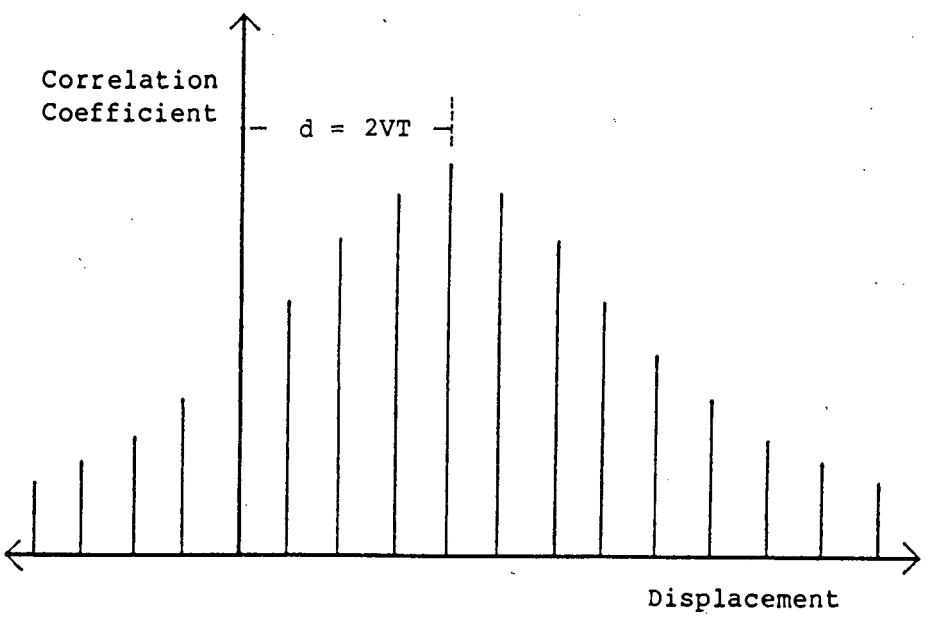

Spatial Correlation Function

FIGURE 6

The width of the spatial correlation function can be estimated as follows:

Consider a projector of dimension D and beamwidth $\theta = \lambda/D$. At a depth Z, the length of sea bed that is insonified by the projector beam is D/Z. If this insonified area is thought of as an acoustic array, then it can be expected that it will radiate at the water surface with a beamwidth of D/Z.
The linear width of this beam or lobe at the water surface will be the beamwidth times the depth Z, or D.
The signal received by receiver transducers that are within this linear width will have a fair degree of correlation. This is because they will be receiving return echoes that have been reflected from common insonified scattering points on the sea bed.
Thus the width of the spatial correlation function is similar to the dimension of the projector.

Experimental spatial correlation functions were produced at the Central Acoustics Laboratory's tank. The experimental procedure and the results, analysis and conclusions are presented in Appendix D.

REFERENCES

1. Denbigh P.N., "Ship velocity determination by Doppler and correlation techniques", I.E.E. Proceedings, Volume 131, Part F, No. 3 (June 1984), pp 315-326.

CHAPTER 3

3. THEORY

3.1 PULSED TRANSMISSIONS

Pulsed transmissions and range gating of the return signal are used. This enables unwanted returns from sources other than the sea bed to be eliminated. These unwanted returns arise from transmitter breakthrough, volume reverberation and other short range back scatter effects.

The length of the transmit pulse should be significant compared with the two-way propagation time. This allows the return from the sea bed to be made up of the total interference pattern resulting from the insonifying beam. Because of this requirement for long pulses, it is not possible to have a large number of short pulses in the water column at one time.

The minimum interpulse period (IPP) should always be greater than the two-way propagation time (T_{TWP}) corresponding to the water depth Z. A suitable relationship for the interpulse period is:

$$IPP \geqslant IPPmin$$

where IPPmin = 1,5 T_{TWP} = 1,5 x $\frac{2Z}{c}$

Take c = 1500 m/s then:

IPPmin = 2Z [ms] Equation 3

The pulse length should be long enough for a valid sea bed return echo but not so long that a guard time cannot be provided between the arrival of the sea bed return and the start of the next transmission pulse.

An adequate pulse length is:

Pulse length = $\frac{1}{4}$ IPPmin = $\frac{1}{4}$ x 2Z [ms] = $\frac{Z}{2}$ [ms] Equation 4

The minimum guard time is calculated when the IPP = IPPmin and is as follows:

Guard time = $2Z - \frac{2Z}{1,5} - \frac{Z}{2}$

= $\frac{Z}{6}$ [ms] Equation 5

Figure 7 shows these quantities.

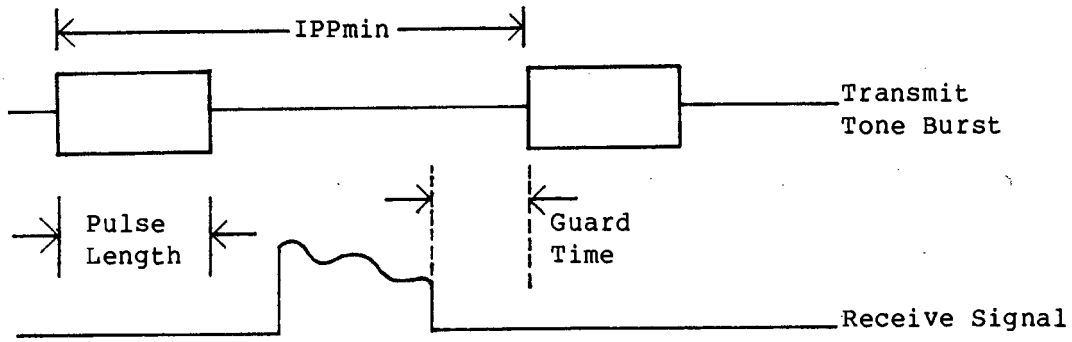

Pulsed Transmission and Gated Return Envelope

FIGURE 7

Provided that the depth is known and the transmit waveform constructed accordingly, the return from the sea bed will be uncontaminated by unwanted acoustic returns. The transmit waveform is thus a function of depth.

For a working system, the depth has to be reliably known. Simple depth sounders suffer from the problem of erroneous readings due to the presence of strong mid-water targets (fish shoals for example) that are mistaken for the sea bed.

A part of this M.Sc. project was devoted to developing a depth sounder that would reject false targets and only accept the sea bottom in determining depth. The depth sounder is described in Chapter 4 and Appendix C.

3.2 SYSTEM PROPOSALS

In the previous chapter a number of proposals as to how the $V = d/2T$ equation can be used in the design of a correlation log were presented. On the basis of pulsed transmission these proposals will now be discussed. They are as follows:

(a) Temporal correlation log

(b) Spatial correlation log

(c) Inter-intrapulse correlation log

3.2.1 VELOCITY DEPTH PRODUCT

Before discussing the system proposals, it is useful to have a parameter to measure the success or failure of the various correlation log proposals. Such a parameter is the velocity depth product VZ. The velocity depth product is fundamental to the successful operation of the correlation log and describes the conditions of velocity and depth under which the correlation log operates.

For example a velocity depth product $VZ \leqslant 20$ implies that if the velocity is known then the operating depth of the correlation log $Z \leqslant 20/V$ for successful operation, or if the depth is known then the range of velocity that can be measured is $V \leqslant 20/Z$. If $Z > 20/V$ or $V > 20/Z$, the correlation log will fail to operate successfully.

3.3 TEMPORAL CORRELATION LOG

The temporal correlation log is based on the following principle:

Fix the distance apart of two receivers. The time shift between the two received signals for which correlation is maximum is now determined. This search can be implemented in one of two ways:

(a) The position of the peak of the crosscorrelation function can be determined. This corresponds to the time shift T.

(b) A delay can be applied to the fore receiver signal and this delayed signal can be correlated with the aft receiver signal to form a correlation coefficient. The delay can be varied until the correlation coefficient is maximal. This value of delay corresponds to the time shift T.

3.3.1 THE TEMPORAL CORRELATION FUNCTION

The implementation of the time correlation function can be described as follows:
For the time correlation function shown in Figure 5 the peak position can be determined.

It must be noted, however that this function was derived for continuous-wave transmission. The use of pulsed transmission modifies the time correlation function as follows:
Figure 3 shows the envelope detected return signals that might be obtained if continuous-wave transmissions were used and if there was no unwanted back scatter.

For the same conditions of velocity, transducer separation d and the same portion of sea bed, Figure 4 shows the range gated envelope detected return signals that might be obtained if pulsed transmission were used.

For the the pulse transmission situation shown in Figure 4 the envelope detected return signal can be thought of as a sample version of the received envelope that would be obtained using a continuous-wave transmission.

When the fore and aft signals of Figure 4(b) and 4(c) are crosscorrelated, the result is a sampled version of the crosscorrelation function that would have been obtained if continuous-wave transmission were used.

If the pulse length of transmission is τ, the width of the samples in the correlation function is 2τ, and the samples are an interpulse period apart.

Depending on the pulse length, interpulse period, displacement and width of the correlation peak, the correlation function may appear in any of the forms shown in Figures 8(b), 8(c) or 8(d). These parameters then are functions of depth, velocity, transducer separation and projector dimension respectively.

Figure 8(c) illustrates clearly the situation in which it is impossible by interpolation to accurately determine the peak of the crosscorrelation function.

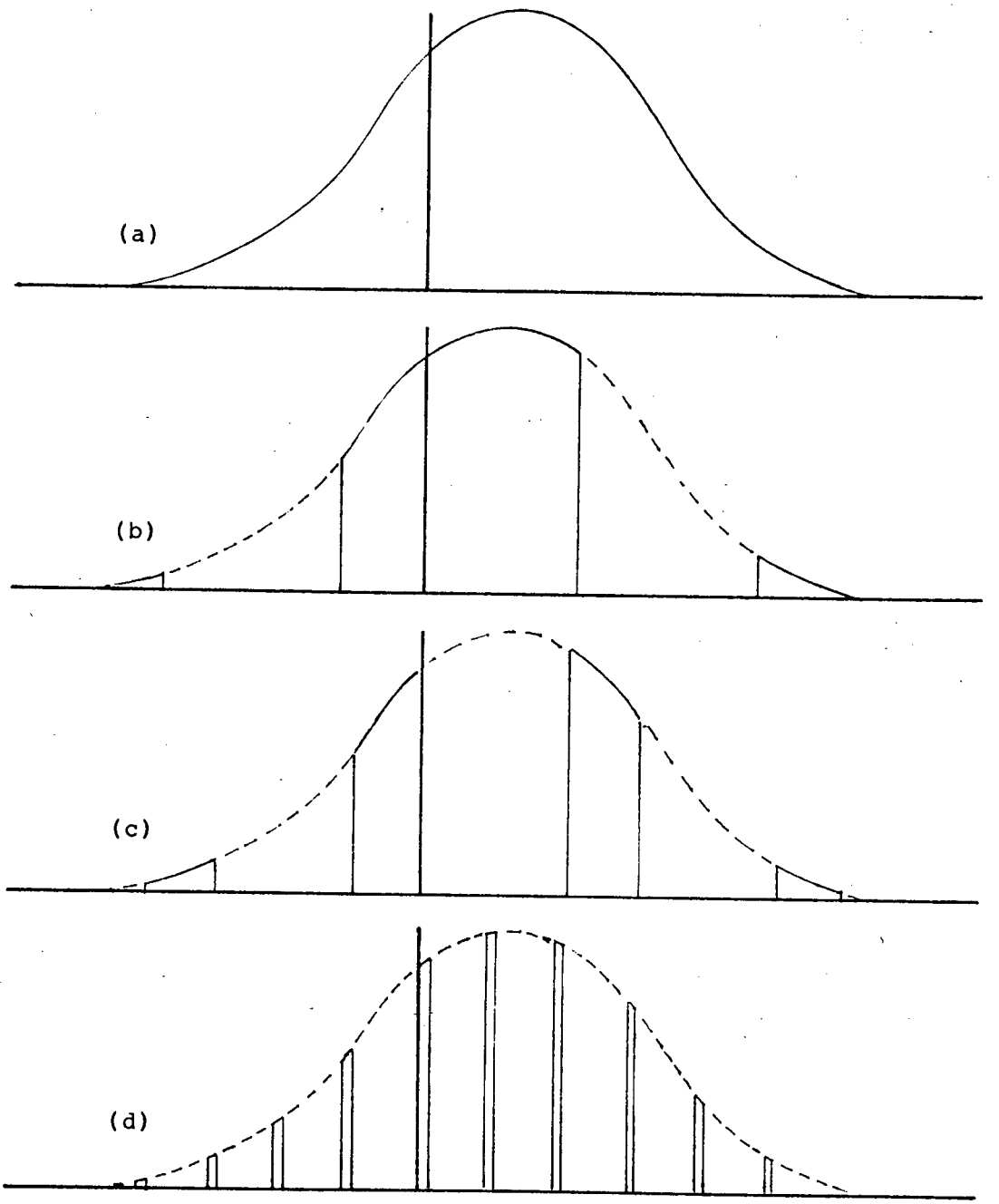

Sampled Correlation Functions

FIGURE 8

Figures 8(b) and 8(d) show situations in which it is possible to determine the position of the correlation peak. For this to occur one of two conditions have to be met:

(a) It is required that the sum of the time shift and the halfwidth of the correlation function should be less than the pulse length of transmission.

From Section 2.4.1, the halfwidth of the correlation function is $D/2\pi V$ and the time shift is $d/2V$.

It follows that:

$$\frac{d}{2V} + \frac{D}{4\pi V} \leqslant \tau \quad \text{where } \tau \text{ is the pulse length.}$$

Now τ the pulse length = $Z/2000$, where Z is the water depth and c = 1500 m/s, from Section 3.1. The above inequality becomes

$$1000\left[d + \frac{D}{2\pi}\right] \leqslant VZ \qquad \text{Equation 6.}$$

Under these conditions, the correlation function would appear as shown in Figure 8(b).

(b) Alternatively, there should be sufficient samples within the correlation peak to facilitate interpolation. A sufficient requirement is that there be at least two interpulse periods within the halfwidth.

From Section 2.4.1, the halfwidth of the correlation function is $D/2\pi V$.

It follows that:

$$IPPmin \leqslant \frac{D}{4\pi V}$$

Now IPPmin = Z/500 where Z is the water depth and c = 1500m/s, from Section 3.1. The previous inequality becomes:

$$VZ < \frac{D \times 125}{\pi} \qquad \text{Equation 7}$$

If this condition is met, the correlation function will appear as illustrated in Figure 8(d).

Take typical values of d = 5cm and D = 6cm

Equation 6 becomes $60 \leqslant VZ$

Equation 7 becomes $VZ \leqslant 2,4$

The above two inequalities can be combined as follows: with the values of d and D chosen, the temporal correlation function will not work for velocity and depth situations for which

$$2,4 < VZ < 60$$

For example, with a velocity of 1 m/s, and the depth Z such that $2,4m < Z < 60m$, then the temporal correlation log using the correlation function will not work.

The previous inequalities apply to a specific transducer geometry. A different choice of transducer separation and projector size will change the combinations of depth and velocity for which the correlation function can be used.

3.3.2 CORRELATION COEFFICIENT

The correlation coefficient implementation can be described as follows:

The correlation coefficient for a given delay T can be thought of as a single sample of the time correlation function. It has been shown that a pulsed transmission system produces sampled time correlation functions and that the position of the peak of the correlation function can only be determined for certain velocity and depth situations. These constraints also apply to the correlation coefficient method.

Besides these problems a difficulty arises in adjusting the delay T so that the correlation coefficient is always maximal. Consider the sampled time correlation functions of Figures 8(b), (c) and (d). It has been shown in Section 2.4.1 that the halfwidth of these functions is $D/2\pi V$. If V is very small, the width of the correlation function will be very large and the function will consequently vary very slowly with time. The sharply defined peak will become flat and it will be impossible to determine the maximum value of the correlation coefficient.

The temporal correlation log using two receive transducers is not a satisfactory device as it cannot operate under all velocity and depth situations.

3.4 SPATIAL CORRELATION LOG

In contrast with the temporal correlation log which seeks the time delay which gives the maximum correlation for a particular receiver spacing, the spatial correlation log seeks the receiver spacing which gives the maximum correlation for a particular time delay.

This search is implemented by forming a spatial correlation function and searching for the displacement which gives the maximum value of the function. With reference to Section 2.4.2 it can be seen that the spatial correlation function is made up of samples. Hence, to determine the displacement of the peak, interpolation techniques are required.

Let us examine the effect of interpolation on the accuracy of the velocity measurement.

Let the positional error be δd. It is expected that δd will be significant with respect to the minimum receiver spacing and could be in the order of 1% to 20% of the spacing. The positional error is expected to be independant of velocity. By differentiating Equation 1 it is possible to relate positional error to velocity measurement error as follows:

$$\delta V = \delta d/2T \qquad \text{Equation 8}$$

Dividing Equation 8 by Equation 1 gives:

$$\frac{\delta V}{V} = \frac{\delta d}{d} \qquad \text{Equation 9}$$

The spatial correlation log exhibits the same constraints with regard to pulsed transmissions as the temporal correlation log. The allowable time delays are given as follows:

$$T \geqslant IPPmin$$

and $$T \leqslant 0{,}25\ IPPmin$$

IPPmin = 1,5 . Two-way propagation time

From Equation 8 it can be seen that the most accurate velocity measurements are obtained when d is large. It is therefore advantageous to choose a time delay which forces the displacement of the correlation peak to be as large as possible, while still remaining within the maximum receiver spacing.

Interpolation can introduce velocity errors which are totally unacceptable. The following example illustrates this point:

Let the water depth be 5 metres, the transducer spacing be 12mm and the positional accuracy δd = 0,6mm. The IPPmin = 10ms and the delay T is made equal to 0,25 IPPmin = 2,5ms. The time delay is the pulse duration.

The velocity error is $\delta V = \frac{\delta d}{2T} = \frac{0{,}6}{2x2{,}5} = 0{,}12m/s$

The measured velocity is $\frac{d}{2T} = \frac{12}{2x2{,}5} = 2{,}4m/s$

The velocity error is 5% which is unacceptable. To improve this accuracy, the time delay should be increased until it is greater than the pulse duration by making it equal to the

interpulse period. The value of d needed to achieve maximum correlation would increase and the velocity error would consequently decrease.

The conclusion that can be drawn from the above analysis is that there will always be an inherant velocity error due to the inaccuracy in determining the displacement of the peak of the spatial correlation function using interpolation techniques.

What is required is a technique which determines the position of the peak of the spatial correlation function without large positional errors. Such a technique is the two-point difference method and it is described as a part of the inter-intrapulse correlation log proposal.

3.5 INTER-INTRAPULSE CORRELATION LOG

3.5.1 INTRODUCTION

The inter-intrapulse correlation log is based on both the temporal and spatial correlation logs. As such it uses a variable time delay T and a number of receive transducer spacings d.

The system operates as follows:

Consider three receive transducers: A reference (Ref), at a distance X_1 behind the reference a receiver 1 (R1) and at a distance X_2 behind the reference a receiver 2 (R2). They are shown in Figure 9.

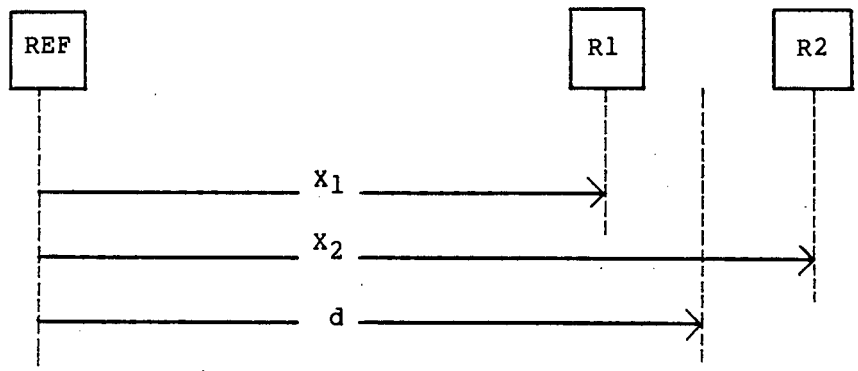

Receiver Transducer Geometry

FIGURE 9

Let the sea bed return echo be received by all three receivers. The signal on the reference receiver is delayed by an amount T and the delayed signal is correlated with the signal on receiver 1 and receiver 2. The delay T is adjusted until the same correlation exists between the reference and receiver 1 and between the reference and receiver 2. It can be assumed that if there was a hypothetical receiver at a distance $d = (X_1 + X_2)/2$ from the reference, the correlation between the delayed reference signal and the hypothetical receiver's signal would be maximum. The velocity

can then be found from Equation 1 V = d/2T. This hypothetical receiver is understood by way of the two-point difference method, described below.

3.5.2 TWO-POINT DIFFERENCE METHOD

The failing of the spatial correlation log is that one cannot interpolate to a satisfactory degree of accuracy the position of the peak of the spatial correlation function. Consider the ideal continuous spatial correlogram shown in Figure 10:

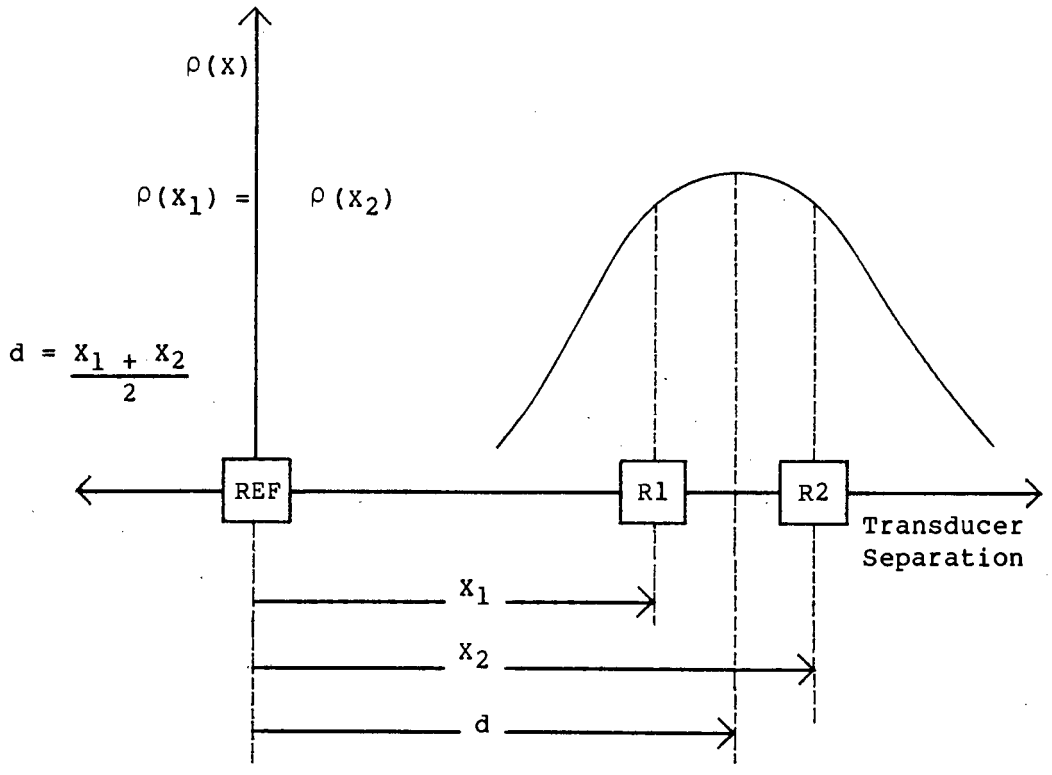

Ideal Spatial Correlogram

Figure 10

If the correlogram is symmetrical (experimental evidence described in Appendix D verifies this) then the following holds:

Let there be two transducer separations, X_1 and X_2 made up from a transducer geometry as shown in Figure 9. Also let the respective correlation coefficients for these transducer separations be $\rho(X_1)$ and $\rho(X_2)$.

If $\rho(X_1) = \rho(X_2)$ as depicted in Figure 10, then the position of the peak of the correlation function is:

$$d = \frac{X_1 + X_2}{2}$$

It has been shown experimentally (see Appendix D) that by varying the applied time delay T, the peak of the correlation function can be forced to change position. It is proposed that the time delay T be varied until the correlation coefficients $\rho(X_1)$ and $\rho(X_2)$ are equal. The position of the peak of the correlation function will thus be d where:

$$d = \frac{X_1 + X_2}{2}$$

The advantages of the two-point difference method are as follows:

(a) The method lends itself to a negative feedback control loop solution.

(b) There is not the same problem of positional accuracy associated with the spatial correlation log. The two separation values are known and any inaccuracy of construction can be eliminated in calibration.

(c) By having a second reference, the full range of velocity and depth situations can be accommodated.

3.5.3 MODES OF OPERATION

The inter-intrapulse correlation log, like the other logs described, uses pulsed transmission and range gating to ensure that the signal used for correlation arises solely from the sea bed return echo.

It has been shown that this imposes certain restrictions on the delay T that can be applied to the reference receiver signal.

Two ways of implementing a delay are suggested:

(a) The delay can be between pulses and as such the delay is equal to the interpulse period. This mode of operation is called the interpulse mode.

(b) The delay can be within a return pulse and as such the delay can be smaller than or equal to the return pulse length. This mode of operation is called the intrapulse mode.

The mode used depends on the measured velocity and the water depth. As was mentioned previously these quantities are described by the velocity depth product VZ. The next two sections derive the mode parameters in terms of the velocity depth product.

3.5.4 INTERPULSE MODE

Consider the spatial correlation function (of Section 2.4.2), for a given separation X between reference and a second transducer. The reference signal is delayed by an amount T and correlated with the signal from the second receiver. This delay T is achieved in the interpulse mode as follows:

Firstly the pulsed transmission criteria (of Section 3.1) have to be fulfilled. Each sea bed return pulse is sampled simultaneously for both receivers. Two series of (n + 1) samples result, being the sampled versions of the reference and second receiver outputs respectively. The time between samples is an interpulse period IPP. The kth sample in the reference series is multiplied by the (k + 1)th sample in the second receiver series.

This product is averaged for n pulses. The time delay T thus imposed is one IPP. The transmit and sampled receive waveforms are shown in Figure 11.

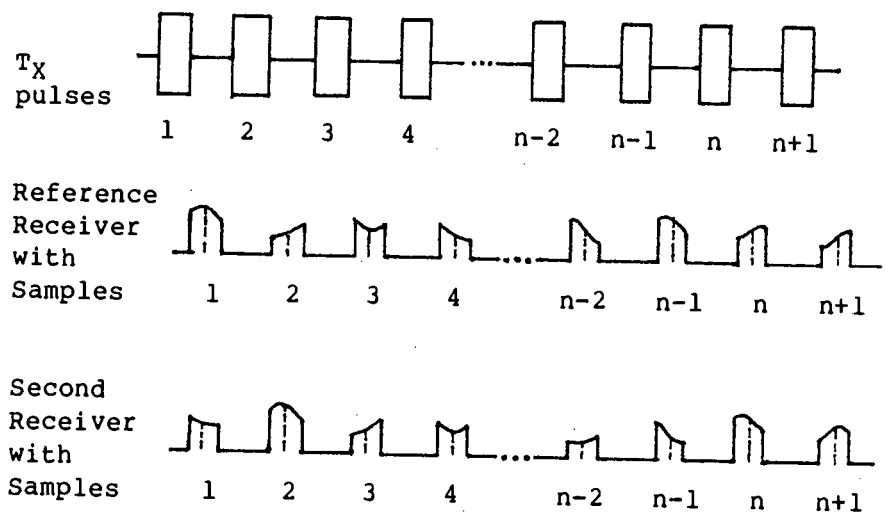

Transmit and Sampled Receive Waveforms for the Interpulse Mode

FIGURE 11

The delay of one IPP imposes restrictions on the operating water depth, and the velocity range that can be measured.

The time delay T = IPP.

The IPP $\geq$ IPPmin = 2Z [ms] from Equation 3

Therefore $T \geq 2Z$

Now the value of the delay T that must be applied to achieve maximum correlation with a receiver spacing X and a velocity V is $T = X/2V$

Therefore $250\ X \geq VZ$ where X is the transducer spacing in metres.

The sample time is derived as follows:

Consider Figure 12(a) which shows the sample time as being measured from the start of the transmit pulse to the sample in the return pulse. The sample time is equal to the two-way propagation time plus a time β. This time β must be greater than the time needed for the return echo to encompass the full interference pattern of the sea bed return.

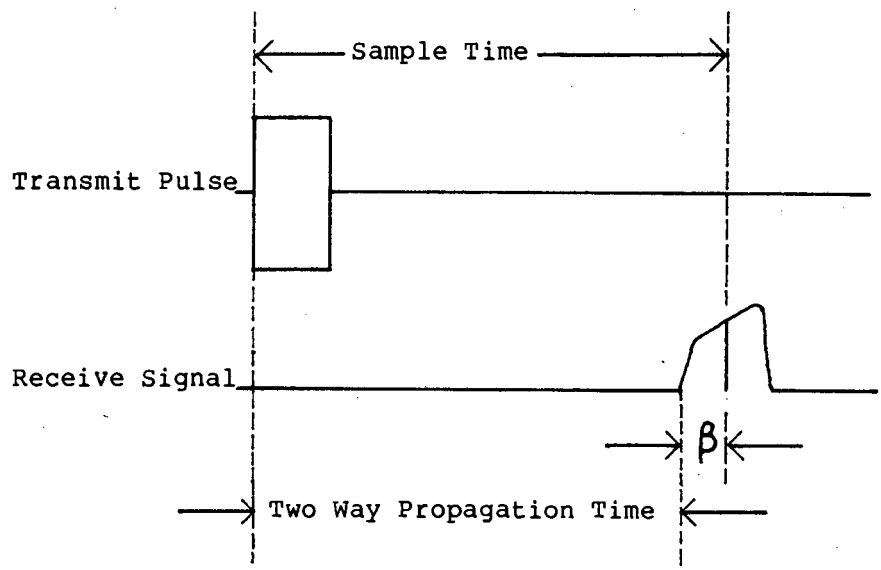

The Sample Time

FIGURE 12(a)

Consider a transmit transducer whose beamwidth is θ and is a distance Z from the sea bed. Such a situation is shown in Figure 12(b).

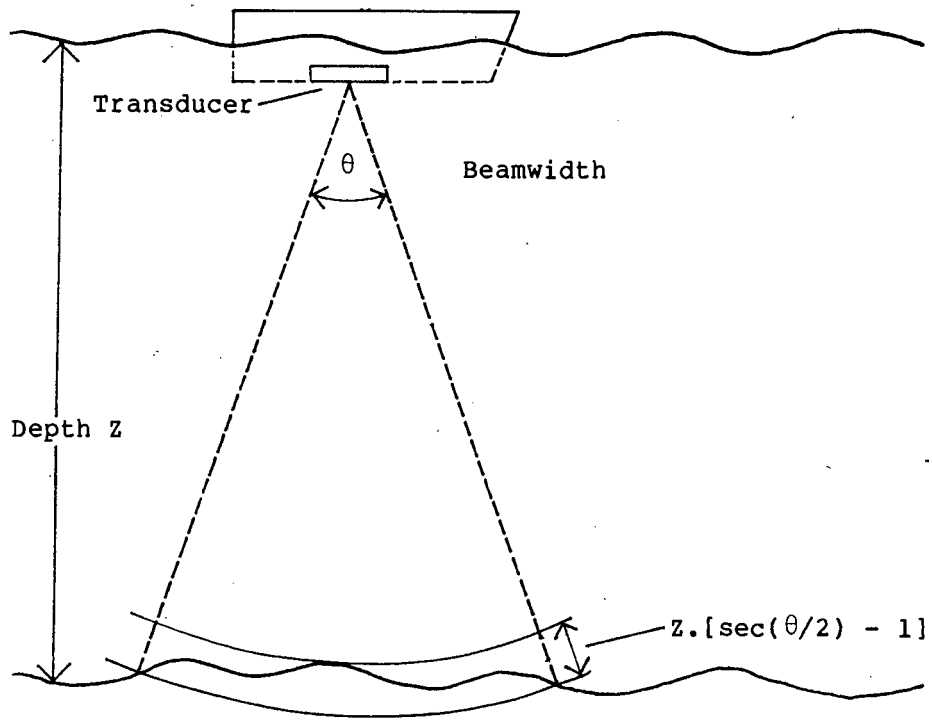

Transmitter Beamwidth

FIGURE 12(b)

The beamwidth of the transmit transducer is the reciprocal of the length of the transducer in wavelengths. Let λ be the transmit wavelength and D the dimensions of the transmit transducer

$$\theta = \frac{\lambda}{D}$$

Typical values of λ = 7,5mm and D = 24mm

This gives $\theta = \frac{7,5}{24}$ = 0,3 rads

The amount of time necessary for complete illumination of the sea bed is:

$$\frac{Z}{c}[\sec(\theta/2) - 1] = 1 \times 10^{-2} Z \text{ [ms]}$$

$$= 7,5 \times 10^{-3} \cdot T_{TWP}$$

The time $\beta > 7{,}5 \times 10^{-3} \cdot T_{TWP}$

Let $\beta = 0{,}25 \cdot T_{TWP}$

The sample time $= T_{TWP} + 0{,}25 \cdot T_{TWP}$

$= 1{,}25 \cdot T_{TWP}$

$= 1{,}25 \cdot \frac{2Z}{1500}$

$= 1{,}7\ Z$ [ms]

3.5.5 INTRAPULSE MODE

The interpulse inequality

$$250X \geqslant VZ$$

implies that for high velocity and large depth situations the interpulse mode of achieving a suitable delay T will fail.

To overcome this, each return echo from the sea bed is sampled twice within the return pulse. This mode of operation is called the intrapulse mode.

The delay T is achieved in the intrapulse mode as follows:

Firstly the pulsed transmission criteria have to be met. (Section 3.1) The IPP is fixed as IPPmin. Each sea bed return pulse is sampled twice, simultaneously

at each receiver. A series of n sample pairs result. The time between sample pairs is variable, but cannot be greater than the pulse length.

The first sample of the kth sample pair of the reference series is multiplied by the second sample of the kth sample pair of the second receiver series. This product is averaged over n pulses. The time delay T thus imposed is the time between sample pairs.

The transmit and sampled receive waveforms are shown in Figure 13.

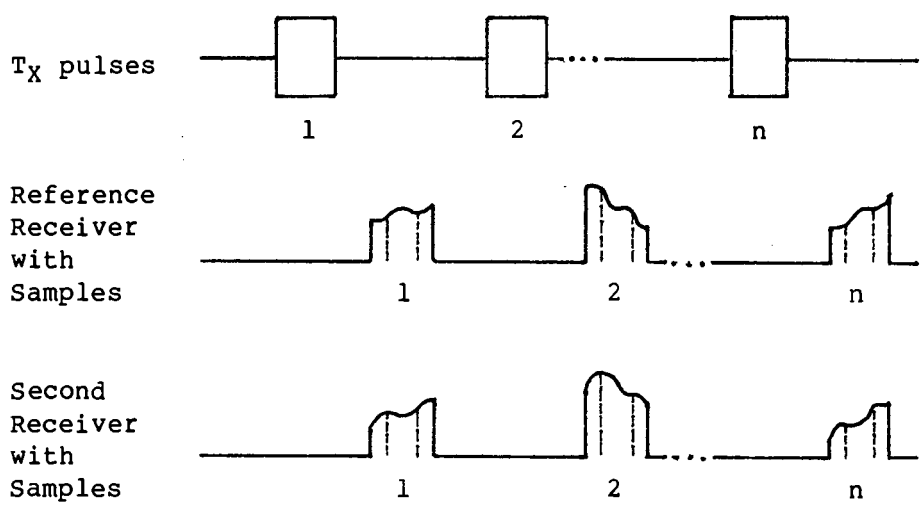

Transmit and Sampled Receive Waveforms for the Intrapulse Mode

FIGURE 13

The delay that can be obtained is always smaller than the pulse length and as such it imposes restrictions on the water depth that can be operated over, and the velocity that can be measured.

The length of the received echo restricts the time between the sample pairs and hence the delay T. There is a time at the beginning and end of the return echo when the echo is not made up of the total interference pattern from the insonifying beam reflecting off the sea bed. In the previous section a typical value for this time was calculated to be 1×10^{-2} Z milliseconds.

To be safe, the first sample can be set at five times this time i.e. 5×10^{-2} Z [ms] from the start of the return echo. Similarly the second sample should be taken less than 5×10^{-2} Z milliseconds from the end of the return echo.

The useful pulse length is thus (total pulse length) - $2(5 \times 10^{-2}$ Z) [ms].

Total pulse length is 0,5Z [ms]

Therefore time between samples $\leqslant 0{,}5Z - 2(5 \times 10^{-2} Z)$

$= 0{,}4Z$ [ms]

Therefore delay $T \leqslant 0{,}4Z$ [ms]

Now the value of delay T that must be applied to achieve maximum correlation with a receiver spacing X and a velocity V is

$$T = \frac{X}{2V}$$

Therefore $1250X \leqslant VZ$ where X is the transducer spacing in metres.

3.5.6 MODE SUMMARY

The following symbols are used:

Z	water depth in metres
X	separation of reference and second transducer in metres
V	velocity in metres/second

The interpulse and intrapulse mode characteristics are as follows:

INTERPULSE MODE

PARAMETER	FUNCTION OF	UNITS	VALUE
IPPmin	Depth	ms	2Z
IPP = Delay T	Velocity	ms	$\geqslant$ IPPmin
Pulse length	Depth	ms	0,5Z
Sample time	Depth	ms	1,7Z
Guard time (min)	Depth	ms	Z/6

$VZ \leqslant 250X$

INTRAPULSE MODE

PARAMETER	FUNCTION OF	UNITS	VALUE
IPP = IPPmin	Depth	ms	2Z
Pulse length	Depth	ms	0,5Z
First sample time	Depth	ms	1,38Z
Delay T	Velocity	ms	$\leqslant$ 0,4Z
Guard time	Depth	ms	Z/6

$1250X \leqslant VZ$

3.5.7 MODE CHANGE OVER

Depending on the measured velocity and water depth situations either the interpulse or the intrapulse mode is used. Consider the two mode inequalities

$250X \geqslant VZ$ Interpulse mode

$VZ \geqslant 1250X$ Intrapulse mode

It seems logical from the above inequalities to use the interpulse mode for low velocity and shallow depth situations and to use the intrapulse mode for high velocity and large depth situations.

If the separation X was the same for both modes then there would be velocity and depth situations in which it would be impossible to operate. What is needed is to use different receiver separations for the two modes.

Let the receiver spacing for maximum correlation for the interpulse mode be d_1 and for the intrapulse mode be d_2.

Consider the two-point difference method (of Section 3.5.2) of finding the receiver spacing for maximum correlation. If the transducer assembly shown in Figure 14 is used then $d_1 = (X_{11} + X_{12})/2$ and $d_2 = (X_{21} + X_{22})/2$

DISTANCE BETWEEN	IS
REF1 & R1	X_{11}
REF1 & R2	X_{12}
REF2 & R1	X_{21}
REF2 & R2	X_{22}

Figure 14 shows four transducers, two of which are reference transducers and two of which are secondary transducers.

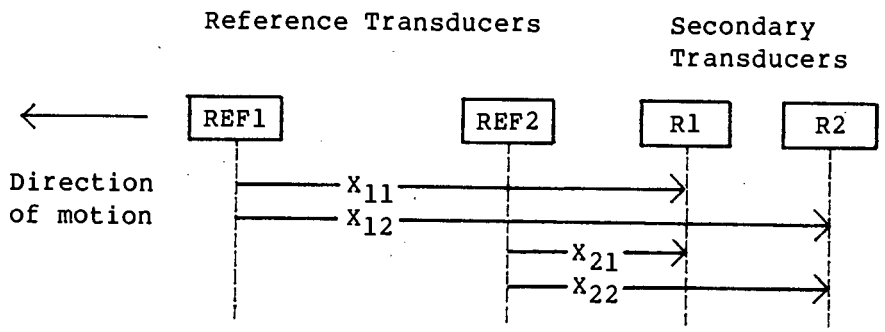

Transducer Geometry

FIGURE 14

For the log to operate in all the velocity and depth situations:

$$d_1 > 5\ d_2$$

A satisfactory condition is to let $d_1 = 6\ d_2$

(a) **Interpulse Mode**

With respect to the two-point difference method (Section 3.5.2) the transducers pairs (REF1 and R1) and (REF1 and R2) are used for X_1 and X_2, respectively.

$$X_1 = X_{11}$$

$$\text{and } X_2 = X_{12}$$

Note that $X_{12} > X_{11}$.

Provided that $250X_{11} \geqslant VZ$, the delay T can be imposed to obtain maximum correlation for both transducer pairs using interpulse techniques.

(b) **Intrapulse Mode**

The transducer pairs (REF2 and R1) and (REF2 and R2) are used for X_1 and X_2 respectively.

$$X_1 = X_{21}$$

$$\text{and } X_2 = X_{22}$$

Note that $X_{22} > X_{21}$

Provided that $1250X_{22} \leqslant VZ$, the delay T can be imposed to obtain maximum correlation for both transducer pairs using intrapulse techniques.

In physical terms, when using the interpulse mode REF1 transducer is used and when using intrapulse mode REF2 transducer is used. Figure 15 shows how this can be realised.

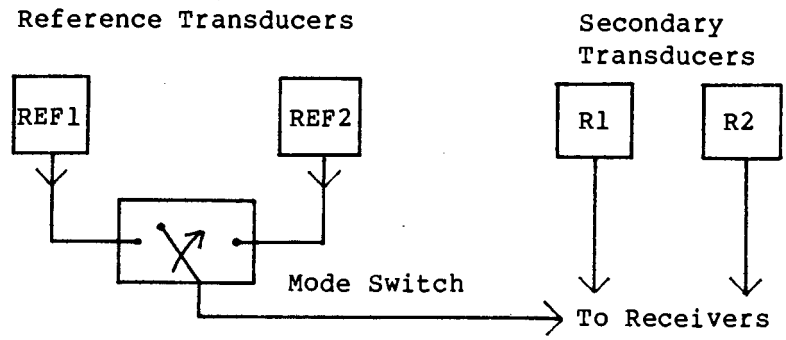

Reference Switching

FIGURE 15

3.5.8 SYSTEM OVERVIEW

The inter-intrapulse correlation log system is based on the two-point difference method of determining the position of the peak of the spatial correlation function. The delay T can be applied via two modes of operation: interpulse or intrapulse, depending on the measured velocity and the water depth situation. The system can be described with the aid of the block diagram shown in Figure 16.

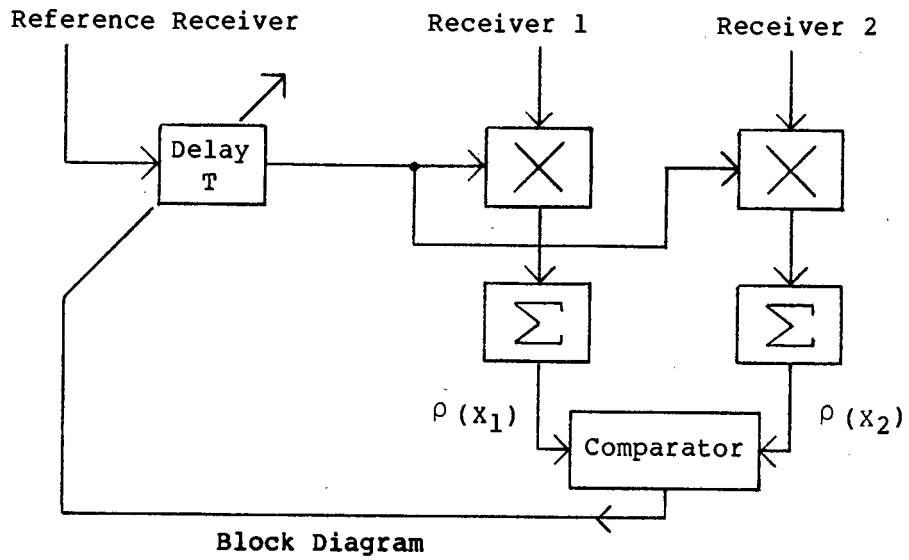

Block Diagram

FIGURE 16

The correlation between the delayed reference signal and receiver 1 and between the delayed reference signal and receiver 2 produce the two correlation coefficients $\rho(X_1)$ and $\rho(X_2)$ repectively. These are compared and the error is used to adjust the delay T until $\rho(X_1)$ equals $\rho(X_2)$.

CHAPTER 4

4. CORRELATION LOG SYSTEM

4.1 INTRODUCTION

This chapter describes the overall system that was built to implement the inter-intrapulse correlation log proposal. A broad overview is offered. For greater detail, the reader is referred to appendices A, B and C. These appendices describe the hardware and software realisation of the system.

4.2 CONSTITUENT SYSTEM ELEMENTS

The system consists of the following four subsystems:

(1) System processor.

(2) Correlation signal processor/generator.

(3) Depth sounder.

(4) Transmit and Receive Transducer Assembly.

(1) System Processor

The system processor is a micro-computer which has the following functions:

(a) The system algorithm implementation.

(b) The reading from the depth sounder.

(c) The writing to and reading from the correlation signal processor/generator.

(d) The two-point difference method implementation.

(2) **Correlation signal processor/generator (Correlator)**

This subsystem has two functions:

(a) Transmitter and receiver sampling waveform generation.

(b) Correlation signal processing.

(3) **Depth Sounder**

The functions of this subsystem are as follows:

(a) The depth sounder is to present to the system processor an updated value of depth on demand.

(b) The depth sounder is to have the ability to reject false depth readings due to marine life (fish shoals) and to accept only the true depth reading due to the sea bottom.

(4) **Transducer Assembly**

The transducer assembly consists of:

(a) four identical receive transducers

(b) one transmit transducer

4.3 TRANSDUCER ASSEMBLY

The transducer assembly used was an existing one built up by Tucker[1]. It was found that the transmit transducer block produced large amplitude side lobes. These were undesirable for the depth sounder and the correlation log system.

A solution to this problem was to use a separate circular transducer as transmitter and to clamp this to the existing transducer assembly.

The transducer assembly is shown in Figure 17.

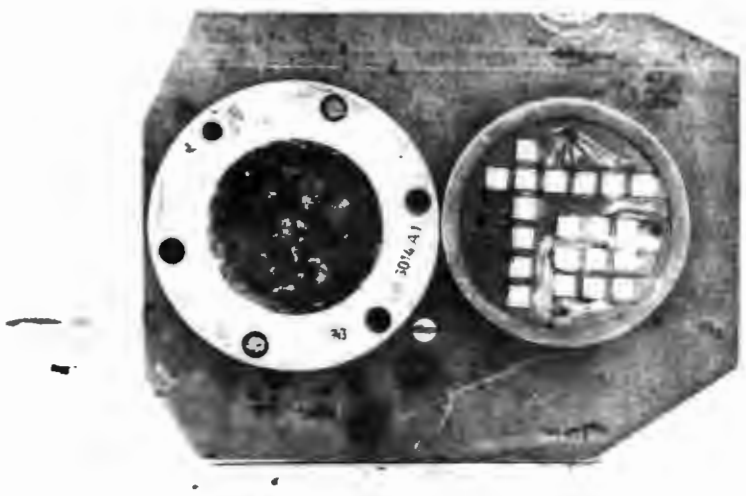

Transducer Assembly

FIGURE 17

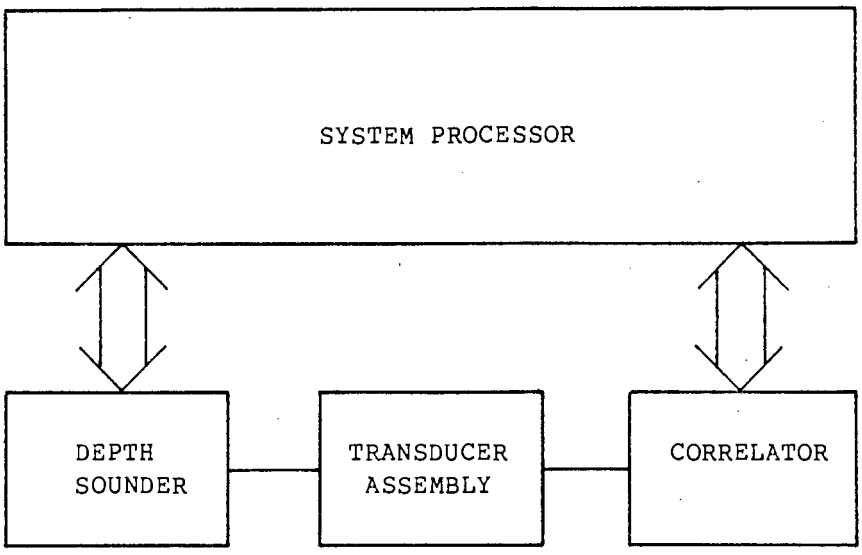

Schematic of Constituent System Elements

FIGURE 18

4.4 SYSTEM ALGORITHM

The correlation log system is based on the two-point difference method of determining the position of the peak of the spatial correlogram. The position of the peak is altered by applying a variable delay between the signals received on the reference transducer and the secondary transducers.

The delay can be applied via two different sampling techniques which depend on the velocity and depth situation.

A decision has to be made as to which mode inter or intrapulse is to be used. Depth is known via the depth sounder. A method of determining approximate velocity is needed. It is thought the taffrail log could be used.

The general algorithm is as follows:

Algorithm

1. Start
2. Input delay T and mode
3. Run depth sounder
4. Read depth
5. Calculate mode parameters
6. Write mode parameters to correlator
7. Run correlator
8. Read correlator results
9. Display correlator results
10. Stop

4.5 SYSTEM PROCESSOR

4.5.1 INTRODUCTION

The most readily available processor in the Central Acoustics Laboratory is the HP 85/86. The programming language is BASIC. A listing of programs used is found in Appendix A.

The HP 85 was used for portability. It was ideal for sea trials in False Bay and to test at the Simonstown Reservoir.

The HP 86 was used for tests in the CAL tank at UCT where the printer and disc storage medium was found invaluable.

4.5.2 MODE PARAMETER CALCULATION AND INPUT/OUTPUT

Consider the algorithm of Section 4.4. Let either mode be selected and the delay T decided upon.
Regardless of which mode is chosen, there are two basic functions that have to be set up.

(1) The transmitter waveform parameters:
   (a) Period which is the Delay T for the interpulse mode.
   (b) Pulse length.

(2) The sampling parameters:
   (a) Time of first sample.
   (b) Time between first sample and second sample which is the Delay T for the intrapulse mode.

Let the processor input the depth as Z metres. Note all parameters in [ms].

INTERPULSE MODE

PARAMETER	VALUE [ms]
IPP	Delay T
Pulse Length	0,5 Z
First Sample Time	1,7 Z
(Second-First) Sample Time	0

INTRAPULSE MODE

PARAMETER	VALUE [ms]
IPP	2 Z
Pulse Length	0,5 Z
First Sample Time	1,38 Z
(Second-First) Sample Time	Delay T

The four digital words above have to be sent to the correlator. The system processor inputs two digital words. The first being the depth Z and the second being the output from the correlator.

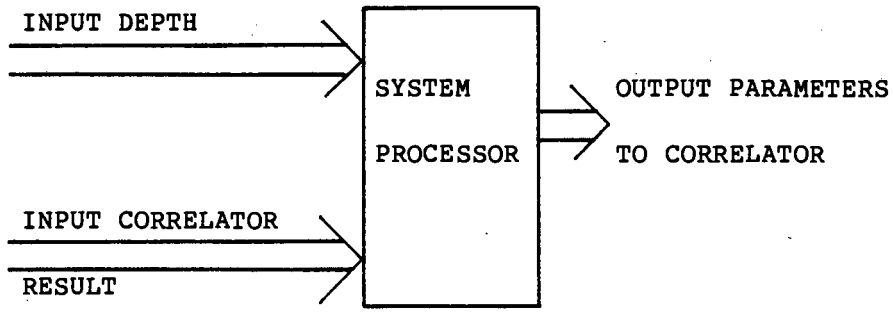

Schematic of System Processor Input/Output

FIGURE 19

4.5.3 THE DELAY T ALGORITHM

The algorithm of Section 4.4 is in open loop form. The loop is closed by implementing the two point difference method. A brief reminder of this method follows:

Consider three receive transducers: Reference, Receiver 1 and Receiver 2.

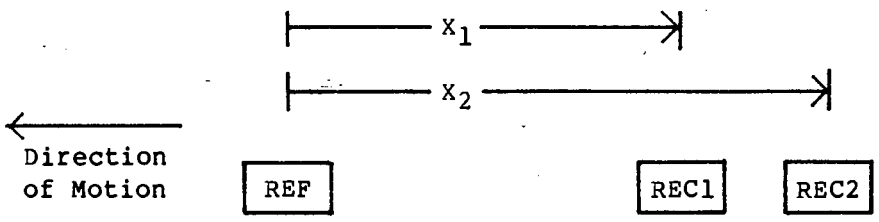

Receive Transducers

FIGURE 20(a)

Assume the correct mode is chosen for the velocity and depth situation. The reference received signal is delayed relative to receiver 1 and receiver 2 by an

amount T and these signals are correlated. The following spatial correlogram results:

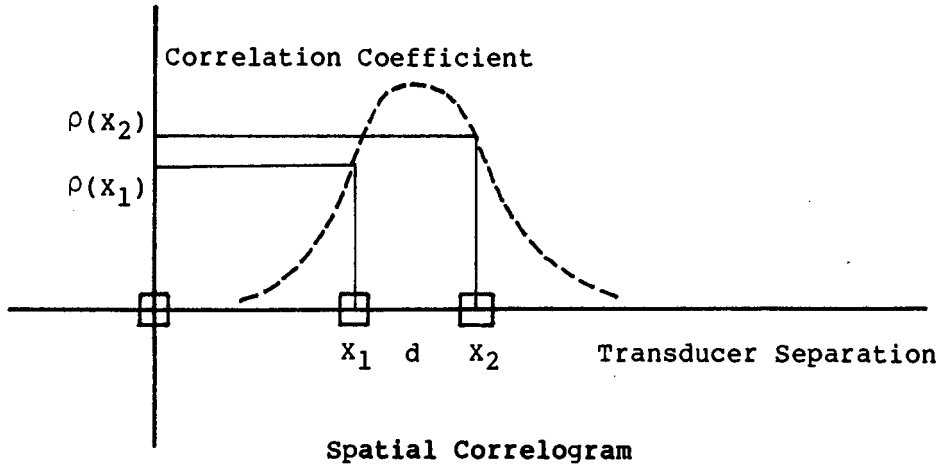

Spatial Correlogram

FIGURE 20

When the two correlation results $\rho(X_2)$ and $\rho(X_1)$ are equal, the peak of the correlogram is found at $d = \frac{X_1 + X_2}{2}$. The values of $\rho(X_1)$ and $\rho(X_2)$ are made equal by adjusting the value of the delay T. This is achieved by shifting the curve to the right or left.

Consider three cases of shift as depicted in Figure 21.

(1) $\rho(X_2) < \rho(X_1)$

(2) $\rho(X_2) = \rho(X_1)$

(3) $\rho(X_2) > \rho(X_1)$

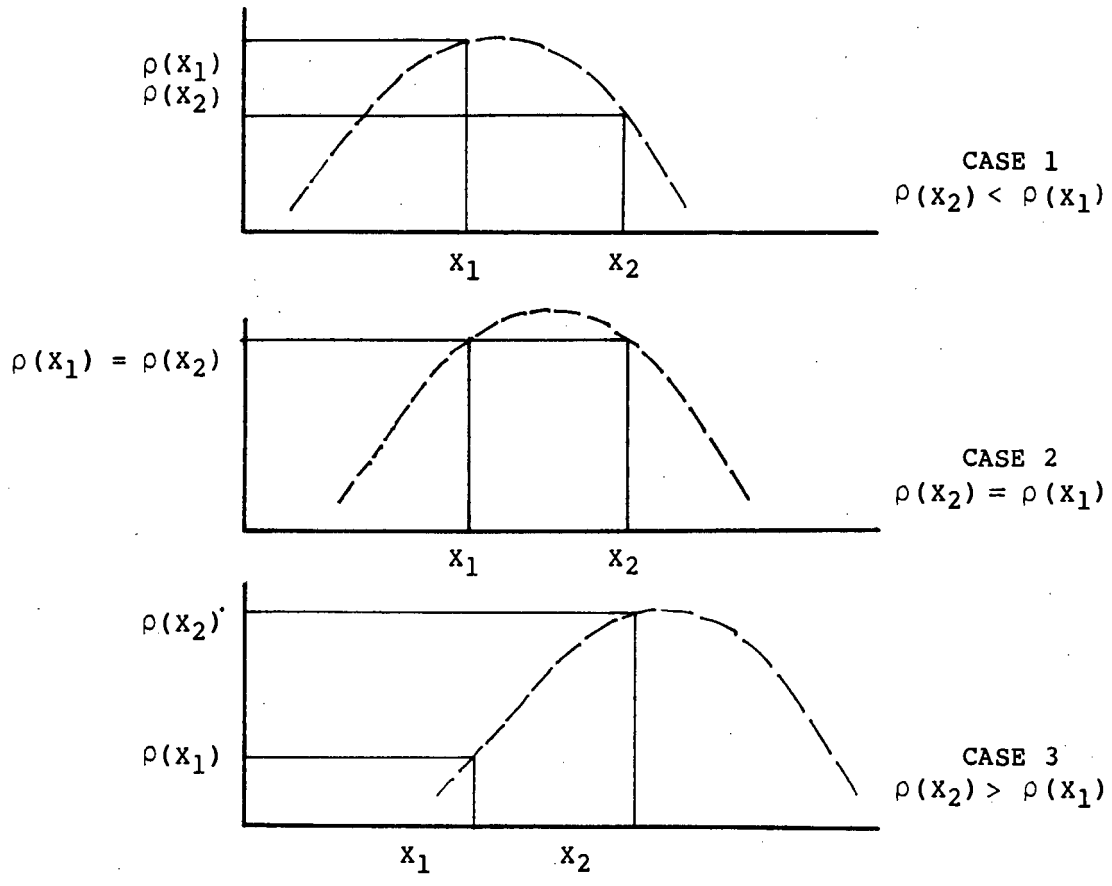

Shifted Spatial Correlograms

FIGURE 20(b)

Note the velocity for all three cases is the same. The delay T is least for Case 1 and most for Case 3. This suggests the following algorithm for implementing two-point difference method:

Algorithm

1. Start with minimum delay T
2. Run correlator with current delay T
3. If $(X_2) - (X_1) < 0$ increase delay T
4. If $(X_2) - (X_1) > 0$ decrease delay T
5. If $(X_2) = (X_1)$ leave delay T unchanged
6. Go to 2

The algorithm of Section 4.4 was implemented. Analysis of the correlation results pointed to some minor modifications to the correlator hardware.

A software correlator was implemented using alternate forms of the correlation equation. The results obtained are described in Chapter 5. Unfortunately time did not permit the two-point difference method algorithm to be implemented and the loop of the general algorithm of Section 4.4 to be closed.

4.6 CORRELATOR

4.6.1 FUNCTIONS AND CONTROLLING ALGORITHM

The functions of the correlator are as follows:

(1) To generate transmitter and receive sampling waveforms as specified by the system processor.

(2) To present to the system processor the result of the correlation.

The controlling algorithm is as follows:

Algorithm

(1) Wait until system processor writes mode parameters to correlator and demands a run.

(2) Interpret mode parameters and set transmitter and receiver sampling waveforms accordingly.

(3) Transmit and sample a preset number N pulses.

(4) Calculate the correlation results.

(5) Present correlation results to system processor.

4.6.2 BLOCK DIAGRAM

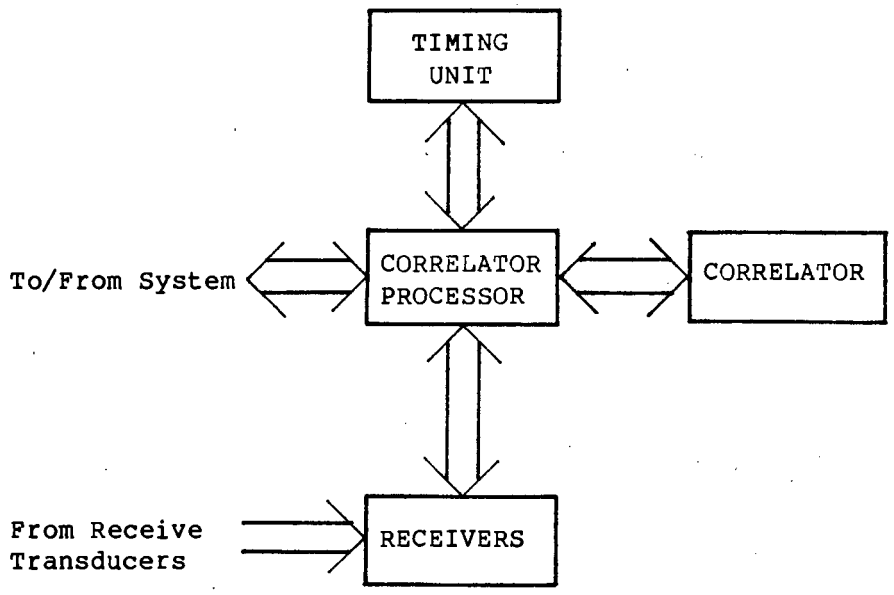

Correlator Block Diagram

FIGURE 22

The correlator subsystem can be thought of as being made up of four subsystems:

(1) Correlator processor;

(2) Receivers;

(3) Timing unit;

(4) Correlator.

General functions of the subsystems are:

1. **Correlator processor**

(a) To implement controlling algorithm of Section 4.6.1.

2. **Receivers**

(a) To amplify and envelope detect return echo signals from receive transducers.

(b) To apply time varying gain to this signal.

(c) To sample and hold and A/D signal on demand.

3. **Timing unit**

(a) To send transmitter gating signal to transmitter with specified pulse length and period.

(b) To send sampling signal to receivers with specified first sample time and delay T time if intrapulse mode used.

4. **Correlator**

(a) To perform two identical correlation calculations. One with the delayed sampled reference signal and the sampled receiver 1 signal. The other being the delayed sampled reference signal and the sampled receiver 2 signal.

(b) To present these results to the correlator processor on demand.

4.6.3 TIMING WAVEFORMS

The system processor specifies the mode parameters to the correlator processor. Consider each mode separately.

Interpulse Mode

In the interpulse mode (n + 1) pulses are transmitted and the (n + 1) return echoes are received on three transducers: Reference 1, Receiver 1 and Receiver 2.
The distance between Reference 1 and Receiver 1 transducer is X_{11}.
The distance between Reference 1 and Receiver 2 transducer is X_{12}.
The resultant signals from the three transducers are fed into their respective receivers. Amplification, time varying gain and envelope detection are applied. Each return pulse is sampled once.

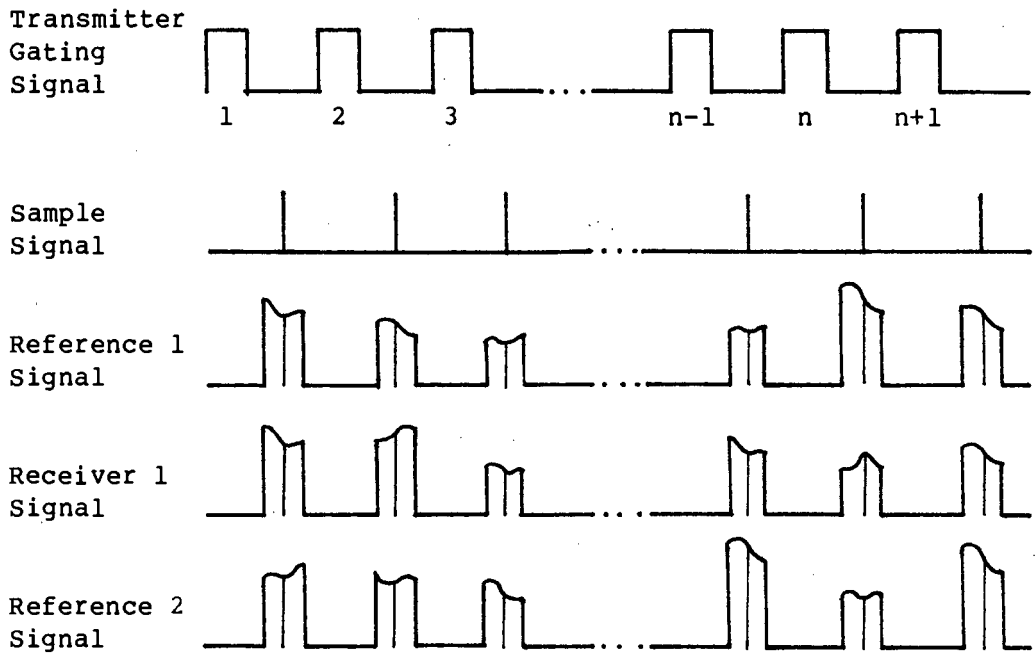

Interpulse Sampling

FIGURE 23

Intrapulse Mode

In the intrapulse mode n pulses are transmitted and the n return echoes are received by three transducers: Reference 2, Receiver 1 and Receiver 2.

The distance between Reference 2 and Receiver 1 transducer is X_{21}.

The distance between Reference 2 and Receiver 2 transducer is X_{22}.

The resultant signals from the three transducers are fed into their respective receivers. Amplification, time varying gain and envelope detection are applied. Each return pulse is sampled twice.

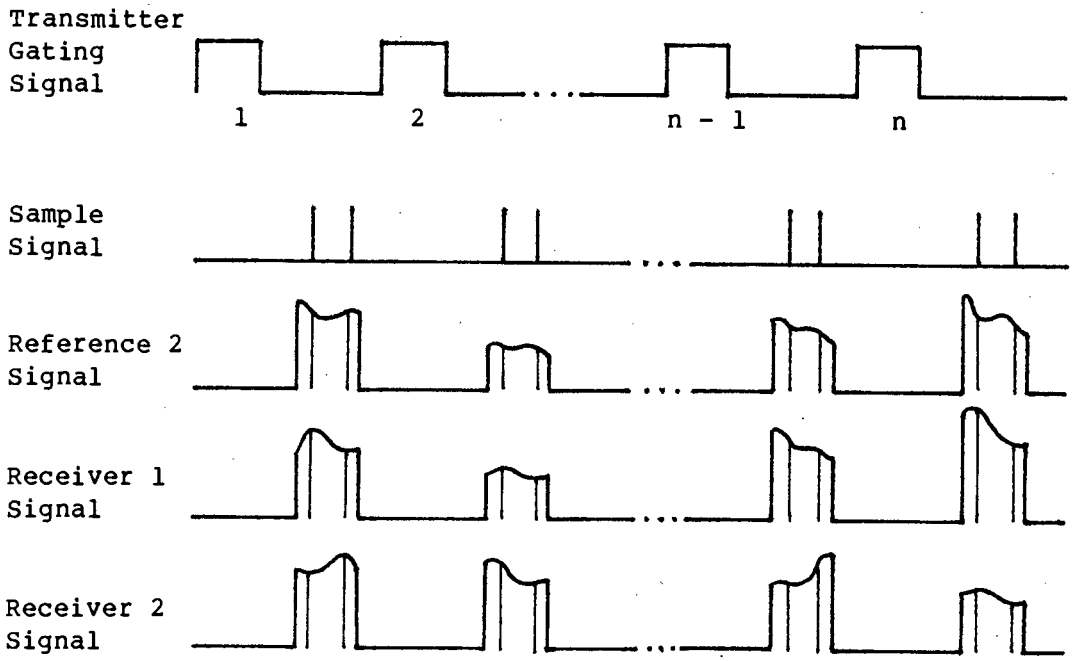

Intrapulse Sampling

FIGURE 24

4.6.4 CORRELATION PROCEDURE

For the Interpulse Mode

The receivers generate the following:

A sampled Reference 1 series $\{REF1_i\}$ for i = 1 to n + 1.

A sampled Receiver 1 series $\{REC1_i\}$ for i = 1 to n + 1.

A sampled Receiver 2 series $\{REC2_i\}$ for i = 1 to n + 1.

The correlation results $\rho(X_{11})$ and $\rho(X_{12})$ are derived as follows:

$\rho(X_{11})$ is calculated by correlating the first n samples of $\{REF1_i\}$ (i = 1 to n) with the last n samples of $\{REC1i\}$ (i = 2 to n + 1).

Similarly $\rho(X_{12})$ is calculated by correlating the first n samples of $\{REF1_i\}$ (i = 1 to n) with the last n samples of $\{REC1_i\}$ (i = 2 to n + 1).

The simplest form of correlation is applied, that of multiplying and summing. The mean is not removed and no normalisation is attempted. In Chapter 5 alternate forms of correlation are discussed.

So $\rho(X_{11}) = \Sigma \{REF1_i\} \cdot \{REC1_{(i+1)}\}$

and $\rho(X_{11}) = \Sigma \{REF1_i\} \cdot \{REC2_{(i+1)}\}$

For the Intrapulse Mode

The receivers generate a series of n sample pairs as follows:

$\{REF2_{(i,j)}\}$ being the sample pairs of Reference 2;

$\{REC1_{(i,j)}\}$ being the sample pairs of Receiver 1;

$\{REC2_{(i,j)}\}$ being the sample pairs of Receiver 2;

for i = 1 to n and j = 1,2.

The correlation results $\rho(X_{21})$ and $\rho(X_{22})$ are derived as follows:

$\rho(X_{21})$ is calculated by correlating the first sample of n sample pairs of $\{REF2_{(i,j)}\}$ (i = 1 to n and j = 1) with the second sample of n sample pairs of $\{REC1_{(i,j)}\}$ (i = 1 to n and j = 2).

Similarly $\rho(X_{22})$ is calculated by correlating the first sample of n sample pairs of $\{REF2_{(i,j)}\}$ (i = 1 to n and j = 1) with the second sample of n sample pairs of $\{REC2_{(i,j)}\}$ (i = 1 to n and j = 2).

So $\rho(X_{21}) = \Sigma \{REF2_{(i,1)}\} . \{REC1_{(i,2)}\}$

and $\rho(X_{22}) = \Sigma \{REF2_{(i,2)}\} . \{REC2_{(i,2)}\}$

4.7 DEPTH SOUNDER

4.7.1 INTRODUCTION

The requirement of the depth sounder is that its output should be a digital word giving water depth. This word should not be affected by unwanted strong returns such as mid-water fish.

The technique by which unwanted targets were rejected is based on the fact that they would not consistently

lie in the same range cell for successive positions of the depth sounder.

This principle is similar to that of the binary moving window detector used in Radar [Skolnik][2].

An added attraction of the detector is its simplicity of implementation.

The sea bottom may be detected at a given range by positioning a range gate, so that it only passes echoes of that given range. This results in a detector receiving, say, n echo pulses of the same range. If m of these n expected returns exceed a preset amplitude threshold then the sea bottom is assumed to be at that range.

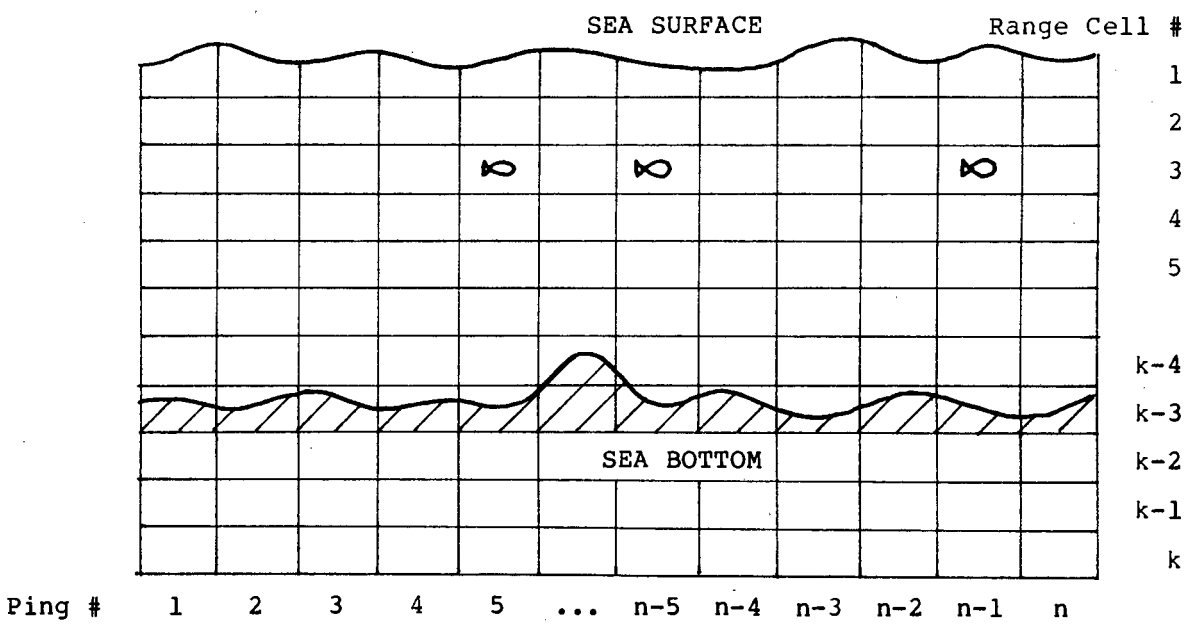

Sea Volume

FIGURE 25

Figure 25 depicts a cross-section of a typical sea volume. The columns represent the successive positions of the depth sounder as the ship moves forward. These columns are called pings.

A given water column is divided into a number of range cells. Range is related to time of propagation as follows:

The two-way propagation time for a sound wave to reflect off a target Z metres away is:

$$\text{Two-way propagation time} = \frac{2Z}{c}$$ c = speed of propagation.

From the above equation, a time cell can be equated to a range cell. Time cells are used because the return echoes display range information in terms of time, i.e. time elapsed from transmission.

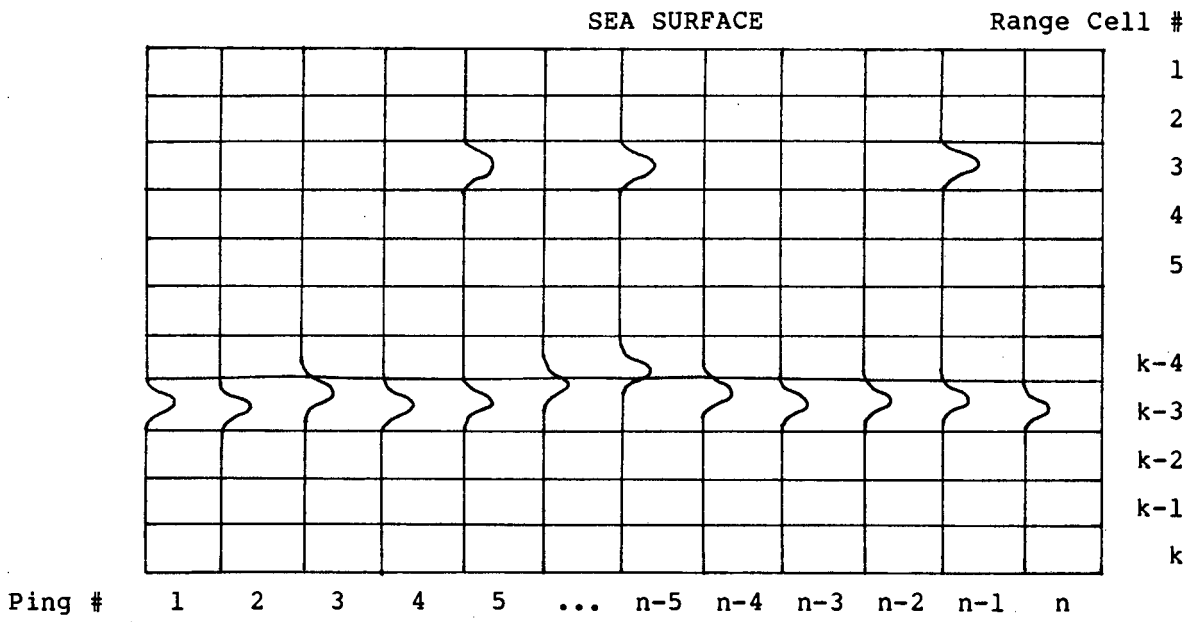

Envelope Detected Returns

FIGURE 26

Figure 26 depicts a series of envelope detected returns that would be expected if a pulse was transmitted for successive positions of the depth sounder. Consider implementing the target detector logic. The target is the sea bed. Let the number m of significant amplitude returns out of the total number of returns n be 5 for target detection. If one considers range cells 3 and k - 4. There are not more than 5 significant returns (that pass an amplitude threshold test) and so the m out of n test fails. For the k - 3 range cell the m out of n test is passed and so that target is detected.

It is required that:

(a) The return signal from the sonar receiver pass through an amplitide threshold detector and that the resulting encoded signal be placed in the appropriate range cell.

(b) The n encoded return signals be stored and updated.

(c) For each new return, the detector must be interrogated about the existence of a target at a given range.

(d) The target range be displayed and updated.

4.7.2 PULSE REPETITION FREQUENCY AND RANGE RESOLUTION

Pulse Repetition Frequency (prf)

There is an upper and a lower bound associated with the value of the prf.

(a) The lower bound of the prf is determined by the desired response time to change of depth. The critical response time occurs when operating in a shallow coastal environment where one is in danger of running aground. This environment is an advantage because the rate of change of depth in shallows is generally low. A depth update every ten seconds or less should cover all eventualities. The prf must thus be greater than 0,1Hz.

(b) The upper bound of the prf is related to the depth sounder's capacity for rejecting strong mid-water targets (e.g. fish shoals). Consider a ship carrying the depth sounder over the fish shoal. The fish shoal is insonified every interpulse period. The number of returns from the fish shoal that pass the threshold test must not exceed m. The number of times the fish shoal is insonified must be kept to a minimum. An insonification rate or prf of five times (or less) per second should be adequate.

The prf was chosen as 1Hz for the depth sounder as a stand alone unit. When connected as part of the correlation log system, the demand for a depth update from the system processor takes into account the above-mentioned upper and lower bounds.

Range Resolution

Consider the choice of range resolution. There are two factors governing range resolution.

(a) The resolution should be fine enough to comply with the correlation log system. It should be noted that the system processor downloads mode parameters in units of 100 s. There is no purpose then, in having a resolution less than 100 s two-way propagation time.

(b) Range resolution also affects the number of range cells used and the number n of pings used in the m out of n detector. One wants the number n as large as possible so that the detector has a lower probability of false alarms. As memory capacity is limited, the number of range cells k has to be relatively small.

With these two factors in mind a range resolution of 100mm was chosen. This corresponds to 133 s of two-way propagation time.

4.7.3 BLOCK DIAGRAM

The following block diagrams fulfill the previously listed requirements.

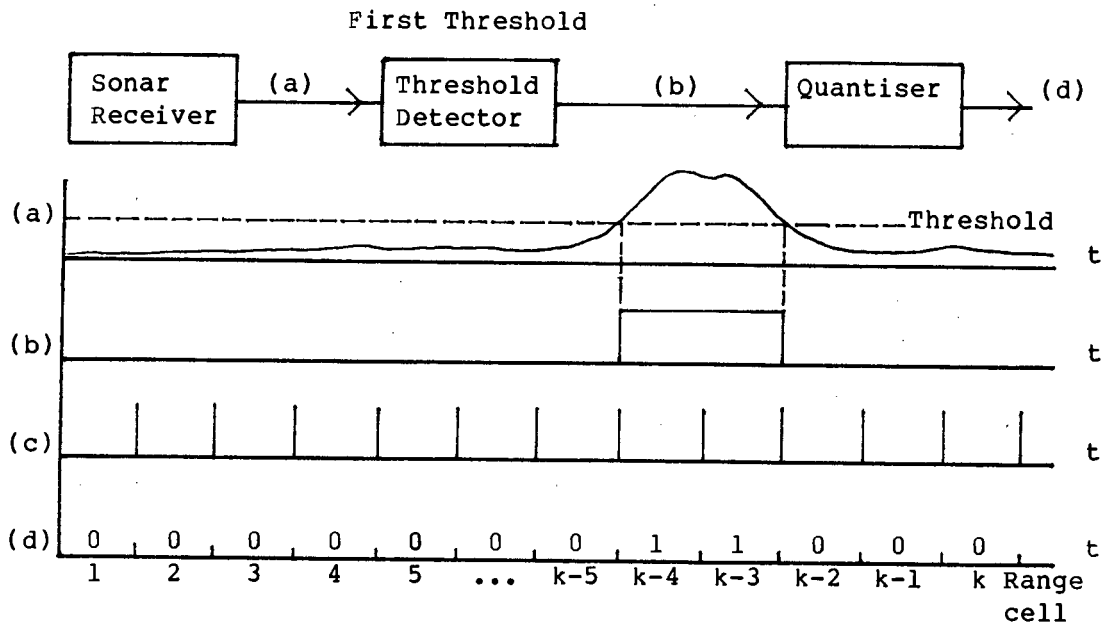

Block Diagram

FIGURE 27

Waveform (a) is one of n envelope detected return echoes. The reverberation and transmitter breakthrough have been gated out. A threshold has been superimposed upon it.

Waveform (b) is the output from the threshold detector which is at either a logic level 1 if the threshold is passed, or a logic level 0 if not.

Waveform (c) is a series of time cells, which can be related to range cells by the speed of sound propagation. If waveform (b) is sampled at the end of each range cell, then the resulting waveform is (d), the output from the quantiser. A digital '1' thus indicates if a range cell contains a return echo that has passed the threshold test. A digital '0' indicates that a range cell does not contain a return echo that has passed the threshold test.

If the return echoes in Figure 26 are passed through the threshold detector and quantiser as shown in Figure 27, the following coded version of the sea volume cross section results (Figure 28); 0's have been omitted.

												Range Cell #
												1
												2
				1		1				1		3
												4
												5
						1						k-4
1	1	1	1	1	1		1	1	1	1	1	k-3
												k-2
												k-1
												k
Ping #	1	2	3	4	5	...	n-5	n-4	n-3	n-2	n-1	n

Coded Version of the Sea Volume

FIGURE 28

Each encoded return is stored sequentially in memory. This process continues until the memory is full and n returns are stored. The next return to be stored is written over the earliest return resident in memory, and this updating sequence is continued for each new return. The memory thus contains the last n returns that were received.

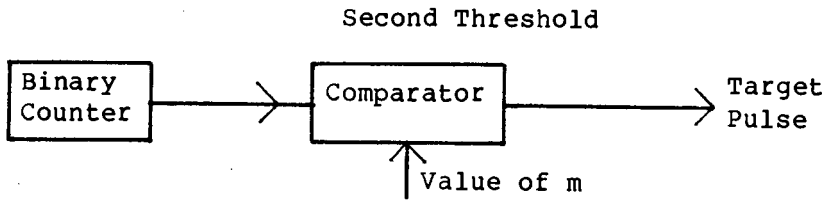

Block Diagram of m out of n Detector

FIGURE 29

Figure 29 is a block diagram of the m out of n detector. The contents of n range cells, of the same range, are counted and compared with a preset value m. If the sum is greater than m then a target pulse is sent.

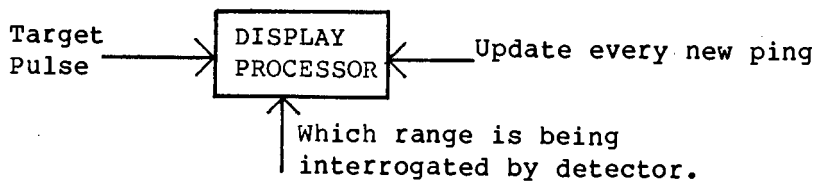

Block Diagram of Display Processor

FIGURE 30

The target pulse is sent to the display processor as shown in Figure 30. The display is updated every ping and the processor displays the range at which the target pulse was received.

4.7.4 DEPTH SOUNDER PARAMETERS

The described system has been realised using analogue and digital techniques. The following parameters apply:

(a) The depth sounder is a self-contained unit that can either stand alone and display depth via a 4-digit display or be interfaced to the HP 85/86.

(b) The length of a range cell is variable. It has been set at 100mm. This is to comply with the metric system. It would be possible to have range cell set to fractions of a fathom, if this was desired.

(c) The number of range cells k = 1024. This number is adequate for the desired resolution. For the range cell length chosen the maximum readable depth is 102,4 metres. It can, though, be varied by changing the range cell length.

(d) The number of pings (water columns) in memory at one time is n = 16. A value of m = 10 was found to be adequate.

For a detailed circuit and control algorithm description see Appendix C.

REFERENCES

1. Tucker A.D., "Speed measurement at sea and sea bed characterization using correlation techniques", M.Sc. thesis, University of Cape Town (1983).

2. Skolnik M.I., "Introduction to Radar Systems", McGraw-Hill Book Company (1980), pp 388-390.

CHAPTER 5

5. RESULTS

5.1 CORRELATION EQUATION

In the context of the correlation log, the correlation coefficient is used to determine the degree of similarity between the sampled signals of the delayed reference receiver and the second receiver.

In the inter-intrapulse correlation log, the two-point difference method is used to determine the position of the peak of the spatial correlogram.

Two correlation coefficients are calculated, one using the sampled signals of the reference receiver and receiver 1, the other using the sampled signals of the reference receiver and receiver 2. The reference signal is delayed by one sample period. The sample period is altered, by either changing the IPP or by changing the second sample time within the return pulse, depending in which mode, inter or intrapulse, is used. The delay is adjusted until the two correlation coefficients are equal. The position of the peak of the spatial correlogram is then found midway between receiver 1 and receiver 2.

Let the sampled reference signal be $\{x_i\}$ and the sampled second receiver signal be $\{Y_i\}$ for i = to N + 1. These samples form (N + 1) data pairs. The extent of correlation with a delay of one sample period between data pairs may be estimated from the sample data by Equation 10[1].

$$\hat{\rho}_{xy} = \frac{\Sigma (x_i - \bar{x})(y_{i+1} - \bar{y})}{\left[\Sigma (x_i - \bar{x})^2 \; \Sigma (y_{i+1} - \bar{y})^2\right]^{1/2}}$$

$$= \frac{\Sigma x_i y_{i+1} - N\bar{x}\bar{y}}{\left[(\Sigma x_i^2 - N\bar{x}^2)(\Sigma y_{i+1}^2 - N\bar{y}^2)\right]^{1/2}}$$

$$= \frac{\Sigma x_i y_{i+1} - N\bar{x}\bar{y}}{\hat{\sigma}_x . \hat{\sigma}_y} \qquad \text{Equation 10}$$

Equation 10 is known as the normalised correlation coefficient. $\hat{\sigma}_x$ and $\hat{\sigma}_y$ are estimates of the variance of $\{x_i\}$ and $\{y_i\}$ respectively. The means $\bar{x}$ and $\bar{y}$ are calculated as follows:

$$\bar{x} = \frac{1}{N} \Sigma x_i \qquad \bar{y} = \frac{1}{N} \Sigma y_{i+1}$$

Due to the complexity of implementing the normalised correlation equation it was thought that Equation 10 could be simplified as follows:

(a) That the variance product $\hat{\sigma}_x.\hat{\sigma}_y$ could be ignored as the variance is not expected to vary from one data set to another. Hence it performs a scaling function in Equation 10.

(b) That the mean product $N\bar{x}\bar{y}$ could be ignored as the mean is not expected to vary from one data set to another. Hence it performs an offset function in Equation 10.

The simplification result in a correlation equation of the form:

$$\text{correlation result} = \Sigma x_i y_{i+1} \quad \text{Equation 11.}$$

5.2 HARDWIRED CORRELATOR PERFORMANCE

The hardwired correlator used in the inter-intra pulse correlation log performs a correlation based on Equation 11. The number N of sample pairs is limited to 16. It was thought at the time that this number would be sufficient to obtain a reliable estimate of the mean and the variance. The simplifications used to derive Equation 11 from Equation 10 would then hold. Two correlation results are obtained from the hardwired correlator for the sampled signals from the receiver pairs (REF and REC1) and (REF and REC2)

5.2.1 WATER TRIALS

The inter-intrapulse correlation log system was tested in its construction stages in the CAL tank and Civil Engineering flume tank at UCT. The constituent elements were found to work according to specification.

Water trials were performed on the sonar raft moored at the Simonstown reservoir. The water bottom is composed mostly of mud and silt. The average water depth was five metres. The depth sounder that is part of the correlation log system was checked against a commercial depth sounder and the two depth readings were always found to tally.

The sonar raft is ideal for speed measurement tests. This is because a section of the deck between the pontoons that provides floatation has been cut away. The cut away section is in the form of a rectangle open to the water. On the edges of the rectangle rails have been laid upon which a trolley rests. The trolley can be moved up and down this rectangle of water. When the transducer assembly is mounted on the trolley, the trolley is moved at constant speed and the system processor computer program is run.

Due to the shallow water and the low speeds that can be attained the interpulse mode was tested. The speed was kept relatively constant at 0,5m/s. By interacting with the computer program, the IPP was varied from 10ms to 60ms and the two correlation results were printed. The separation of the receive transducer pairs (REF and REC1) and (REF and REC2) was 48mm and 60mm respectively.

5.2.2 HARDWIRED CORRELATOR RESULTS

It was found that there was no trend, as the IPP changed, that one of the correlation results would grow bigger and then smaller that the other correlation result. This is what one would expect if one considers Figure 21 of Chapter 4 Section 4.5.3.

An explanation for these poor results is found if one considers that the hardwired correlator is based on a simplified version of Equation 10. With only 16 samples the estimates of $\hat{\sigma}x.\hat{\sigma}y$ and $N\bar{x}.\bar{y}$ do vary from one data set to another. This was found to be true when the software correlator's (which modelled Equation 10) results were analysed. The estimates do not just perform a scaling and offset function and hence the simplification breaks down for a small number of samples.

If the sample size were large enough so that true estimates of the variance and mean could be obtained, the Equation 11 could be used in the hardwired correlator.

It is evident that the hardwired correlator was based on simplifications that are not valid for small sample sizes. A software correlator was designed (see Appendix A Section 4.2) to model the hardwired correlator and to implement the normalised correlation equation (Equation 10). In replacing the hardwired correlator, the correlation results are not given in real time. This is due to the slowness of the HP 86 which was used the implement the correlator.

5.3 SOFTWARE CORRELATOR

The software correlator was implemented as follows:
The Biomation waveform recorder's four inputs were connected as follows: One input recorded the transmitter gating pulses from the correlator system. The other three parts recorded the REF OUT, REC1 OUT and REC2 OUT analogue signals from the correlator system. The Biomation performs a 12 bit A/D on these inputs. The resultant digital words are downloaded to the software correlator (the HP 86) via a second BCD interface with interface code 4.

The system processor now controls the Biomation, depth sounder and correlator system via the HP86 running the AUTOLOG program (see Appendix A Section 4.2)

5.3.1 TANK TESTS

With the software correlator incorporated, the inter-intrapulse correlation log was set up in the CAL tank at UCT. The tank used has a gantry on which the transducer assembly was mounted. The gantry can be moved the length of the tank and in this way a fairly constant velocity can be obtained. The gantry was pulled along by a length of cord attached to a weight. The cord passed through a pulley-like arrangement so that when the gantry was let go the weight would drop to the floor pulling the cord and hence the gantry across the tank. The water resistance to transducer motion dampened the acceleration due to the weight, so that an approximately constant velocity of 1m/s was achieved.

The separation of the two receive transducer pairs is 12mm for (REF and REC1) and is 24mm for (REF and REC2). Consider the first receiver pair. The separation is 12mm and the velocity is 1m/s. By Equation 1 the time delay needed for maximum correlation is:

$$T = \frac{d}{2V} = \frac{12}{2} = 6\text{ms}$$

Thus an IPP of 6ms should give maximum correlation for the (REF and REC1) transducer separation. Similarly an IPP of 12ms should give maximum correlation for the (REF and REC2) transducer separation.

The two-point difference method used to find the peak of the spatial correlogram is based on the premise that if the correlation coefficients for two receiver displacements are the same then the peak of the spatial correlogram is found at a displacement:

$$d = \frac{X_1 + X_2}{2}$$

Consider the test situation where the two displacements are 12 and 24mm and the velocity is 1m/s:

$$d = \frac{12 + 24}{2} = 18\text{mm}$$

If the displacement is 18mm, the time delay needed to achieve maximum correlation is:

$$T = \frac{d}{2V} = \frac{18}{2} = 9\text{ms}$$

Thus at 9ms delay the correlation coefficients of the 12 and 24mm separation should be equal.

5.3.2 RESULTS

With the velocity held constant at 1m/s, the IPP was varied from 6ms to 25ms. Correlation results were calculated for each IPP. Table 1 lists the two

correlation coefficients COR1 and COR2 obtained using the transducer pairs (REF and REC1) and (REF and REC2) respectively. With the same data correlation results were calculated using Equation 11 (the simplified correlation equation used in the hardwired correlator) and Equation 12. Equation 12 is a simplified version of Equation 10 where the variance product $\hat{\sigma}_x.\hat{\sigma}_y$ is left out:

$$\text{Correlation result} = \Sigma x_i y_{i+1} - N\bar{x}\bar{y} \quad \text{Equation 12.}$$

5.3.3 ANALYSIS

The analysis of the results tabulated in Table 1 is as follows:

(a) Consider the normalised correlation coefficients calculated using Equation 10. The pertinent results are tabulated in Table 2.

	EQUATION 11		EQUATION 12		EQUATION 10	
IPP [ms]	COR1 x 10^2	COR2 x 10^2	COR1	COR2	COR1	COR2
6	5037	4766	3540	1244	0,911	0,365
7	6159	600	9668	8345	0,937	0,755
8	5505	5401	6789	4696	0,878	0,549
9	7330	7122	5998	7291	0,870	0,871
10	5595	5622	5160	5591	0,787	0,776
11	6343	6509	2621	3258	0,698	0,762
12	5185	5211	2570	6180	0,532	0,933
13	6172	6082	3877	5040	0,474	0,638
14	7698	7542	3590	3909	0,652	0,845
15	5737	5903	1513	5816	0,295	0,876
16	5423	5290	1581	3317	0,425	0,735
17	5330	5306	2201	2964	0,571	0,672
18	4858	4821	894	3807	0,213	0,795
19	6347	6246	1272	5436	0,211	0,778
20	4881	4827	1919	2674	0,548	0,678
21	5330	5641	-3287	4823	-0,401	0,708
22	6586	6591	1983	4188	0,359	0,650
23	5361	5459	782	2704	0,178	0,650
24	5485	5359	1921	3229	0,421	0,571
25	6638	6469	-1058	541	-0,142	0,054

TABLE 1

A table of results obtained from the software correlator for different IPP and at a velocity of 1m/s.

$$\hat{\rho}_{xy} = (\Sigma x_i y_{i+1} - N\bar{x}\bar{y}) / (\hat{\sigma}_x \hat{\sigma}_y) \qquad \text{Equation 10}$$

$$\text{correlation result} = \Sigma x_i y_{i+1} - N\bar{x}\bar{y} \qquad \text{Equation 12}$$

$$\text{correlation result} = \Sigma x_i y_{i+1} \qquad \text{Equation 11}$$

PARAMETER	PREDICTED IPP [ms]	RECORDED IPP [ms]
COR1 MAX	6	7
COR2 MAX	12	12
COR1 = COR2	9	9

TABLE 2

The predicted results of Section 5.3.1 and the recorded results agree very well. The trend of:

COR1 > COR2 for IPP < 9ms

COR1 = COR2 for IPP = 9ms

COR1 < COR2 for IPP > 9ms

is readily apparent.

(b) Consider the normalised correlation coefficients calculated using Equation 10 and the correlation results obtained using Equation 12. The correlation result using Equation 10 and 12 follow the same trend. The correlation results using Equation 12 do not convey any information as to the degree of correlation. These results do not exhibit a constant scaling factor when compared with the results of Equation 10. This shows that the sample size is too small to obtain a true estimate of the variance $\hat{\sigma}_x$ and $\hat{\sigma}_y$.

The results obtained using Equation 12 show that the correlator based on Equation 12 cannot be used to adjust

the time delay T in the feedback loop of the two-point difference method.

(c) Consider the normalised correlation coefficients calculated using Equation 10 and the correlation results obtained using Equation 11. The correlation results using Equation 10 and 11 do not follow the same trend.

The results of Equation 11 do not exhibit a constant offset when compared with the results of Equation 12. This shows that the sample size is too small to obtain a true estimate of the mean $\bar{x}$ and $\bar{y}$. The hardwired correlator based on Equation 11 has been shown in this software model to be non-viable. This is due to the limited sample size.

Like the software correlator based on Equation 12, a correlator based on Equation 11 will not convey information as to the degree of correlation. It cannot then be used to adjust the time delay in the feedback loop of the two-point difference method.

5.3.4 SUMMARY

The normalised correlation coefficient (that using Equation 10) must be used as the basis of the correlator of the inter-intrapulse correlation log. The two-point difference method has been shown to be a viable working system when using normalised correlation coefficients.

5.4 NUMBER OF SAMPLES

The number of samples used in the normalised correlation coefficient calculation has a direct relationship to whether a non-zero correlation coefficient reflects a statistically significant correlation. The number of samples used was N = 16.

To determine the value of $\hat{\rho}xy$ that gives a statistically significant correlation for N = 16 one tests the hypothesis that $\hat{\rho}xy = 0$. If this hypothesis is rejected then a significant correlation is indicated.[1]

The acceptance region for the hypothesis of zero correlation is given by

$$-z_{\alpha/2} \leq \frac{\sqrt{N-3}}{2} \ln\left[\frac{1+\hat{\rho}xy}{1-\hat{\rho}xy}\right] \leq z_{\alpha/2} \qquad \text{Equation 13}$$

where Z is the standardized normal variable. Values outside the above interval would indicate statistical correlation at the α level of significance.

For the 95% level of confidence that the negative hypothesis will hold $Z_{\alpha}/2 = 1.96$. Rearranging the above inequality and replacing $Z_{\alpha}/2$ by 1.96 and N by 16, the negative hypothesis will not hold if $\hat{\rho}_{xy} > 0,5$. So for all correlation coefficients $\hat{\rho}_{xy} > 0,5$ the correlation is statistically significant.

From this analysis it can be seen that the correlator must use many more samples than 16 in its calculation. This is so that correlation coefficients $\hat{\rho}_{xy} \leqslant 0,5$ need not be rejected as not statistically significant.

5.5 CONCLUSIONS

(a) The system concepts of the inter-intrapulse correlation log have been shown to be sound.

(b) The results obtained have shown that the hardwired correlator based on the correlation equation of multiplying and summing, without normalisation, is not viable.

(c) Replacing the hardwired correlator with a software correlator, whose correlation coefficients are normalised, has shown that the two-point difference method is a viable means of determining the peak position of the spatial correlogram.

The depth sounder that is part of the inter-intrapulse correlation log system performed depth readings accurately and consistently under widely varying sea bed characteristics.

5.6 FURTHER WORK

(a) For the inter-intrapulse correlation log to perform consistently in real-time a dedicated normalising correlator needs to be built. The number of samples used in the correlation must be much greater than 16. It is envisaged that this number should be 16^2 or greater. This would mean that statistical validity could be given to low correlation coefficients. The correlator should be made from a dedicated micro-processor that has facilities for high speed multiplication. The hardwired correlator board could be replaced by the correlator-microprocessor board and in this way leave the other elements of the system unchanged. This construction work is unfortunately out of the range of this M.Sc. because of the time factor involved.

(b) The control problems involved in implementing a negative feedback control loop for the two-point difference method have to be investigated. The envisaged controller should be in the form of a

proportional, integral and differential (PID) controller. The problem of initial conditions for cold starts and the associated strategy needs to be looked into.

(c) The accuracy of the inter-intrapulse correlation log needs to be examined. Work must be performed to ascertain if the geometric centres of the transducers match the acoustic centres. Also an investigation is needed to determine whether the acoustic centres change with time or physical operating conditions.

(d) The depth sounder has not been tested to see if it will reject fish shoal returns and give reliable depth readings. It is envisaged that these tests could be performed in a large tank where fish can be introduced. The other possibility is to go to sea and find a fish shoal and take depth readings.

REFERENCE

1. Bendat J. and Piersol A. , "Random Data. Analysis and Measurement Procedures", pp 126-129.

CHAPTER 6

6. CONCLUSION

The inter-intrapulse correlation log is an instrument that measures ship speed relative to the sea bed. It utilises a transducer assembly, consisting of a single circular transmitter and four closely spaced receivers. The transducers point vertically downwards at the sea bed. Tone bursts are transmitted at the sea bed and the resultant backscatter is received by the receive array. The beamwidth of the transmit transducer is large and so a low operating frequency can be employed. Because the attenuation of acoustic signals is less for low frequencies than for high frequencies, and that the transmitter transmits vertically at the sea bed, the correlation log can operate at great depth.

With the transducer assembly moving relative to the sea bed, the envelope detected returns from two receivers will be identical except for a time shift T. If this time shift T and the separation of two receivers d is known then the ship velocity can be calculated using the equation $V = d/2T$.

A number of alternate proposals have been suggested, as to the manner in which knowledge of T and d can be attained. The proposals' pro's and con's have been discussed and the one that looks like giving the most accurate measurement of speed for all operating depths is the inter-intrapulse correlation log. It is a combination of the temporal and spatial correlation log. The operating principle is to have two receivers at spacings X_1 and X_2 from a reference receiver. A search is undertaken to find the time shift T that gives the same correlation between the reference receiver and receiver 1 and between reference receiver and receiver 2. It can then be assumed that the peak of the spatial correlation function is found midway between receivers 1 and 2 at a distance $d = (X_1 + X_2)/2$ from the reference receiver.

The inter-intrapulse correlation log has two modes of operation. The mode in use depends on the velocity that is to be measured and the operating depth. The interpulse mode is used for low velocity and shallow depth situations. In this mode the return pulse is sampled once on all receivers and the delay T is imposed by delaying the sampled reference signal by one interpulse period.
The intrapulse mode is used for high velocity and large depth situations. In this mode the return pulse is sampled twice on all receivers, and the delay T is imposed by delaying the first sample of reference signal by a time equal to the time between sample pairs.

The inter-intrapulse correlation log was designed and constructed. As the depth parameter plays such a crucial role in the operating system, a depth sounder was designed and built. This depth sounder can not

only provide a digital read-out of depth accurate to 10cm, it also has the facility to reject strong mid-water return signals (for example fish shoals).

Water trials of the inter-intrapulse correlation log have shown that the system is viable. It automatically sets up the pulsed transmission and sampling functions for varying depths. The hardwired correlator which is based on the simplified correlation coefficient equation, did not give valid results. Investigation of the correlation equation which culminated in a software correlator showed that the simplifications were erroneous for a small sample size. The software correlator results using the normalised correlation coefficient showed that the two-point difference method (which is the basis of the inter-intrapulse correlation log), is a viable means of determining the position of the peak of the spatial correlogram.

The minor modification of replacing the present correlator board, with a correlator board that performs a normalised correlation coefficient function, should result in the constructed correlation log being able to measure in real time ship speed relative to the sea bed, for all ranges of speed and depth.

APPENDICES

APPENDIX A

SYSTEM PROCESSOR

CONTENTS

1. INTRODUCTION

1.1 COMPUTER CHOICE

The computer used for the system processor is the HP 85/86. It was chosen for its ease of use and its availability. The programming language is BASIC, and so it is a fairly slow machine (an average line of BASIC is executed in about 4ms). For real time operation, all high speed functions (correlation for example) are hardwired.

1.2 BLOCK DIAGRAM

The system processor consists of three elements:

(a) the HP 85/86;

(b) the BCD interface;

(c) the computer interface.

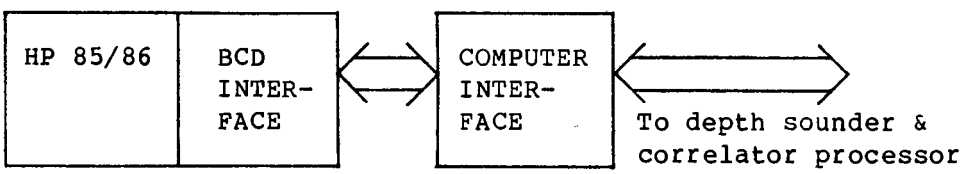

System Processor Block Diagram

FIGURE A-1

1.3 ALGORITHM

The system processor implements the system algorithm in software. As mentioned in Chapter 4, the open loop algorithm

was implemented first. Analysis of the open loop results showed the need for modifications to the hardwired correlator. A software correlator was implemented and unfortunately time did not permit a hardwired version to be built and the closed loop algorithm to be realised.

The open loop algorithm is as follows:

ALGORITHM

(1) Start;

(2) Input delay T and mode;

(3) Run depth sounder;

(4) Read depth;

(5) Calculate mode parameters;

(6) Write mode parameters to correlator subsystem;

(7) Run correlator;

(8) Read correlator results;

(9) Display correlator results;

(10) Stop.

1.4 DESCRIPTION OF SYSTEM ELEMENTS

(a) The HP 85/86

The HP 85 and HP 86 are identical in their operating systems and so programs written for the HP 85 can be run on the HP 86. The advantage of having two machines

running the same programs is that they can be used for different environments.

The HP 85 has its mass storage medium (tape), VDU and printer built into the machine. As such it is highly portable and can be used in tests outside the laboratory (for example at sea or in a reservoir).

The HP 86 is used in the laboratory where portability is not important.

The HP 85/86 does not have any direct interfacing capabilities. It does, however, have a series of slots where peripherals may be inserted. The peripheral used to interface the HP 85/86 to the rest of the system processor is the BCD interface.

(b) **The BCD Interface**

The BCD interface is used to INPUT and OUTPUT digital words and control commands to and from the HP 85/86. It has a limited bus capacity and latching facility and so a computer interface is needed to perform these functions.

(c) **The Computer Interface**

The computer interface is a hardwired digital board that provides bus facilities. These facilities include latching, tri-state switching and timing compatability between the BCD interface and the rest of the system.

1.5 MODE PARAMETERS

1.5.1 TIMING

All system timing is generated by counters. These counters are loaded with their respective binary words and then clocked down at a fixed frequency until their respective borrow conditions exist.

The maximum envisaged time interval that is to be generated is 255ms. This can be achieved by an 8 bit word being loaded into a counter and counted down at a frequency of 1kHz.

The problem of poor fractional accuracy is encountered when small time periods are measured (say less than 25ms). This problem is critical because the measured velocity is directly related to the delay T and hence the measured velocity will also suffer from poor fractional accuracy.
A solution is to examine and modify the proposed timing interval so as to improve the fractional accuracy.

An algorithm that describes the decision process necessary to improve fractional accuracy is as follows:

ALGORITHM

(1) Examine a mode parameter.

(2) Is mode parameter greater than 25ms?

(3) If it is, then set counter clock to 1kHz. If it is not, then multiply mode parameter by ten and set counter clock to 10kHz.

(4) Are there more mode parameters to examine?

(5) If there are more, then call next mode parameter and go to (2). If there are no more, then go to (6)

(6) Stop.

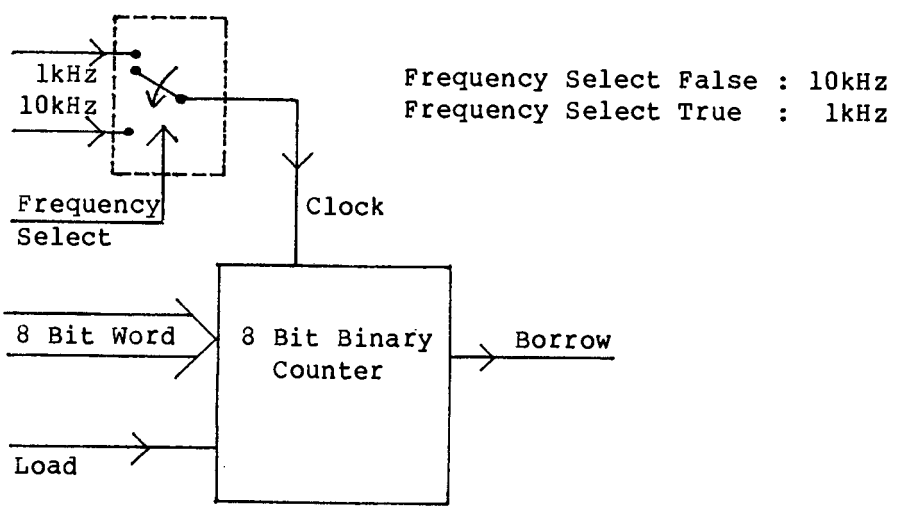

Block Diagram of Typical Mode Parameter Timer

FIGURE A-2

1.5.2 PARAMETERS

A mode parameter is described by the following:

(a) An 8 bit word that specifies its value;

(b) A 1 bit word that specifies the frequency at which the time interval is measured.

Depending on the mode, inter or intrapulse, there are three or four parameters that have to be described.

INTER	INTRA
Period (Pulse Length) Mark Sample	Period Mark Sample Delay

Which mode is in use, is indicated by the MODE line.

1.6 CONTROL AND STATUS LINES

To control the depth sounder and correlator, the system processor needs the following:

(a) Lines whereby the depth sounder or correlator subsystem is told to begin its assigned function. The lines are called the PING and GO line, respectively.

(b) Knowledge of the status of the depth sounder or correlator subsystem (i.e. busy or free) is needed to ensure that the read or write sequence of the system processor occurs at the right time.

1.7 DEPTH READING AND CORRELATION RESULTS

The system processor reads the depth from the depth sounder via a 16 bit BCD word called DEPTH. The two correlation results are read from the correlator subsystem via two 8 bit binary words called COR1 and COR2.

1.8 SUMMARY

The digital words and control lines that the system processor inputs and outputs are as follows.

WORDS		CONTROL LINES	
INPUT	OUTPUT	INPUT	OUTPUT
COR1 COR2 Depth Status	Period Mark Sample Delay Frequency		Ping Go Mode

2. BCD INTERFACE

2.1 DESCRIPTION

One of the peripherals the HP 85/86 uses to input/output is the BCD interface. The interface plugs into the back of the

computer and two cables, A and B, are provided. The interface can be configurated in many ways (either by software or by a set of internal switches).

The configuration used is as follows:

Ten 4 bit BCD ports P_0 - P_9;

One 1 bit I/O A line; One 1 bit CTL A line;

One 1 bit FLG A line;

One 4 bit special BCD port P_{10}.

These lines are found in cables A and B which are terminated in 37 pin Cannon D type connectors.

2.2 BINARY TO DECIMAL AND DECIMAL TO BINARY CONVERSION

Denote a 4 bit binary word as $W = w_3w_2w_1w_0$ and its decimal equivalent D, which has a value 0 - 15.

Input

The interface is configurated for one 4 bit port. Input the word W via the port:

```
INPUT 3; A$
```

The interface interprets the binary code as a BCD code and assigns the BCD code an ASCII representation. The string A$ is the ASCII code for W. The ASCII codes are assigned as in Table A-1. Positive logic is used for port lines.

BCD CODE	ASCII CODE	DECIMAL EQUIVALENT OF ASCII CODE
0000	0	48
0001	1	49
0010	2	50
0011	3	51
0100	4	52
0101	5	53
0110	6	54
0111	7	55
1000	8	56
1001	9	57
1010	:	58
1011	;	59
1100	<	60
1101	=	61
1110	>	62
1111	?	63

TABLE A-1

If one converts the ASCII code into its decimal equivalent and subtracts 48, then the binary word W is converted by the interface so that the computer reads it in decimal form.

In BASIC the input and conversion is as follows:

```
INPUT 3; A$
D = NUM(A$) - 48
```

An example is $W = 1000_2$, $D = 8_{10}$

and $W = 1111_2$, $D = 15_{10}$.

If the binary word is greater than 4 bits, then examine each 4 bit nibble separately and reconstruct the decimal equivalent.

Denote the 8 bit word as R = $r_7r_6r_5r_4r_3r_2r_1r_0$.

R has a most significant nibble X = $r_7r_6r_5r_4$ and a least significant nibble W = $r_3r_2r_1r_0$.

The decimal equivalents of X and W are D2 and D1, respectively.

The word R thus has a decimal equivalent of D = D1 + 16*D2.

Output

The interface is configured for one 4 bit port. To output the decimal value D via the interface, D has to be converted to its corresponding ASCII form. If A$ is the ASCII value, then:

```
A$ = CHR$(D + 48)
```

and it is output via the statement

```
OUTPUT 3; A$
```

The interface interprets the ASCII string and outputs the corresponding BCD code (which is the binary word W) to the port.

The interface is configured for two 4 bit ports. If the decimal value X is less than or equal to 255, then the number is converted to two 4 bit nibbles.

Let Y = X/16,

Also D1 = (Fractional part of Y) * 16,

D2 = Integer part of Y,

and A$ = CHR$(D2 + 48) and CHR$(D1 + 48).

This string is then output via the statement

```
OUTPUT 3; A$
```

The interface interprets the ASCII string and outputs the

corresponding BCD code to the two ports. The port with the lowest number receives the most significant nibble and the port with the higher number receives the least significant nibble.

The words that are input and output in this manner are:

INPUT	OUTPUT
COR1 COR2	Period Mark Sample Frequency

2.3 BCD TO DECIMAL CONVERSION

The 16 bit BCD word from the depth sounder is read by the interface as follows:

Four 4 bit ports are configured P_0, P_1, P_2 and P_3. The most significant nibble of the DEPTH word is assigned to P_0 and the least significant nibble to P_3.

The DEPTH word is input via:

```
INPUT 3; A$
```

The ASCII string is made up of four characters which are the ASCII equivalent of the four BCD nibbles from the four ports. Each character is converted to its decimal equivalent as in Table A-1 and then by subtracting 48 from each decimal equivalent, the computer reads each BCD nibble in decimal form.

The four decimal values are combined in order of significance.

The individual ASCII characters are extracted from the string A$ as follows:

most significant	:	A$[1,1]
second most significant	:	A$[2,2]
third most significant	:	A$[3,3]
least significant	:	A$[4,4]

The corresponding decimal values are as follows:

```
D1 = NUM(A$[1,1]) - 48
D2 = NUM(A$[2,2]) - 48
D3 = NUM(A$[3,3]) - 48
D4 = NUM(A$[4,4]) - 48
```

These are combined to form the decimal depth value D as follows:

```
D = D1*100 + D2*10 + D3 + D4*0.1
```

2.4 MECHANISM OF INPUT AND OUTPUT

The interface is configured for a trailing edge handshake. There are three handshake lines: I/O A, CTL A and FLG A. Trailing edge refers to the CTL line going false on the trailing edge of the FLG line going false. Refer to Figures A-3 and A-4 where input and output sequences are described.

Input

For an input from the depth sounder or the correlator subsystem, the interface drives the I/O A line false. To initiate the transfer, the interface sets the CTL A line true. The computer interface responds by setting FLG A line true. FLG A line is the output from a monostable that is triggered by the CTL A line. The period of the monostable pulse is 80μs, which is much greater than the 15μs minimum FLG duration. On the trailing edge of the FLG A line, the interface drives CTL A false, inputs the data and sends it to the HP 85/86.

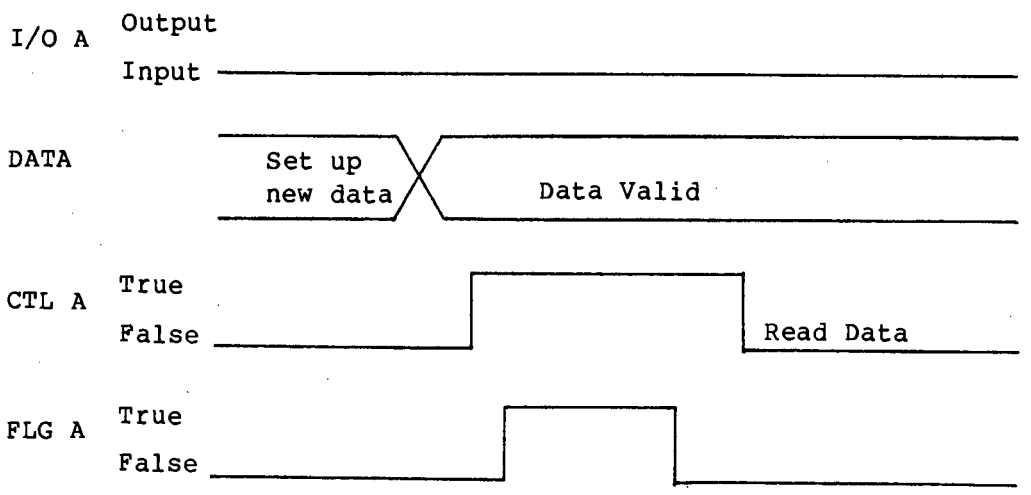

Input Handshake Timing

FIGURE A-3

Output

For an output to the depth sounder or correlator subsysytem, the BCD interface drives the I/O A line true. The HP 85/86 places the data on the lines of the ports prior to the handshake. When all the data is ready, the BCD interface sets the CTL A true. The computer interface responds by setting FLG A line true. FLG A line is the output from a monostable that is triggered by the CTL A line. The period of the monostable pulse is 80μs which is much greater than the 15μs minimum FLG duration. On the trailing edge of the FLGA line, CTL A line is driven false and the HP 85/86 can then send a LATCH command to the computer interface to latch the data present at the ports.

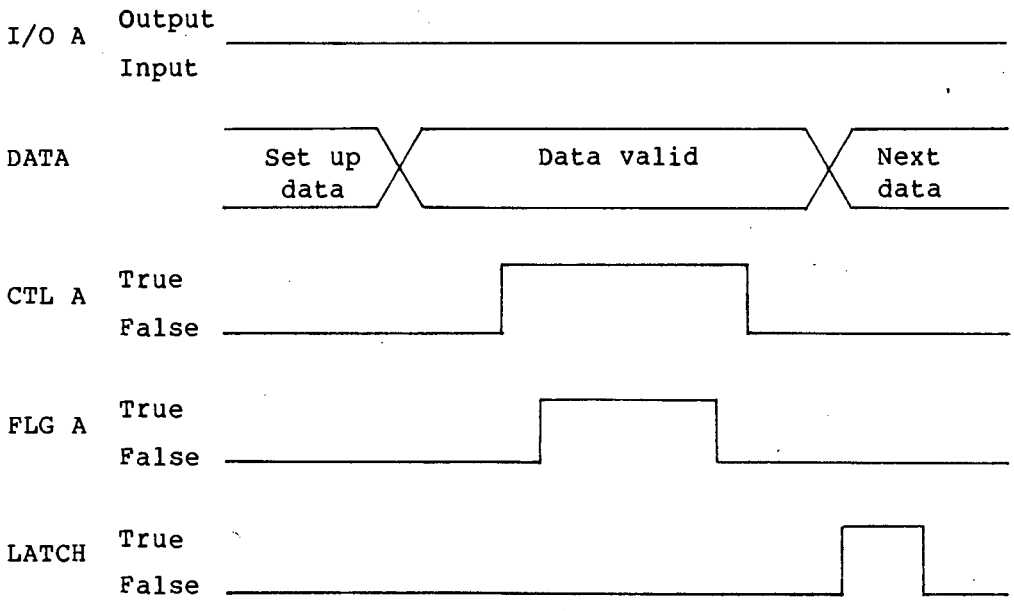

Output Handshake Timing

FIGURE A-4

2.5 CONFIGURATION

2.5.1 BCD INTERFACE REGISTERS

The BCD interface has 11 registers of interest that control reading and writing sequences. The registers may be set by software or by hardwired switches. The registers are as follows:

Register 0: This register has the value 3 indicating that the peripheral is the BCD interface.

Register 1: This register has the value 0 indicating that the interrupt facilities are not used.

Register 2: This register specifies input or output as well as the value of Port 10.
For input the register has the value 0.
For output the register has the value 128 plus whatever value the 4 bit Port 10 has.

Register 3: This register indicates how many mantissa digits are specified for each channel.
Only channel A is used with 10 mantissa digits. The value of this register is 10.

Register 4: This register indicates how many exponent digits are specified for each channel. No exponent digits are required. The value of this register is 0.

Register 5: This register indicates how many function digits are specified for each channel. No function digits are required. The value of this register is 0.

Register 6: This register indicates how many mantissa digits to the right of the decimal point are specified. No decimal point is required. The value of this register is 0.

Register 7: This register indicates the logic sense of the control and handshake lines. Positive-true logic sense is required. The value of this register is 0.

Register 8: This register indicates the logic sense of each bit of the data digits in each channel. Positive-true logic sense is required. The value of this register is 0.

Register 9: This register indicates the logic sense of each bit of the function digits in each

channel. Positive-true logic sense is required. The value of this register is 0.

Register 10: This register indicates the logic sense of sign bits and Port 10 data bits. The sign bits are irrelevant as they are not used. The Port 10 bits logic sense are set according to which mode (inter or intra-pulse) is used. The value is either 7 for inter or 15 for intrapulse.

2.5.2 Port 10 and the PING, GO, LATCH and Mode Lines

Port 10 is used to output the following control lines: PING, GO, LATCH and MODE.

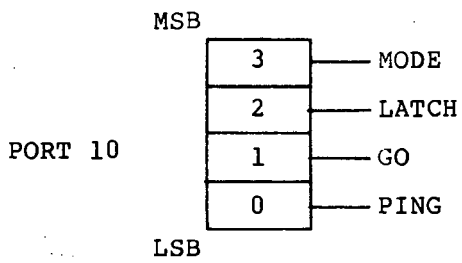

Port 10 Configuration

FIGURE A-5(a)

They are switched in software as follows:

(a) **Mode**

The MSB of Port 10 is always reset to 0. Interpulse mode is indicated by the MODE line being false and

this is generated by all the bits except the MSB of Port 10 having negative-true logic. In software REGISTER 10 is set to 7.

Intrapulse mode is indicated by the MODE line being true and this is generated by all the bits of Port 10 having negative-true logic. In software REGISTER 10 is set to 15.

MODE	True	REGISTER 10 = 7	REGISTER 10 = 15
	False		

Mode Indicator

FIGURE A-5(b)

(b) **PING, GO and LATCH**

As negative-true logic is applied to the three least significant bits of Port 10, they will be true unless they are set, in which case they will be false.

PING and GO lines are accessed in software as follows:

ASSERT 3; X

X = 1 for Port 10 bit 0 to be set - PING line.

X = 2 for Port 10 bit 1 to be set - GO line.

The LATCH line is used to trigger latches in the computer interface to latch output data from the

BCD interface. Hence the BCD interface must be configured for output mode.

The LATCH line is accessed in software by

ASSERT 3; X + 128

Note: 128 indicates output mode.

X = 4 for Port 10 bit 3 to be set - LATCH line.

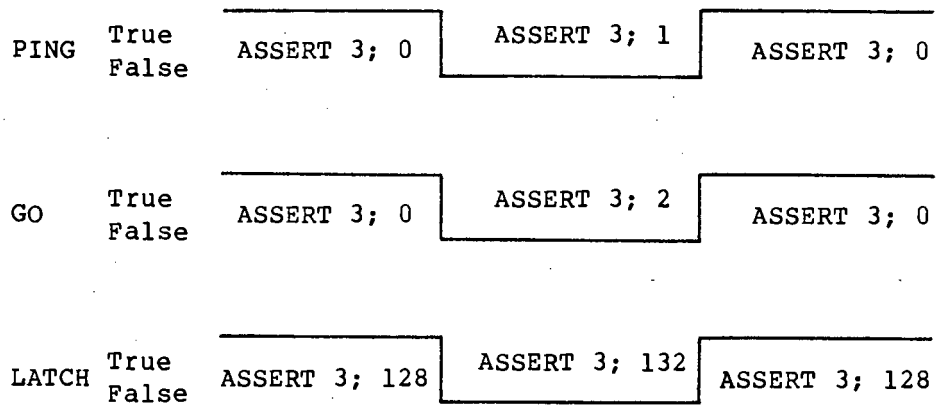

PING, GO and LATCH Switching

FIGURE A-5(c)

2.5.3 STATUS WORDS

The two status words, one from the depth sounder and one from the correlator processor, are not treated numerically, but as a character string. Consider a 4 bit STATUS word.

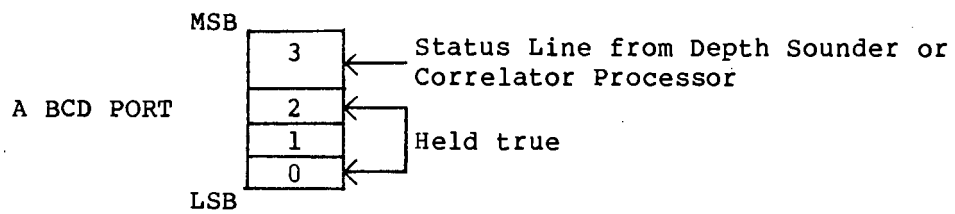

STATUS Word

FIGURE A-6

Assume the BCD interface is configured for one port. The MSB is the STATUS line. If the other three bits are held true, then on input of the word via the port; INPUT 3; A$, the string A$ can take on one of two characters:

either a '?' which indicates free STATUS,

or a '7' which indicates busy STATUS.

These conditions are easily checked in software.

2.5.4 PORT ALLOTMENT

The BCD interface provides eleven 4 bit ports. They are allotted as in Table A-2. Input and output takes place on the same lines. The computer interface provides bus facilities to cope with this. The computer interface is described in Appendix A, Section 3.

PORT	INPUT		OUTPUT	
0	MSN§	COR 1	MSN	PERIOD
1	LSN	COR 1	LSN	PERIOD
2	MSN	COR 2	MSN	MARK
3	LSN	COR 2	LSN	MARK
4	MSN	DEPTH	MSN	SAMPLE
5	2nd MSN	DEPTH	LSN	SAMPLE
6	2nd LSN	DEPTH	MSN	DELAY
7	LSN	DEPTH	LSN	DELAY
8	Correlator	STATUS	-	-
9	Depth Sounder	STATUS	FREQUENCY	
10	-	-	PING, GO, LATCH, MODE	

§ MSN stands for Most Significant Nibble
LSN stands for Least Significant Nibble

TABLE A-2

3. COMPUTER INTERFACE

3.1 INTRODUCTION

The computer interface is a hardwired digital board that provides bus facilities to ensure compatability between the BCD interface and the other system elements.

The digital board is mounted in a robust box. Five Cannon-D connectors are provided for inter-bus connection. A block diagram of these connections is found in Figure A-7.

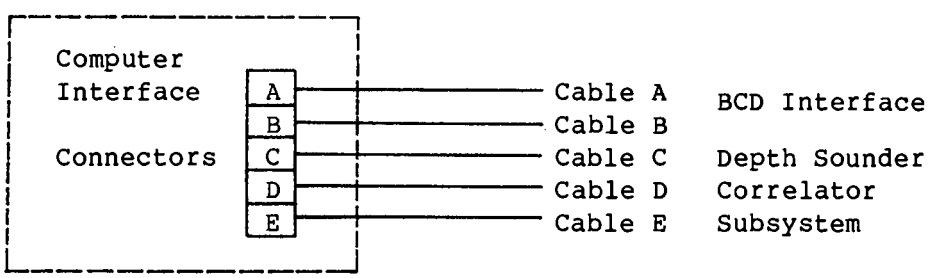

Connection Block Diagram

FIGURE A-7

Cables A and B are provided by the BCD interface and cables C, D, and E are made up of computer ribbon. These cables connect the computer interface to the depth sounder and correlator subsystem.

3.2 FLG A GENERATION

As was mentioned in Appendix A, Section 2.4, a flag line is needed to complete any data transfer for the BCD interface.

As the other system elements do not have facilities for a flag line, the computer interface provides one.

The FLG A line is generated by a monostable that is triggered by the CTL A line of the BCD interface. A block diagram of this is given in Figure A-8.

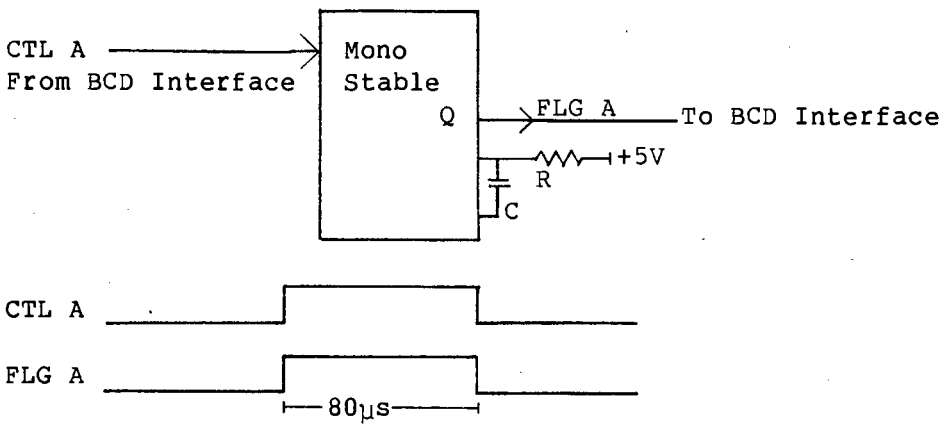

Block Diagram of FLG A Generator

FIGURE A-8

The pulse width of the monostable is set by the resistor-capacitor network. A value of 80μs was chosen. The value of the resistor is 1kΩ and of the capacitor 120pF.

3.3 BUS FACILITIES

Two bus facilities are required:

(a) going into tri-state mode;

(b) latching.

Let the BCD interface input the 8 bit word X and output the 8 bit word W, all on the same 8 bit bus. There will be a bus clash unless the word X is buffered by a tri-state buffer. On input the buffer will be transparent and on output the buffer will go into tri-state, thus preventing a clash. The I/O line of the BCD interface is used for this purpose. An 8 bit latch is used to latch the word W, initiated by a LATCH control line. A block diagram of the buffer and latch is shown in Figure A-9.

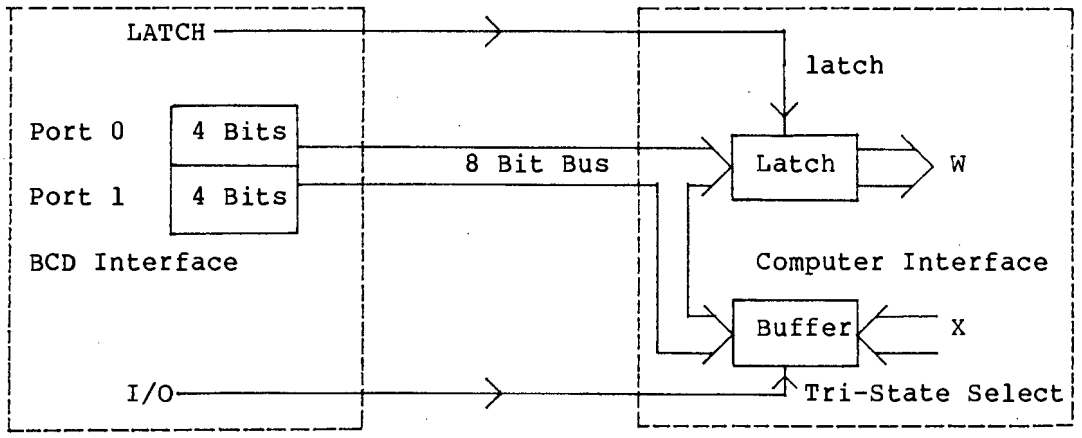

Block Diagram of Buffer and Latch

FIGURE A-9

There are five 8 bit busses like the one shown in Figure A-9 and the complete bus configuration is shown in Figure A-10. It was found that the LATCH line had a fan-out problem and this was solved by buffering it in the computer interface.

3.4 CIRCUIT DIAGRAMS

The circuit diagram and board layout is shown in Figure A-11. Table A-3 gives an explanation of the symbols used.

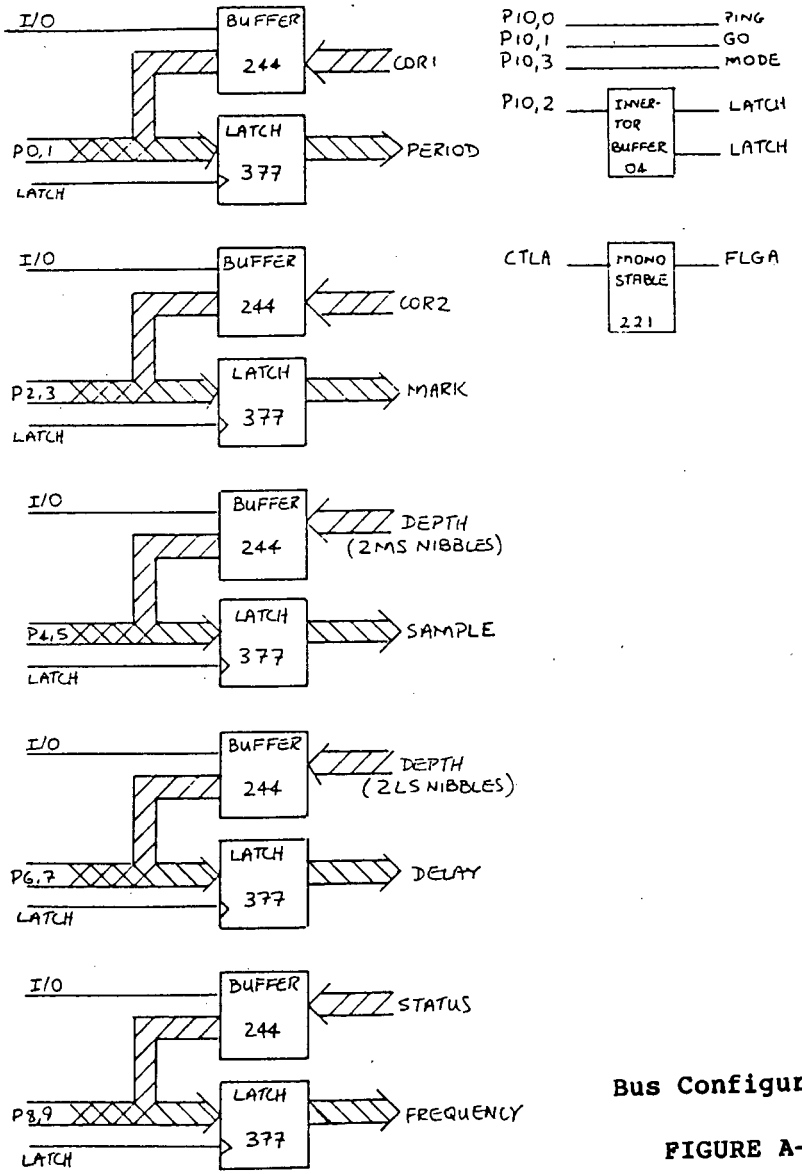

Bus Configuration

FIGURE A-10

CONNECTOR A

1	P4,0	P0,3	20
2	P4,1	P10,0	21
3	P4,2	P10,1	22
4	P4,3	P10,2	23
5	P3,0	P10,3	24
6	P3,1		25
7	P3,2		26
8	P3,3		27
9	P2,0		28
10	P2,1		29
11	P2,2		30
12	P2,3		31
13	P1,0		31
14	P1,1	I/O	32
15	P1,2		33
16	P1,3	FLG	34
17	P0,0	CTL	35
18	P0,1	GND	36
19	P0,2	GND	37

CONNECTOR C

1	D0		14
2	D1		15
3	D2		16
4	D3	GND	16
5	D4		17
6	D5		18
7	D6		19
8	D7		20
9	D8	S0	21
10	D9	PING	22
11	D10	D15	23
12	D11	D14	24
13	D12	D13	25

CONNECTOR B

1	P9,0	P5,3	20
2	P9,1		21
3	P9,2		22
4	P9,3		23
5	P8,0		24
6	P8,1		25
7	P8,2		26
8	P8,3		27
9	P7,0		28
10	P7,1		29
11	P7,2		30
12	P7,3		31
13	P6,0		32
14	P6,1		33
15	P6,2		34
16	P6,3		35
17	P5,0		36
18	P5,1		36
19	P5,2		37

CONNECTOR D

1	S4		20
2	S5		21
3	S6		22
4	S7		23
5	CR1,0		24
6	CR1,1		25
7	CR1,2		26
8	CR1,3		27
9	CR1,4		28
10	CR1,5		29
11	CR1,6		30
12	CR1,7		31
13	CR2,0		32
14	CR2,1		33
15	CR2,2	F7	33
16	CR2,3	F6	34
17	CR2,4	F5	35
18	CR2,5	F4	36
19	CR2,6	CR2,7	37

CONNECTOR E

1			20
2	GO		20
3	SM7	GND	21
4	SM6	PRD7	22
5	SM5	PRD6	23
6	SM4	PRD5	24
7	SM3	PRD4	25
8	SM2	PRD3	26
9	SM1	PRD2	27
10	SM0	PRD1	28
11	DL7	PRD0	29
12	DL6	M7	30
13	DL5	M6	31
14	DL4	M5	32
15	DL3	M4	33
16	DL2	M3	34
17	DL1	M2	35
18	DL0	M1	36
19	MD	M0	37

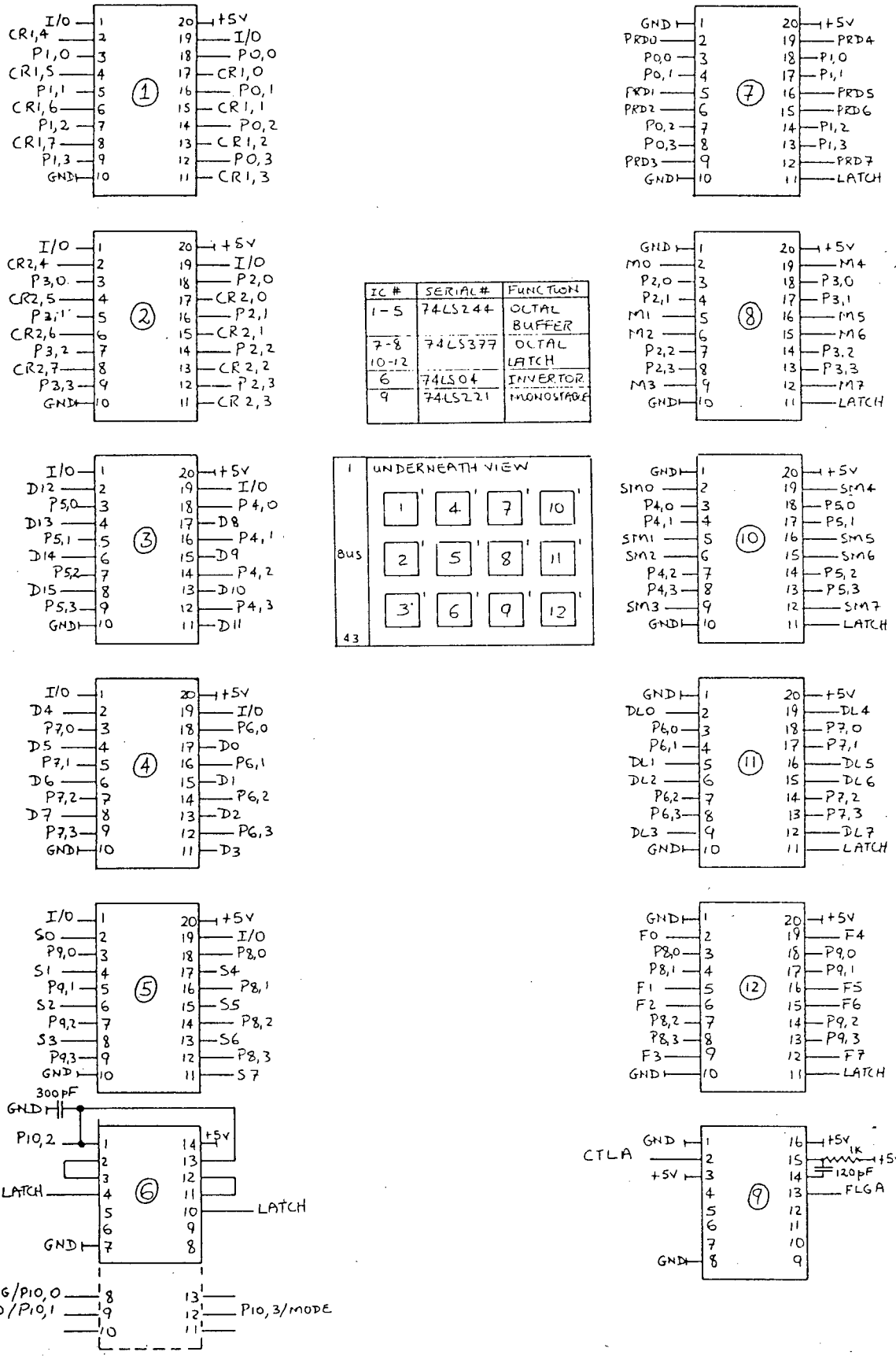

Computer Interface Board

FIGURE A-11

MNEMONIC	REFERS TO THE WORD	BIT #
D_X	Depth	x
S_X	Status	x
F_X	Frequency	x
$CR1_X$	Correlation Result 1	x
$CR2_X$	Correlation Result 2	x
PRD_X	Period	x
M_X	Mark	x
SM_X	Sample	x
DL_X	Delay	x

MNEMONIC	REFERS TO	BIT #
$P_{y,x}$	Port y	x

TABLE A-3

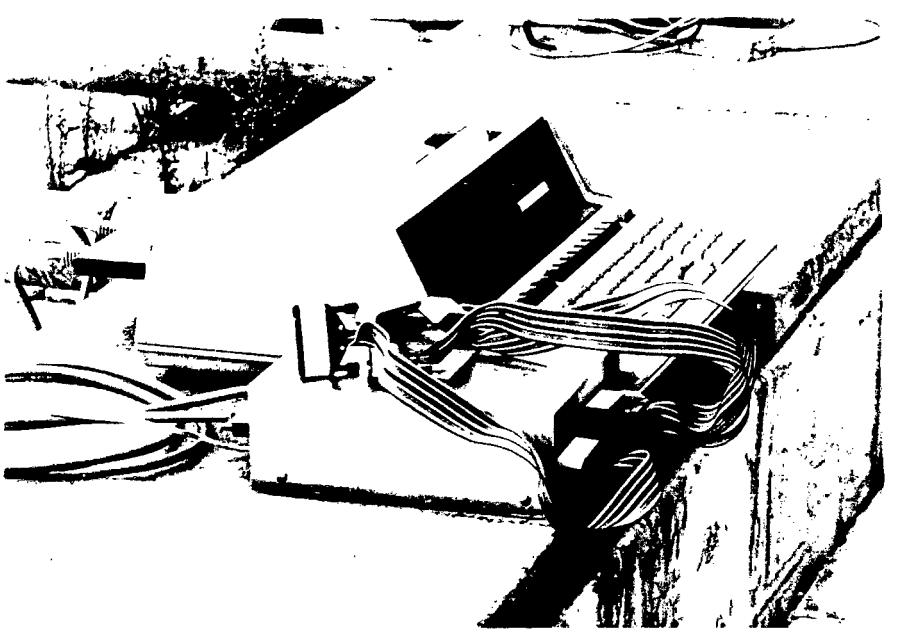

HP 85, BCD Interface and Computer Interface

FIGURE A-12

4. SOFTWARE

4.1 MENU

From the collection of programs written on the HP 85/86 for the correlation log, three are selected as general examples. The menu for these programs is as follows:

MENU	
PROGRAM NAME	DESCRIPTION
DEPTH	This program enables the HP 85/86 to obtain and display an updated depth reading from the depth sounder.
CORLOG	This program enables the HP 85/86 to implement the algorithm of Appendix A, Section 1.3 using the hardwired correlator.
AUTOLOG	This program enables the HP 85/86 to implement the algorithm of Appendix A, Section 1.3. The hardwired correlator's results are not read and the output of the correlator's receivers are stored on the Biomation data storage device. The stored samples are then read by the HP 85/86 via a second BCD-interface (interface code 4). The HP 85/86 performs a software correlation on the receive data and displays the results obtained.

4.2 LISTINGS

```
10 ! ************************************************
20 ! *                                              *
30 ! *                    DEPTH                     *
40 ! *                                              *
50 ! *  THIS PROGRAM GIVES A CONSTANT UPDATE ON DEPTH  *
60 ! *                                              *
70 ! ************************************************
80 SET TIMEOUT 3;1000
90 ON TIMEOUT 3 GOTO 260
100 OPTION BASE 1
110 DIM B(8)
120 CONTROL 3,2 ; 0,10,0,0,0,0,0,0,15
130 ASSERT 3;1
140 ASSERT 3;0
150 ENTER 3 ; B$
160 Z$=B$[10,10]
170 IF Z$="?" THEN 180 ELSE 150
180 ENTER 3 ; A$
190 FOR I=6 TO 9
200 B(I-1)=NUM (A$[I,I])-48
210 NEXT I
220 C3=B(5)*100+B(6)*10+B(7)*1+B(8)*.1
230 DISP C3
240 CLEAR
250 GOTO 130
260 BEEP
270 DISP "***TIMEOUT ERROR***"
280 END
```

```
10 ! ************************************************************
20 ! *                                                          *
30 ! *                        CORLOG                            *
40 ! *                                                          *
50 ! *          THIS PROGRAM FIRST FINDS THE WATER DEPTH        *
60 ! * CORRELATOR RESULTS ARE READ FROM CORRELATOR AND DISPLAYED *
70 ! *                                                          *
80 ! ************************************************************
90 OPTION BASE 1
100 DIM B(8),X(4),R(4),Y(5),E$[100]
110 DEF FNS$(N) = CHR$ (INT (N/16)+48)&CHR$ (FP (N/16)*16+48)
120 CLEAR
130 DISP "ENTER COMMENT"
140 INPUT E$
150 PRINT E$
160 CLEAR
170 DISP "INTER OR INTRA MODE R/A"
180 INPUT W$
190 IF W$="R" THEN Q=7 ELSE Q=15
200 CONTROL 3,2 ; 0,10,0,0,0,0,0,0,0
210 CLEAR
220 IF Q=7 THEN PRINT "INTER PULSE MODE" ELSE PRINT "INTRA PULSE MODE"
230 IF Q=7 THEN DISP "INPUT I.P.P." ELSE DISP "INPUT DELAY"
240 IF Q=7 THEN INPUT X(1) ELSE INPUT X(4)
250 IF Q=7 THEN PRINT "I.P.P.=";X(1);"m=" ELSE PRINT "DELAY=";X(4);"m="
260 PRINT "DEPTH";TAB (15);"RES1";TAB (26);"RES2"
270 ASSERT 3;0
280 ASSERT 3;1
290 ASSERT 3;0
300 ENTER 3 ; B$
310 Z$=B$[10,10]
320 IF Z$="?" THEN 330 ELSE 300
330 ENTER 3 ; A$
340 FOR I=6 TO 9
350 B(I-1)=NUM (A$[I,I])-48
360 NEXT I
370 C3=B(5)*100+B(6)*10+B(7)*1+B(8)*.1
380 IF Q=7 THEN 390 ELSE 430
390 X(2)=.5*C3
400 X(3)=C3/.6
410 X(4)=1
420 GOTO 460
430 X(1)=2*C3
440 X(2)=.5*C3
450 X(3)=1.467*C3
460 Y(1)=X(1)
470 Y(2)=X(2)
480 Y(3)=X(3)
490 Y(4)=X(4)
500 Y(5)=15
510 FOR I=1 TO 4
520 IF X(I)>25 THEN 550 ELSE 530
530 Y(I)=X(I)*10
540 Y(5)=Y(5)-2^(I-1)
550 NEXT I
560 P1$=FNS$(Y(1))
570 P2$=FNS$(Y(2))
```

```
580 P3$=FNS$(Y(3))
590 P4$=FNS$(Y(4)-1)
600 P5$=CHR$ (48)&CHR$ (Y(5)+48)
610 D$=P1$&P2$&P3$&P4$&P5$
620 ASSERT 3;128
630 OUTPUT 3 ;D$
640 ASSERT 3;132
650 ASSERT 3;128
660 ASSERT 3;0
670 ASSERT 3;2
680 ASSERT 3;0
690 ENTER 3 ; B$
700 Z$=B$[11,11]
710 IF Z$="?" THEN 720 ELSE 690
720 ENTER 3 ; A$
730 FOR I=2 TO 5
740 B(I-1)=NUM (A$[I,I])-48
750 NEXT I
760 C1=B(1)*16+B(2) @ C2=B(3)*16+B(4)
770 PRINT C3;TAB (15);C1;TAB (26);C2
780 CLEAR
790 DISP "******CORLOG******"
800 GOTO 270
810 END
```

```
10 ! ************************************************************************
20 ! *                                                                      *
30 ! *                                AUTOLOG                               *
40 ! *                                                                      *
50 ! *          THIS PROGRAM FIRST FINDS THE WATER DEPTH.                   *
60 ! * CORRELATION RESULTS ARE THEN CALCULATED FOR A GIVEN DELAY T.         *
70 ! *                                                                      *
80 ! ************************************************************************
90 OPTION BASE 1
100 DIM B(8),X(4),R(4),Y(5),T(10),D(4096),D1(50),D2(50),D3(50),Z1$[50]
110 DEF FNS$(N) = CHR$ (INT (N/16)+48)&CHR$ (FP (N/16)*16+48)
120 CLEAR
130 DISP "ENTER COMMENT"
140 INPUT Z1$@ PRINT Z1$
150 CLEAR
160 DISP "INTER OR INTRA MODE R/A"
170 INPUT W$
180 IF W$="R" THEN Q=7 ELSE Q=15
190 CONTROL 3,2 ; 0,10,0,0,0,0,0,0,0
200 CONTROL 4,2 ; 0,0,0,4,0,32,0,0,16
210 CLEAR
220 IF Q=7 THEN DISP "INTER PULSE MODE" ELSE DISP "INTRA PULSE MODE"
230 DISP "INPUT DELAY [ms]";@ INPUT S5
240 X(1)=S5 @ X(4)=S5
250 IF Q=7 THEN DISP "I.P.P.=";X(1);"ms" ELSE DISP "DELAY=";X(4);"ms"
260 ASSERT 3;0
270 ASSERT 3;1
280 ASSERT 3;0
290 ENTER 3 ; B$
300 Z$=B$[10,10]
310 IF Z$="?" THEN 320 ELSE 290
320 ENTER 3 ; A$
330 FOR I=6 TO 9
340 B(I-1)=NUM (A$[I,I])-48
350 NEXT I
360 C3=B(5)*100+B(6)*10+B(7)*1+B(8)*.1
370 IF Q=7 THEN 380 ELSE 420
380 X(2)=.5*C3
390 X(3)=C3/.6
400 X(4)=1
410 GOTO 450
420 X(1)=2*C3
430 X(2)=.5*C3
440 X(3)=1.467*C3
450 Y(1)=X(1)
460 Y(2)=X(2)
470 Y(3)=X(3)
480 Y(4)=X(4)
490 Y(5)=15
500 FOR I=1 TO 4
510 IF X(I)>25 THEN 540 ELSE 520
520 Y(I)=X(I)*10
530 Y(5)=Y(5)-2^(I-1)
540 NEXT I
550 P1$=FNS$(Y(1))
560 P2$=FNS$(Y(2))
570 P3$=FNS$(Y(3))
```

```
580 P4$=FNS$(Y(4)-1)
590 P5$=CHR$ (48)&CHR$ (Y(5)+48)
600 D$=P1$&P2$&P3$&P4$&P5$
610 ASSERT 3;128
620 OUTPUT 3 ;D$
630 ASSERT 3;132
640 ASSERT 3;128
650 ASSERT 4;0
660 ASSERT 4;8
670 ASSERT 4;0
680 ASSERT 4;4
690 ASSERT 4;0
700 WAIT 13
710 ASSERT 3;0
720 ASSERT 3;2
730 ASSERT 3;0
740 ENTER 3 ; B$
750 Z$=B$[11,11]
760 IF Z$="?" THEN 770 ELSE 740
770 ENTER 3 ; A$
780 FOR I=2 TO 5
790 B(I-1)=NUM (A$[1,1])-48
800 NEXT I
810 C1=B(1)*16+B(2) @ C2=B(3)*16+B(4)
820 DISP C1;C2
830 FOR N=1 TO 4095
840 ENTER 4 ; Y$
850 D(N)=DTD (Y$)
860 NEXT N
870 ASSERT 4;1
880 ASSERT 4;0
890 J=-1 @ J7=0 @ J8=0 @ J9=0
900 FOR I=1 TO 1023
910 A=D(3072+I)/D(3071+I)
920 IF A<1.2 THEN 930 ELSE 950
930 J7=MAX (J7,D(I)) @ J8=MAX (J8,D(I+1024)) @ J9=MAX (J9,D(I+2048))
940 GOTO 990
950 J=J+1
960 IF J=0 THEN 980 ELSE 970
970 D1(J)=J7 @ D2(J)=J8 @ D3(J)=J9
980 J7=0 @ J8=0 @ J9=0 @ DISP J
990 NEXT I
1000 J=J+1
1010 D1(J)=J7 @ D2(J)=J8 @ D3(J)=J9
1020 FOR K=1 TO 15
1030 PRINT D1(K);D2(K);D3(K)
1040 NEXT K
1050 DIM AA(15),BB(15),CC(15)
1060 FOR I=1 TO 15
1070 AA(I)=D1(I) @ BB(I)=D2(I) @ CC(I)=D3(I)
1080 NEXT I
1090 D=0 @ E=0 @ F=0 @ H=0 @ L=0 @ J=0
1100 FOR I=1 TO 14
1110 D=AA(I)+D @ E=BB(I+1)+E @ F=CC(I+1)+F
1120 NEXT I
1130 D=D/14 @ E=E/14 @ F=F/14
1140 FOR I=1 TO 14
```

```
1150 H=(AA(I)-D)^2+H
1160 J=(BB(I+1)-E)^2+J
1170 L=(CC(I+1)-F)^2+L
1180 NEXT I
1190 N=1
1200 G=0 @ G1=0 @ K=0 @ K1=0
1210 FOR I=1 TO 15-N
1220 G=(AA(I)-D)*(BB(I+N)-E)+G
1230 G1=AA(I)*BB(I+N)+G1
1240 K=(AA(I)-D)*(CC(I+N)-F)+K
1250 K1=AA(I)*CC(I+N)+K1
1260 NEXT I
1270 M1=G/(H*J)^.5
1280 M2=G/(15-N)
1290 M3=G1/(15-N)
1300 P1=K/(H*L)^.5
1310 P2=K/(15-N)
1320 P3=K1/(15-N)
1330 IMAGE M.3D,X,M8D.DD,X,M8D.DD
1340 IMAGE 3D.D,X,3D.D,X,3D.D
1350 PRINT N
1360 PRINT USING 1330 ; M1;M2;M3
1370 PRINT USING 1330 ; P1;P2;P3
1380 PRINT USING 1340 ; D;E;F
1390 PRINT
1400 PRINT
1410 PRINT
1420 PRINT
1430 PRINT
1440 END
```

APPENDIX B

CORRELATOR SYSTEM

CONTENTS

1. INTRODUCTION

The correlator system consists of four subsystems:

(a) Correlator processor.

(b) Timing unit.

(c) Receivers.

(d) Correlator.

The subsystems are realised by hardwired digital and analogue boards that are connected together by a bus system. The entire system is contained in a supporting rack. The hardwired digital design allows the correlator system to operate in real time.

2. BLOCK DIAGRAM

The general and detailed block diagrams of the correlator system are shown in Figures B-1(a) and B-1(b).

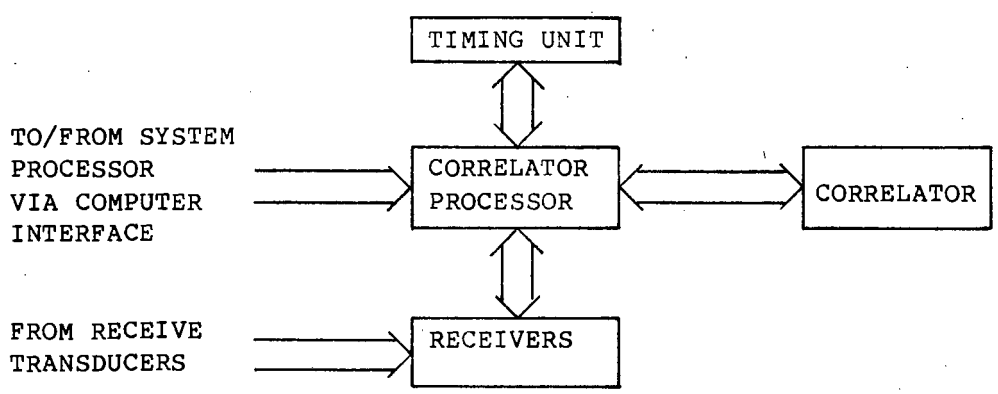

General Block Diagram of Correlator System

FIGURE B-1(a)

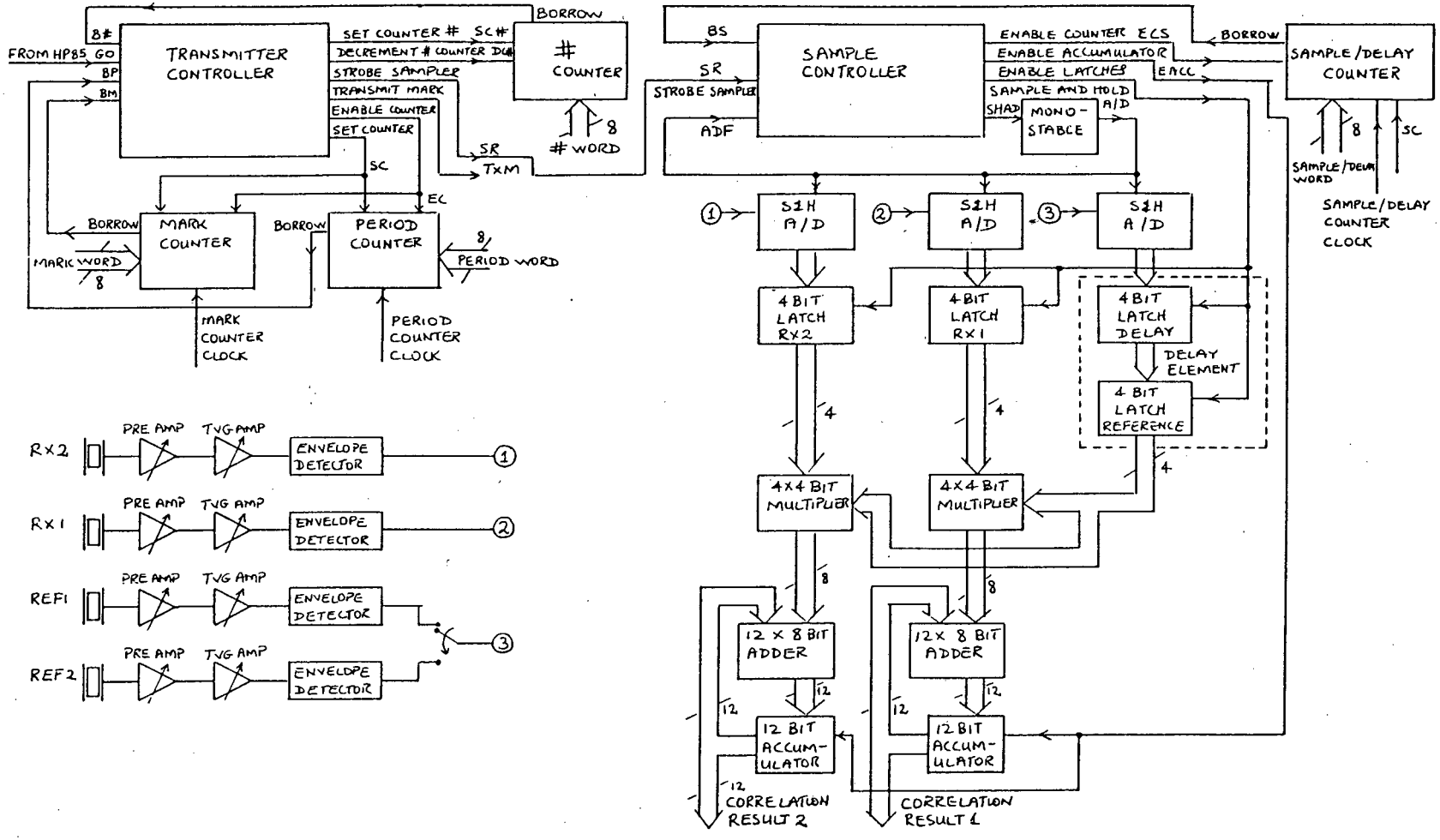

Detailed Block Diagram of Correlator System

FIGURE B-1(b)

3. TIMING

All timing is achieved via 8 bit counters. A counter is loaded with a given 8 bit word and counted down at a specified clock frequency until a borrow condition exists.

The four mode parameters that are timed are: period, mark, sample and delay. The delay parameter is only used when operating in the intrapulse mode. These parameters are derived from the system processor and are presented as four 8 bit digital words. As was discussed in Appendix A, Section 1.5.1, the countdown clock frequency is switched between 1kHz and 10kHz to improve fractional accuracy when measuring small time intervals. The system processor presents the correlator system with a 4 bit digital word, each bit being either false or true, which selects either 10kHz or 1kHz as a countdown clock frequency for a particular counter.

3.1 SAMPLE AND DELAY PARAMETER

The two mode parameters, sample and delay, share the same 8 bit counter. When in the intrapulse mode, the counter is first loaded with the 8 bit digital word SAMPLE and counted down until a borrow condition exists. The counter is reset and then loaded with the 8 bit digital word DELAY. The countdown procedure is repeated until the borrow condition re-exists. In this way two sampling instants can be set up: one at the beginning of the return pulse and one during the return pulse. The time between these two samples is the delay T.

When in the interpulse mode only the sample parameter is loaded into the counter and hence only one sampling instant is set up, in the middle of the return pulse.

The sampling instants for the inter and intrapulse modes are shown relative to the transmitter gating waveform in Figures B-2(a) and B-2(b).

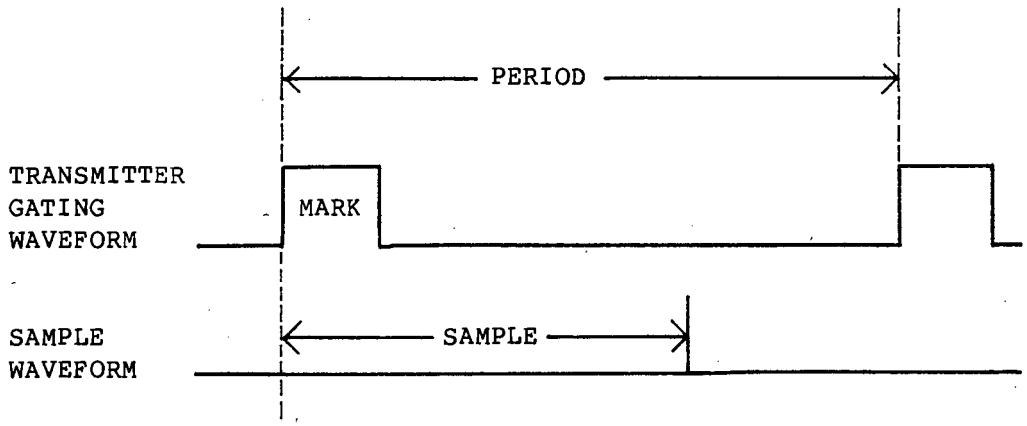

Interpulse Transmitter Gating and Sampling Waveform

FIGURE B-2(a)

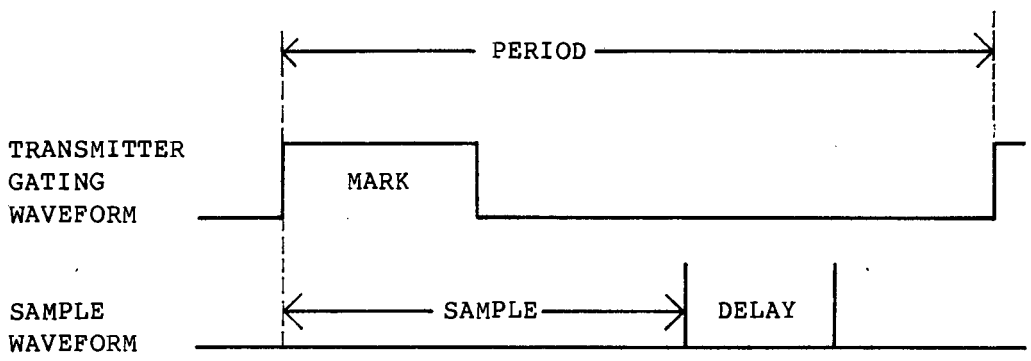

Intrapulse Transmitter Gating and Sampling Waveform

FIGURE B-2(b)

3.2 MARK AND PERIOD PARAMETER

The transmitter gating waveform of the pulsed transmission system consists of two parameters: mark and period. The gating waveform is illustrated in Figure B-2(a) and B-2(b). It should be noted that the waveform is the same for the inter and intrapulse modes. The two mode parameters, mark and period, each have an 8 bit counter associated with them. Both counters are loaded with their respective 8 bit digital words MARK and PERIOD. They are then counted down until their respective borrow conditions exist. Because the mark parameter will always be smaller than the period parameter, the mark borrow condition will always exist first. In this way the transmitter gating waveform can be generated.

Figure B-3 shows the three counters associated with the four mode parameters.

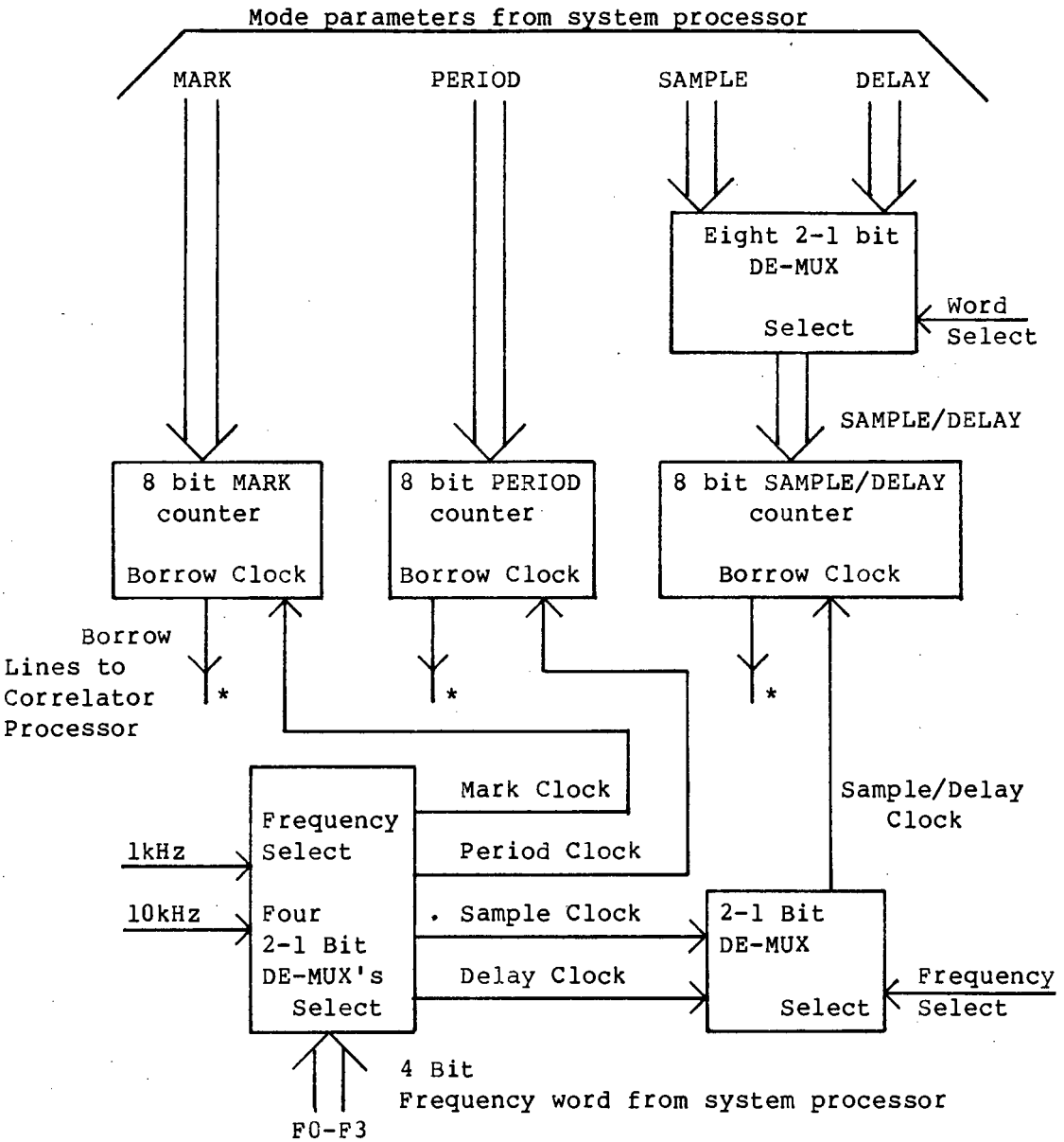

Mode Parameter Counters

FIGURE B-3

3.3 MASTER CLOCK

The correlator system has a crystal controlled 1MHz clock that is used for:

(a) Driving the correlator processor at 1μs per instruction. This is fast enough for real time operation.

(b) Dividing down by 100 and 1000 for the 10kHz and 1kHz countdown clocks used to time the mode parameters.

(c) Dividing down by 1000 for a 1kHz count up clock used to generate a gain versus time law for the time varying gain receivers.

The 1MHz clock is gererated via the 74LS124 VCO shown in Figure B-4.

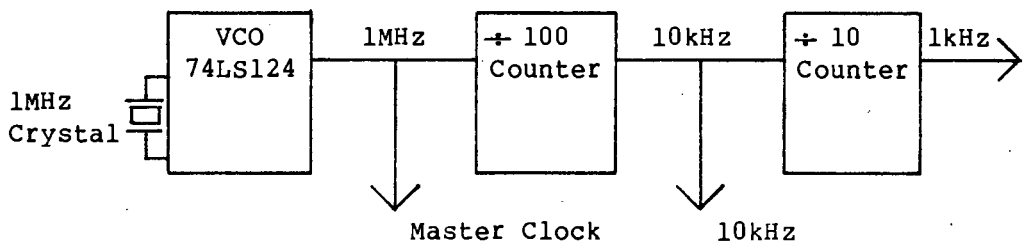

Master Clock

FIGURE B-4

3.4 NUMBER OF PULSES

The number of pulses that are correlated is set by an 8 bit counter. This counter is loaded with a given value whose maximum is 255. For each pulse received the counter is decremented. When a borrow condition exists the prescribed number of pulses will have been received, and the correlation results can be read by the system processor. Figure B-5 shows the number counter.

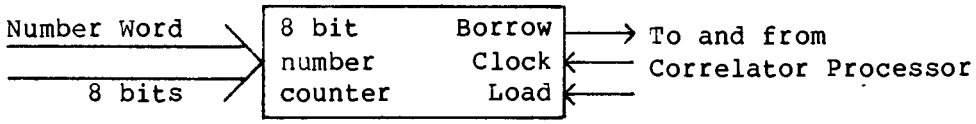

Number Counter

FIGURE B-5

4. CORRELATOR PROCESSOR

4.1 ALGORITHM

To facilitate real time operation,the correlator processor uses hardwired digital design techniques. The controlling algorithm of the processor is written step-wise and then symbol-wise for implementation in an algorithm state machine (ASM) design.

The controlling algorithm is broken up into two parts:

(a) A transmitter routine that generates the transmitter gating waveform.

(b) A sampling routine that generates the appropriate sampling and correlator control signals.

4.1.1 GENERAL ALGORITHM

Transmitter Routine

(1) Proceed to next step if GO command is received from HP 85/86.

(2) Reset GO command latch. Set numbers of pulses counter.

(3) Set mark and period counters. Strobe the sampling routine.

(4) Enable mark and period counters. Decrement number of pulses counter.

(5) Hold transmitter gating waveform true until mark counter borrow.

(6) Proceed to next step on period counter borrow.

(7) If number counter = 0, proceed to (1).
If number counter = 0, proceed to (3).

Sampling Routine*

(1) Proceed to next step on STROBE command from transmitter routine.

(2) Enable sample counter. Reset STROBE command latch.

(3) Proceed to next step on sample counter borrow.

(4) Initiate sample and hold and A/D procedure.

(5) Proceed to next step on end on A/D conversion.

(6) Latch A/D's.

(7) Enable correlator accumulators.

(8) Proceed to (1).

* For the intrapulse mode the sampling routine is entered into twice: the first time with the digital word SAMPLE and the second time with the digital word DELAY.

4.1.2 ASM TRANSLATABLE ALGORITHM

TRANSMITTER ROUTINE

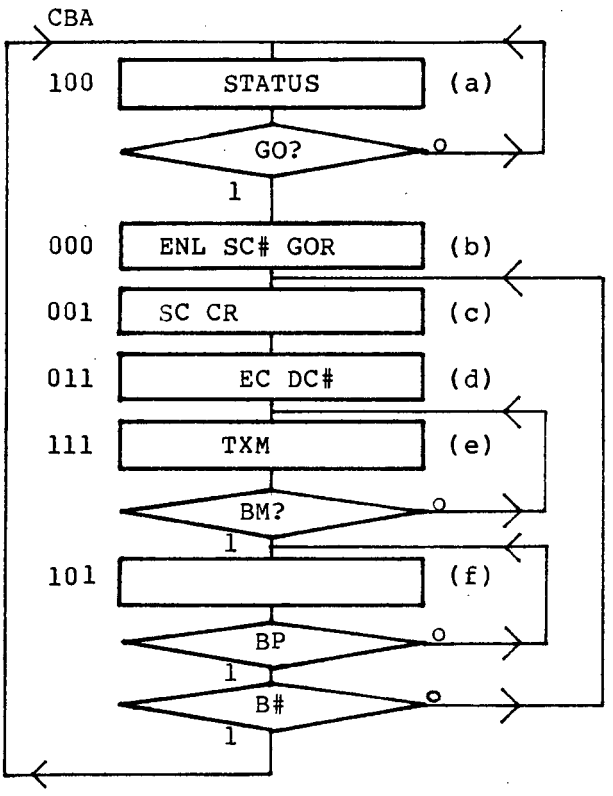

GO	Restart Sequence
BM	Borrow from Mark Counter
BP	Borrow from Period Counter
B#	Borrow from # Counter
ENL	Enable Latches
SC#	Set # of Pulses Counter

SC	Set Mark and Period Counters
GOR	Reset Restart Sequence
DC#	Decrement the # Counter
SR	Strobe the Receiver
EC	Enable Mark and Period Counters
TXM	Transmit Mark
STATUS	Correlator Status

SAMPLE ROUTINE

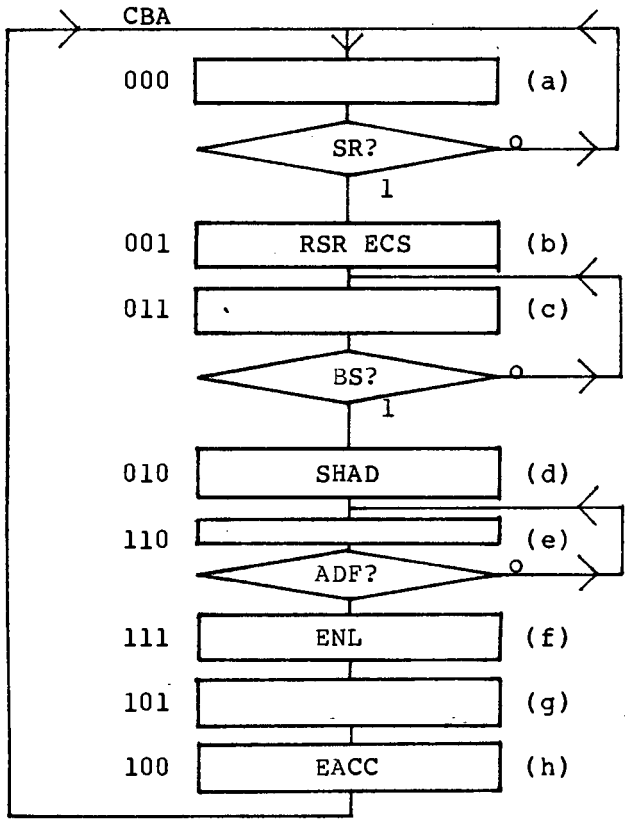

SR	Strobe the Receiver
RSR	Reset Strobe the Receiver
ECS	Enable Sample Counter
BS	Borrow from Sample Counter
SHAD	Sample and Hold and A/D

ADF A/D Finished

ENL Enable Latches

EACC Enable Accumulator

4.2 ASM DESIGN

Following the ASM design procedure, the algorithms were implemented in J-K flip-flop logic.

4.2.1 TRANSMITTER ROUTINE

State Assignments

C \ BA	00	01	11	10
0	b	c	d	-
1	a	f	e	-

State Variables

C \ BA	00	01	11	10
0	1	-	-	-
1		-	-	-

$J_A = \overline{C}$

C \ BA	00	01	11	10
0	-			-
1	-	BP. BN		-

$K_A = C.\overline{B}.BP.BN$

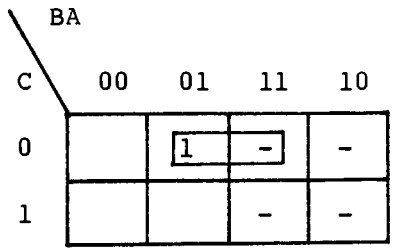

$J_B = \overline{C}.A$

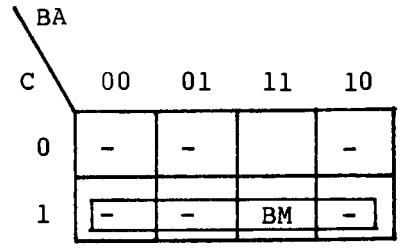

$K_B = C.BM$

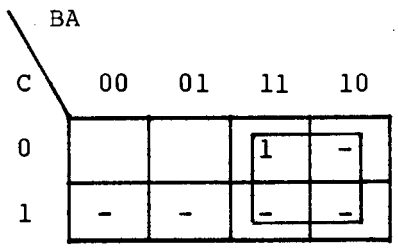

$J_C = B$

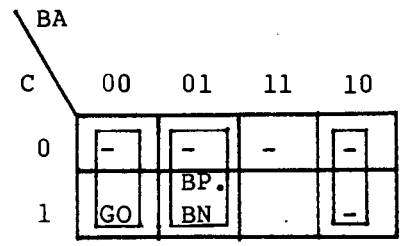

$K_C = GO.\overline{A}+BP.\overline{BN}.\overline{B}.A$

4.2.2 SAMPLE ROUTINE

State Assignments

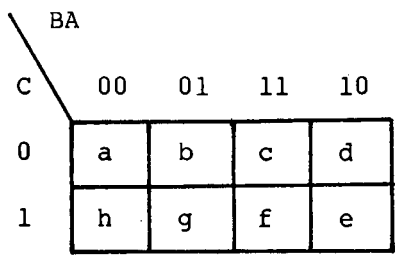

State Variables

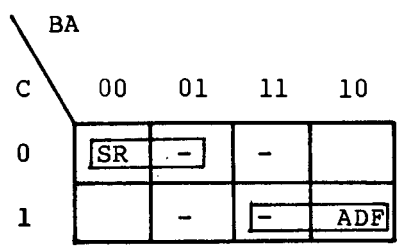

$J_A = SR.\overline{C}.\overline{B}+ADF.C.B$

$= \overline{\overline{SR.\overline{C}.\overline{B}}.\overline{ADF.C.B}}$

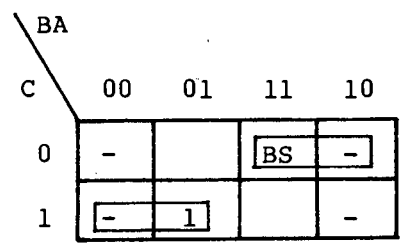

$K_A = C.\overline{B}.+BS.\overline{C}.B$

$= \overline{\overline{C.\overline{B}}.\overline{BS.\overline{C}.B}}$

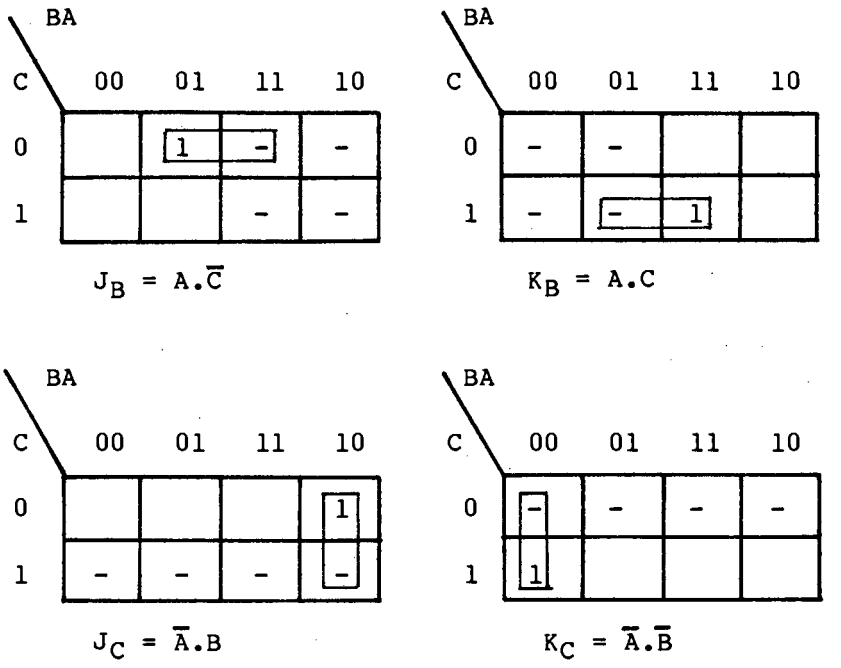

5. INTERFACING TO THE HP85/86

5.1 INTERCONNECTION

As was mentioned in Appendix A Section 3.1, the computer interface provides two cables, D and E, which carry the appropriate bus information for the correlator system. These cables are terminated by three 25-way Cannon-D type connectors, designated connectors 1, 2 and 3. These connectors plug into the correlator rack and are then connected to the appropriate correlator system bus. The connectors of the computer interface and correlator system are given in Figure B-6. For further interfacing information, refer to Appendix A.

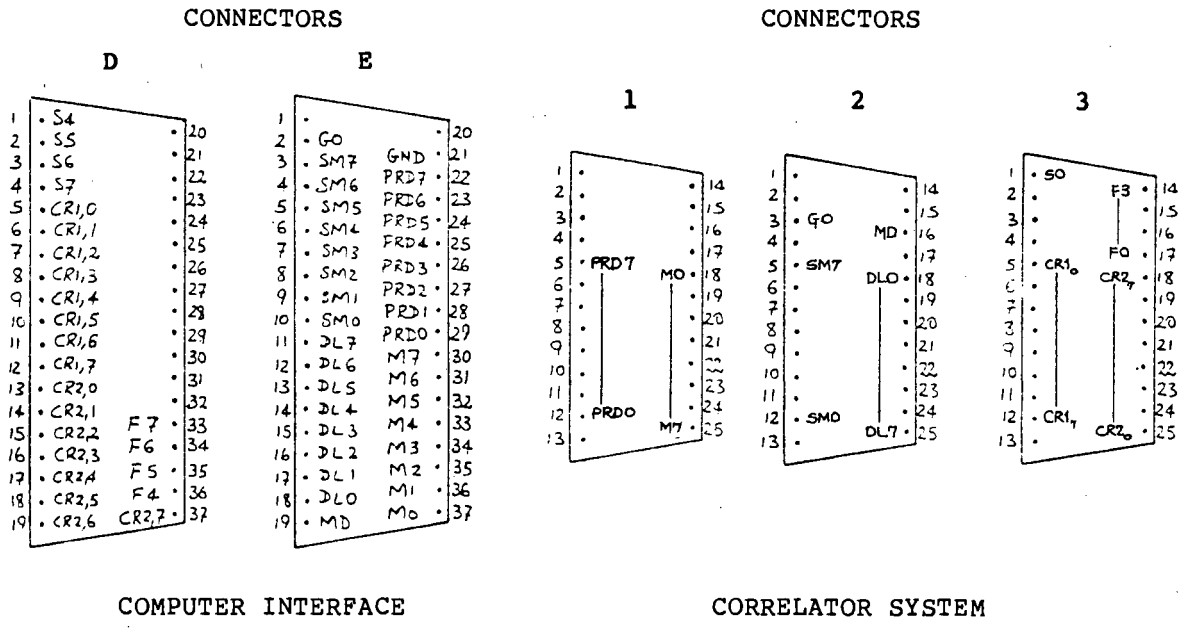

Connector Diagram

FIGURE B-6

5.2 DATA TRANSFER

The correlator system requires the following data input from the computer interface:

INPUT

8 BIT WORD	MNEMONIC	1 BIT CONTROL LINE	MNEMONIC
Mark	M0-M7	Start Correlator	GO
Period	PRD0-PRD7	Mode	MD
Sample	SM0-SM7		
Delay	DL0-DL7		
Frequency	F0-F3		

The computer interface requires the following data output from the correlator processor:

OUTPUT

8 BIT WORD	MNEMONIC	1 BIT CONTROL LINE	MNEMONIC
Correlation Result 1 Correlation Result 2	$CR1_0$-$CR1_7$ $CR2_0$-$CR2_7$	Status	STATUS

STATUS

Valid input and output of data can only be undertaken when the correlator processor is waiting for a GO command from the system processor. This state is the decoded state STATUS of the transmitter routine of Appendix B Section 4.1.2. When the correlator system is free for input and output the STATUS line will be true and when it is busy the STATUS will be false. This is shown in Figure B-7.

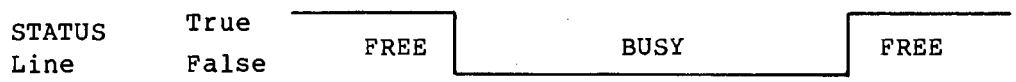

Status Line

FIGURE B-7

MODE

The system processor indicates to the correlator system which mode, inter or intrapulse, is to be used. This is achieved via the mode line MD and is shown in Figure B-8.

Mode Line

FIGURE B-8

GO

The system processor commands the correlator processor to begin via a true to false transition of the GO line as shown in Figure B-9.

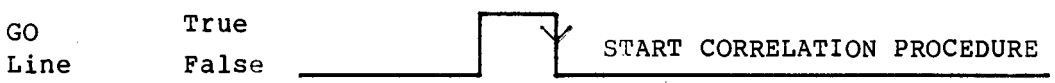

Go Line

FIGURE B-9

6. TRANSMITTER

Tone bursts of 194kHz (the resonant frequency of the receive transducers) are transmitted vertically towards the sea bed. The correlator system and the depth sounder use the same transmit transducer. The transmitter circuitry is described in Appendix C

Section 7. The tone bursts are generated by supplying a gating signal (available from a BNC connector on the correlator system rack) to the transmit circuit of the depth sounder.

The decoded state TXM of the transmitter routine is used as the gating signal. (Refer to Appendix B Section 4.2.1) The gating signal and corresponding tone bursts are shown in Figure B-10.

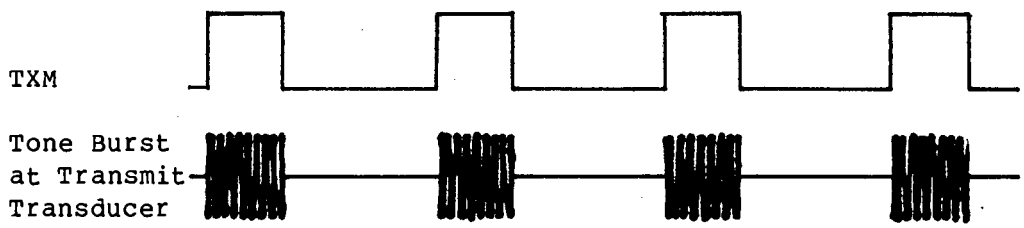

Transmitter Gating Signal

FIGURE B-10

7. RECEIVERS

7.1 TIME VARYING GAIN (TVG) CONCEPT

Refer to Appendix C Section 8.1, to cancel out the effect of the return amplitudes inverse proportionality to deoth, the gain of the receiver must be proportional to depth.

i.e. Gain $G \propto Z$

and Depth $Z = \frac{T_{TWP} \times C}{2}$

where c = speed of sound propagation

T_{TWP} = two-way propagation time

Let $G \propto T_{TWP}$

The gain-time law that is used is shown in Figure B-11.

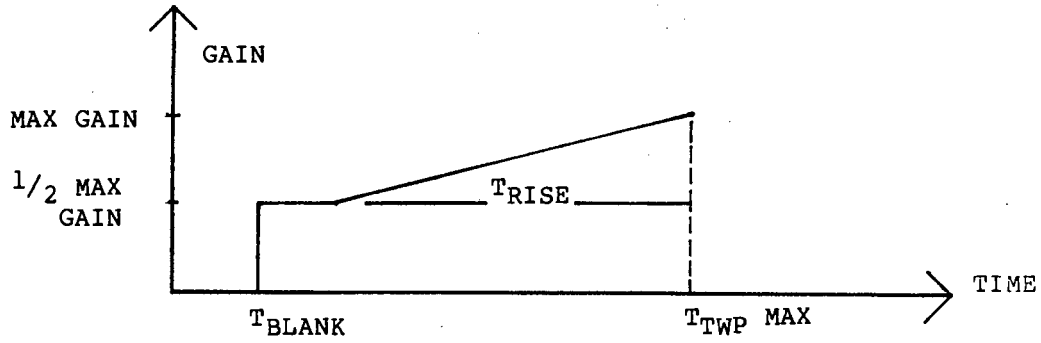

Gain-Time Law

FIGURE B-11

The TVG is realised by using a multiplying D/A shown schematically in Figure B-12.

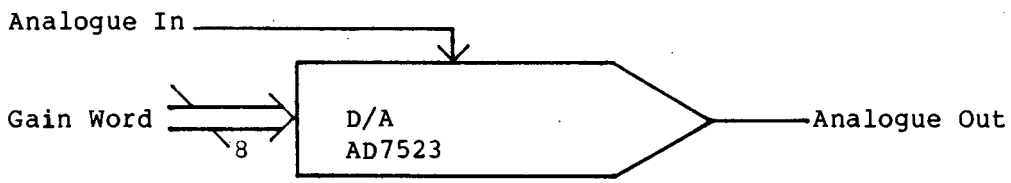

Multiplying D/A

FIGURE B-12

$$\text{Analogue out} = \text{Analogue in} \times \frac{\text{Gain Word}}{255}$$

The gain word is made up as shown in Figure B-13

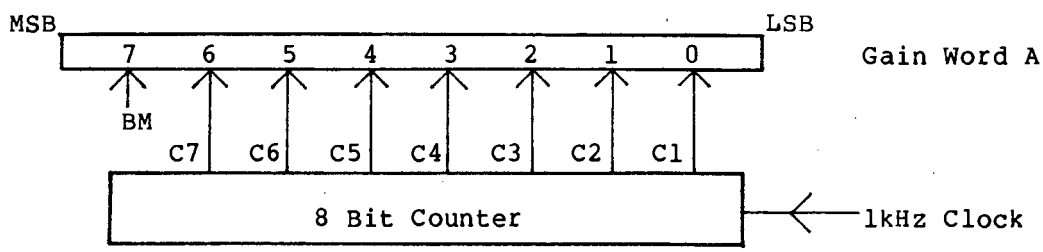

Gain Word

FIGURE B-13

The MSB of the gain word A is A_7 derived from the mark counter borrow line, BM. The borrow line only goes true at the end of the transmitter mark. This gives a time of no gain, T_{BLANK}, so that reverberation and transmitter breakthrough can be gated out.

The other 7 bits of the gain word A are derived from the most significant 7 bits of an 8 bit counter driven at a frequency of 1kHz. The time, T_{RISE}, when the gain increases from half maximum value to the maximum value is T_{RISE} = 255ms.

7.2 GAIN STAGES

Four identical receivers are required for the inter-intrapulse correlation log. A printed circuit board construction technique was employed to help reduce noise and to make the receivers identical. Two receivers are laid down per board. The boards are fitted with 25-way edge connectors and connect into a screened area of the correlator rack.

The receivers consist of four stages:

(a) a low noise long tail pair front end with gain of approximately 46dB;

(b) a wideband amplifier, the MC1590 with an LM318 op-amp as buffer. The gain of this stage can be varied by changing the AGC bias point on the 1590.

(c) a TVG amplifier using the AD7523 8 bit D/A with LM318 op-amp as buffer;

(d) an envelope detector made up of a fullwave rectifier and a low pass filter with cut-off frequency of 20kHz.

The block diagram of a typical receiver is shown in Figure B-14.

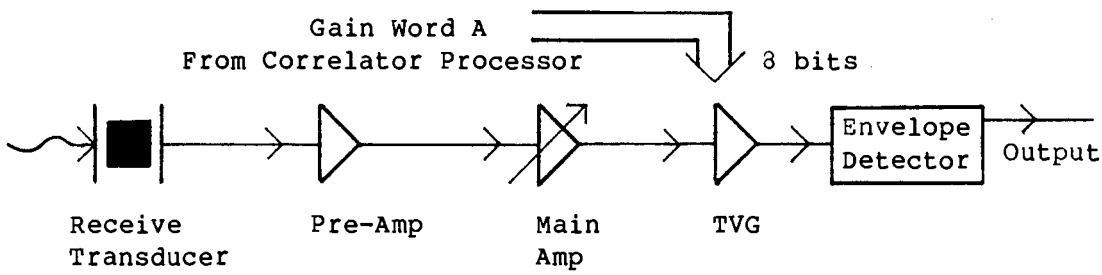

Block Diagram of Receiver

FIGURE B-14

The receiver is a broadband design and is tuned to the carrier frequency of the return echo by a parallel LC circuit at the output to the MC1590.

The carrier frequency chosen was the resonant frequency of the receive transducers and is 194 kHz.

f resonant = 194kHz

The L was chosen to be 165μH with ± 15μH variability wound with 25 turns of Litz wire on a 3H1 A315 core.

Now $f = \frac{1}{2\pi\sqrt{LC}}$ for a parallel LC circuit.

Therefore

$$C = \frac{1}{L(2\pi f)^2} = \frac{1}{180\mu H \times (2\pi \times 194kHz)^2}$$

$C = 3,7nF$ for $180\mu H$

and $C = 4,5nF$ for $150\mu H$

choose $C = 3,9nF$.

A detailed circuit diagram of a receiver is shown in Figure B-25

8. SAMPLE AND HOLD AND A/D TIMING

8.1 TIMING

The timing that initiates the sample and hold function and A/D of the receiver signal is shown in Figure B-15.

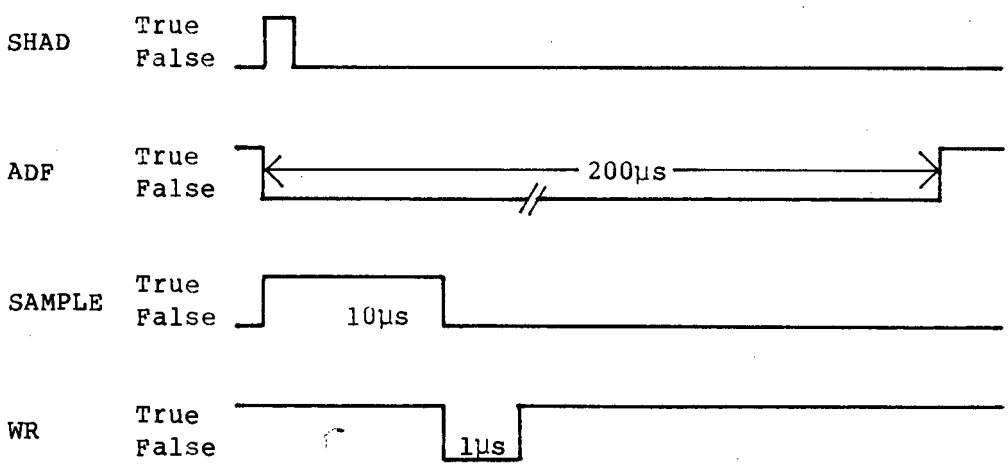

Sample and Hold and A/D Timing

FIGURE B-15

The SHAD command of the correlator processor initiates the following functions:

(a) The A/D finished instruction ADF is generated by a monostable set to give a true value after 200μs. In this time the sample and hold and A/D conversion takes place.

(b) The SAMPLE instruction is generated by a monostable set to give a 10μs pulse. When SAMPLE is true the sample and hold LF398 tracks the input signal from the receiver and when it goes false the LF398 holds the signal. The hold time is long enough so as not to cause errors in the A/D.

(c) The start of conversion WR of the A/D ADC0804 is generated by a monostable set to give a true value 1μs after it has been triggered by the trailing edge of the SAMPLE pulse. This allows time for the LF398 to stop ringing, at the start of the hold sequence.

8.2 BLOCK DIAGRAM

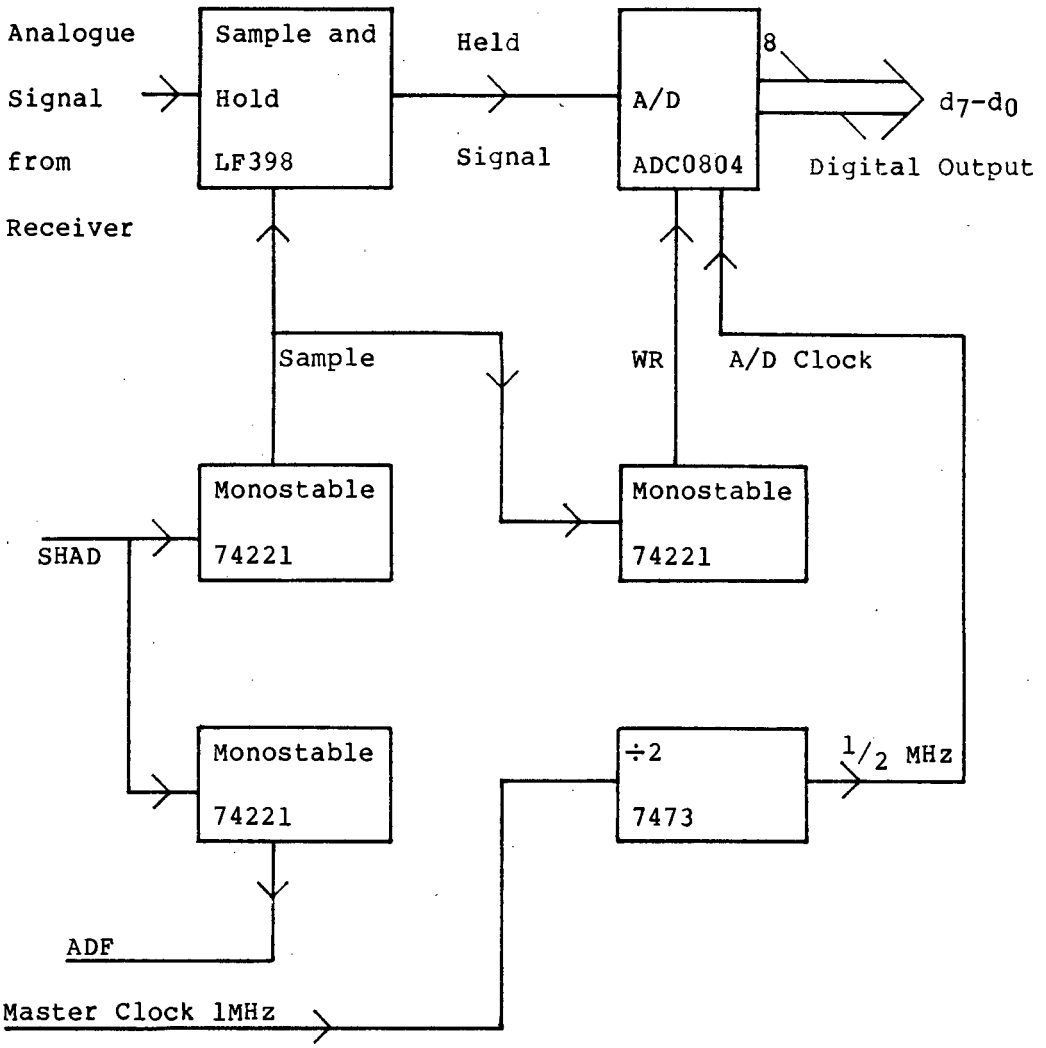

Sample and Hold and A/D Block Diagram

FIGURE B-16

8.2.1 SAMPLE AND HOLD

To improve noise immunity the LF 398 is supplied with a ±12V regulated supply. This voltage regulation is provided by regulating the ±12V power supply with the positive and negative voltage regulators LM340T12 and LM7912.

A hold capacitor of 1nF provides an acquisition time of less than 10µs. To avoid errors the A/D thus starts the conversion 11µs after the start of sampling and 1µs after the start of the hold.

8.2.2 A/D

The A/D provides an 8 bit output d_7 - d_0. The $^1/_2$ full range voltage is 2,5V which is regulated by the voltage regulator LM340T5 for improved noise immunity.

The A/D clock of 500kHz is derived by the master clock of 1MHz. The resultant rate of conversion results in a conversion time of 140µs which is within the 200µs window of the ADF command. (Refer to Appendix A Section 8.1)

Detailed circuits of the three sample and hold and A/D converters are found in Figure B-24, the sample and hold

and A/D board. The two reference receiver signals are connected via a manual switch on the correlator rack to one of the LF398's.

9. CORRELATOR

9.1 INTRODUCTION

Two correlation results $\rho(X_1)$ and $\rho(X_2)$ are calculated by the hardwired correlator. They are read as two 8 bit words COR1 and COR2 by the system processor. This occurs only when the correlator processor's status is free.

The correlator performs two parallel correlations, one with the sampled signals of the reference and receiver 1 and the second with the sampled signals of the reference and receiver 2. The correlation coefficient is calculated by multiplying the sampled signals and summing their product. In both the inter and intrapulse modes the sampled reference signal is delayed by one sample.

9.2 BLOCK DIAGRAM

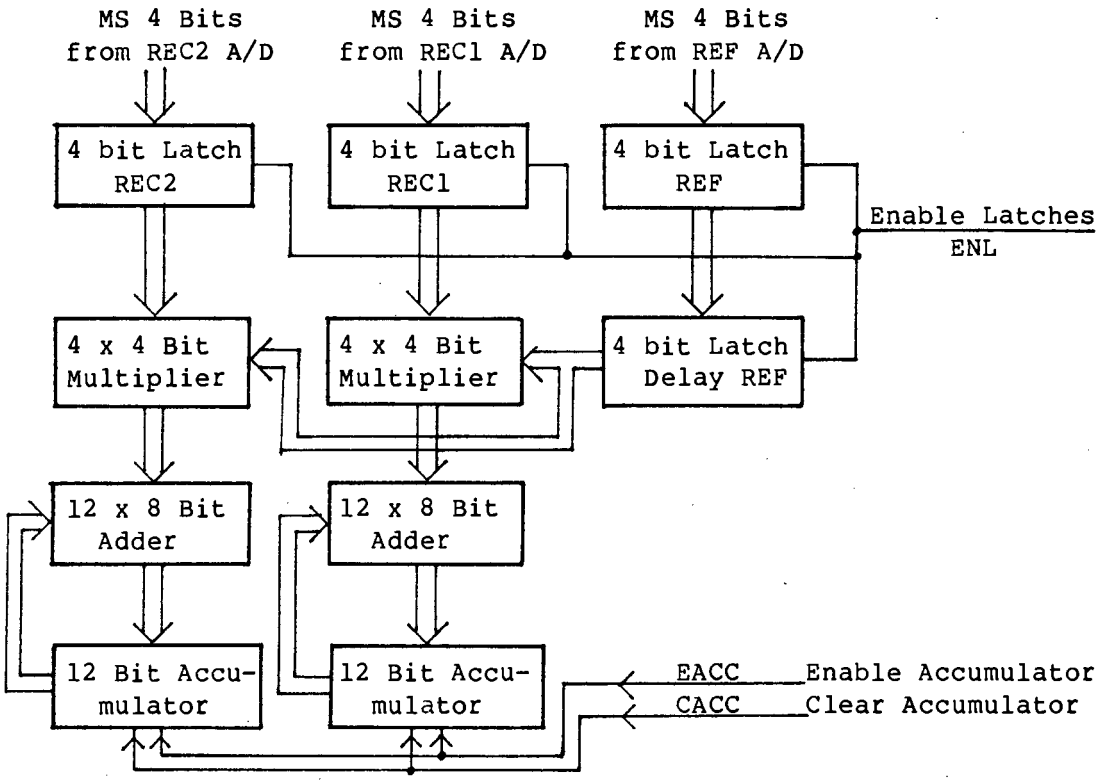

Correlator Block Diagram

FIGURE B-17

9.3 TIMING

The correlator timing sequence is different for the two modes of operation. In the interpulse mode the return pulse is sampled once and the delay that is applied to the REF sisnal is one IPP or one sampling period. In the intrapulse mode the return pulse is sampled twice. The delay that is applied to the REF signal is the period between samples. The delays are realised as follows:

9.3.1 INTERPULSE MODE

The timing sequence of the correlator is shown in Figure B-18 for the first three return pulses.

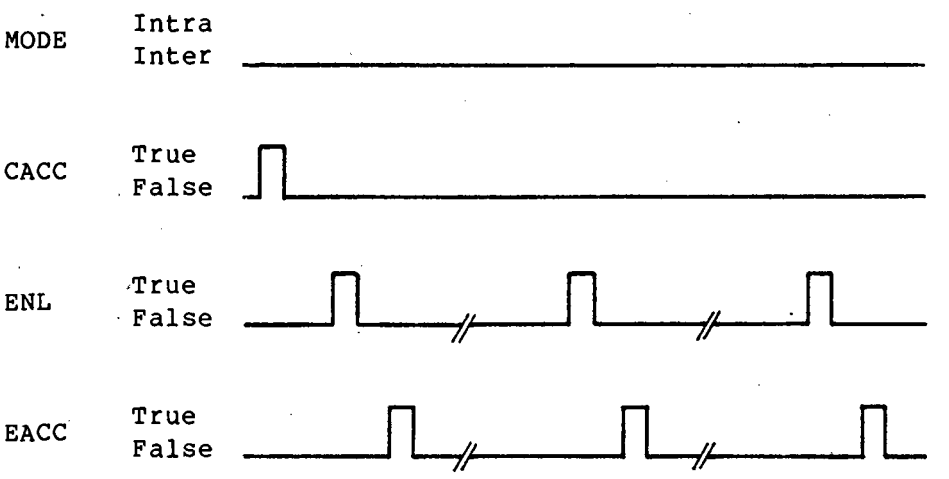

Timing Sequence of Correlator in the Interpulse Mode

FIGURE B-18

This sequence is generated by the sampling routine of the correlator processor (see Appendix B Section 4.1.2).

Delay

The three 4 bit digital words REF, REC1 and REC2 are latched by the 4 bit latches (shown in Figure B-17) on the rising edge of the ENL pulse.

By having two latches for the REF digital word, the first latch can latch the current sample and the second

latch can latch the preceding latched sample of the first latch. A delay of one sample is thus applied to the REF digital word.

Accumulator

One microsecond exists between the ENL and EACC command. This gives the multiplier IC and 8 x 12 bit adder time to reach a stable output before being latched.

At the start of each correlation, the accumulator is cleared via the CACC command.

The most significant 8 bits of the accumulator are read by the system processor as the correlation result. This occurs when the correlator processor's status is free.

9.3.2 INTRAPULSE MODE

The timing sequence of the correlator, for the first two return pulses is shown in Figure B-19. The sequence is generated by the sampling routine of the correlator processor (Refer to Appendix B Section 4.1.2).

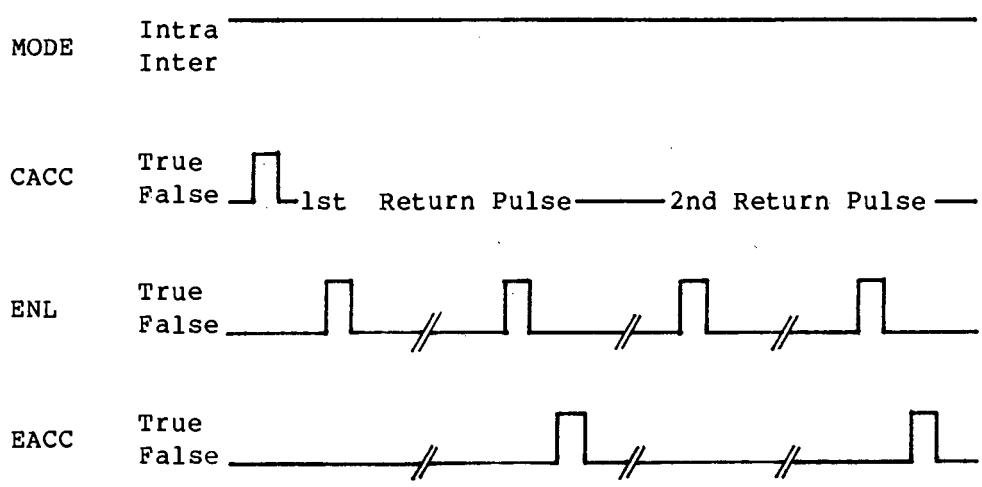

Timing Sequence of Correlator in the Intrapulse Mode

FIGURE B-19

Delay

As in the interpulse case a delay of one sample is applied to the REF digital word by having two successive latches.

Accumulator

The accumulator is enabled by the EACC command only after the second sample within the return pulse has been latched. This ensures that products from the multiplier are only accumulated when the correct delay is applied. At the start of each correlation the accumulator is cleared via the CACC command.

One microsecond exists between the ENL and EACC command. As in the interpulse mode, this gives the multiplier IC and 8 x 12 bit adder time to reach a stable output before being latched.

9.4 NUMBER OF PULSES

The number of return pulse samples used in the correlation coefficient calculation is restricted by the capacity of the accumulator. The accumulator is a 12 bit latch with an 8 x 12 bit adder.

The largest sum that can be accumulated is $(2^{12}-1) = 4095$.

The maximum product of the 4 x 4 bit multiplier is 15 x 15 = 255.

Let this product be accumulated n times. The resulting sum is 255n.

The maximum number of accumulations n before the accumulator overflows is thus n = 4095/255 = 16,06.

The maximum number of pulses that can be used for correlation without an overflow error is thus 16.

The number of pulses counter (see Appendix B Section 3.4) is thus set at 16.

10. RACK SYSTEM

10.1 CORRELATOR RACK

The rack is designed to hold 120mm wide, plug-in boards. These boards plug into a series of edge connectors that are wired together. The edge connectors provide the various boards with power, bus facilities and control lines.

10.2 BOARD LAYOUT

Seven boards are needed to realise the correlator system. Their various functions are tabulated below.

BOARD #	FUNCTION
1	Clock Generator
2	Transmitter Controller
3	Sample Controller
4	Correlator
5	Sample and Hold and A/D
6	Receiver x 2
7	Receiver x 2

The circuit diagrams of the various boards are found in Figures B-20 to B-25. Wire wrap construction was used for all digital circuitry.

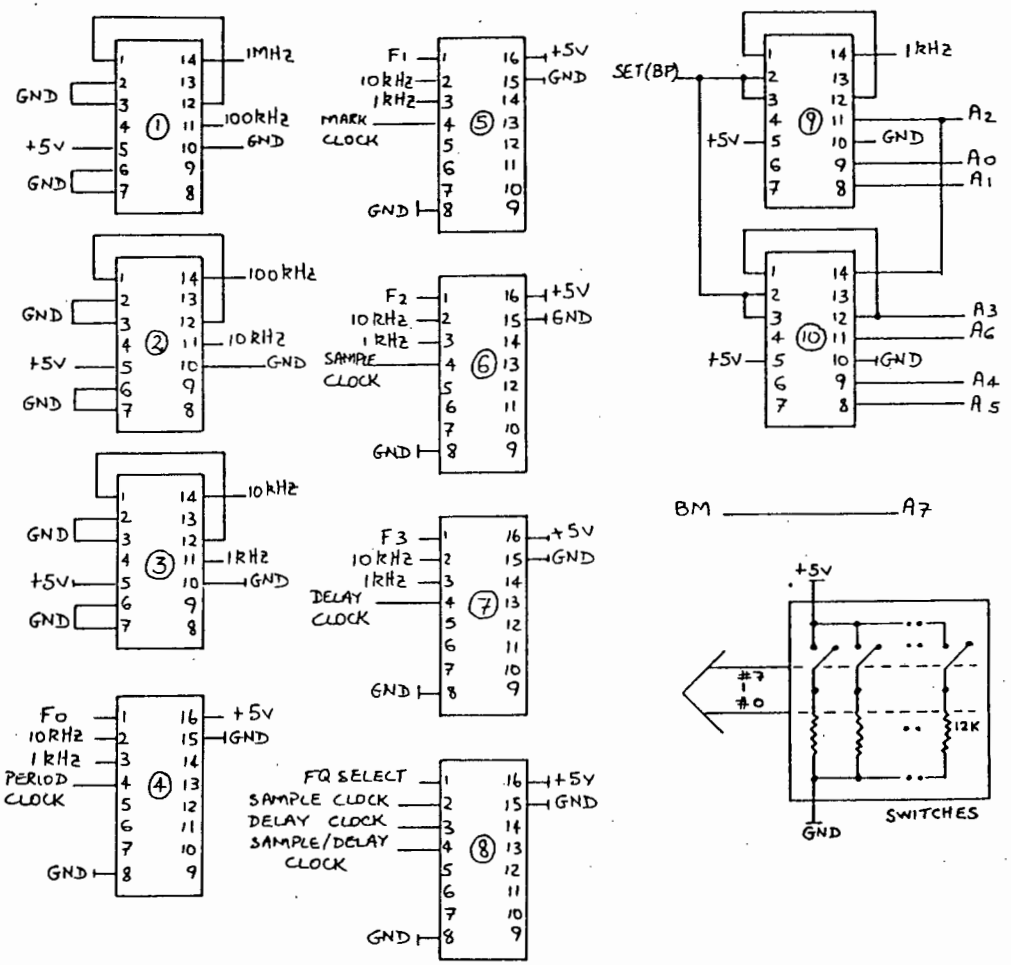

Bus #	DESCRIPTION
1	+5V
2	#7
3	#6
4	#5
5	#4
6	#3
7	#2
8	#1
9	#0
10	
11	
12	
13	
14	
15	A0
16	A1
17	A2
18	A3
19	A4
20	A5
21	A6
22	A7
23	
24	FQ SELECT
25	1MHz CLOCK
26	MARK CLOCK
27	PERIOD CLOCK
28	SAMPLE/DELAY CLOCK
29	
30	BM
31	BP
32	
33	
34	
35	
36	
37	N/C
38	F0
39	F1
40	F2
41	F3
42	
43	GND

IC #	FUNCTION	SERIAL #
1	÷10	74LS90
2	÷10	74LS90
3	÷10	74LS90
4	2-1 DEMUX	74LS157
5	2-1 DEMUX	74LS157
6	2-1 DEMUX	74LS157
7	2-1 DEMUX	74LS157
8	2-1 DEMUX	74LS157
9	÷16	74LS93
10	÷16	74LS93

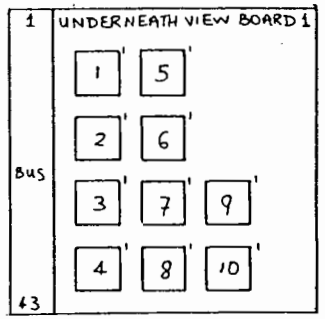

Board 1

FIGURE B-20

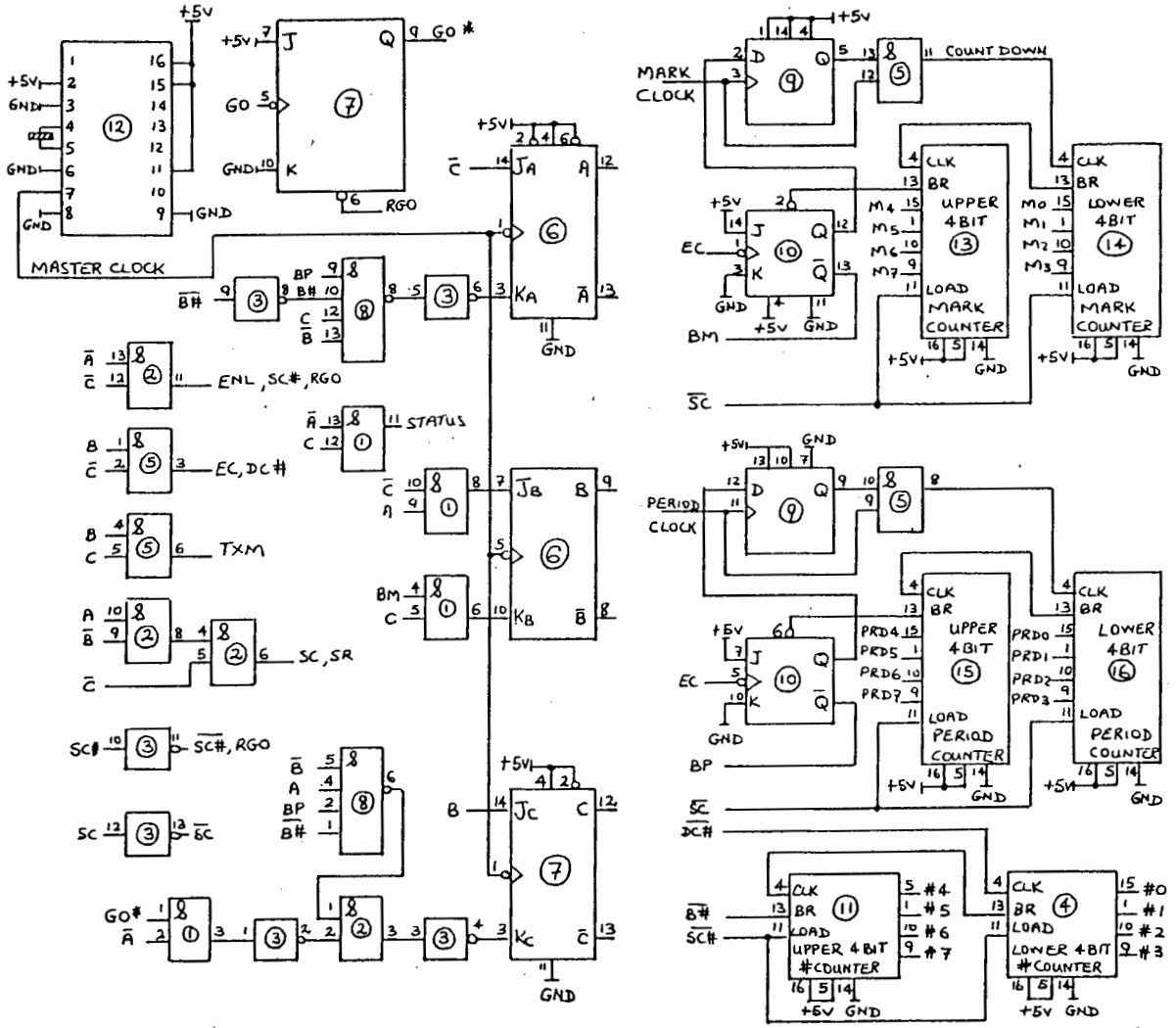

BUS #	DESCRIPTION
1	+5V
2	
3	
4	STATUS
5	M7
6	M6
7	M5
8	M4
9	M3
10	M2
11	M1
12	M0
13	PRD7
14	PRD6
15	PRD5
16	PRD4
17	PRD3
18	PRD2
19	PRD1
20	PRD0
21	#7
22	#6
23	#5
24	#4
25	MASTER CLOCK
26	MARK CLOCK
27	PERIOD CLOCK
28	GO
29	SR
30	TXM
31	SC
32	RGO
33	
34	
35	BM
36	BP
37	
38	
39	#3
40	#2
41	#1
42	#0
43	GND

IC #	FUNCTION	SERIAL #
1	QUAD 2I/P AND	74LS08
2	QUAD 2I/P AND	74LS08
3	HEX INVERTER	74LS04
4	4 BIT COUNTER	74LS193
5	QUAD 2I/P AND	74LS08
6	DUAL J-K FF	74LS73
7	DUAL J-K FF	74LS73
8	DUAL 4I/P NAND	74LS20
9	DUAL D FF	74LS74
10	DUAL J-K FF	74LS73
11	4 BIT COUNTER	74LS193
12	VCO	74LS623
13	4 BIT COUNTER	74LS193
14	4 BIT COUNTER	74LS193
15	4 BIT COUNTER	74LS193
16	4 BIT COUNTER	74LS193

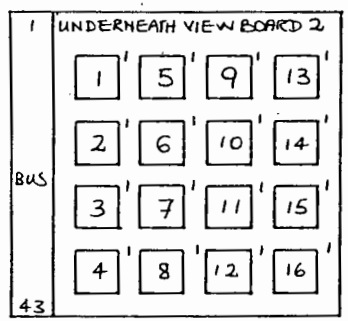

Board 2

FIGURE B-21

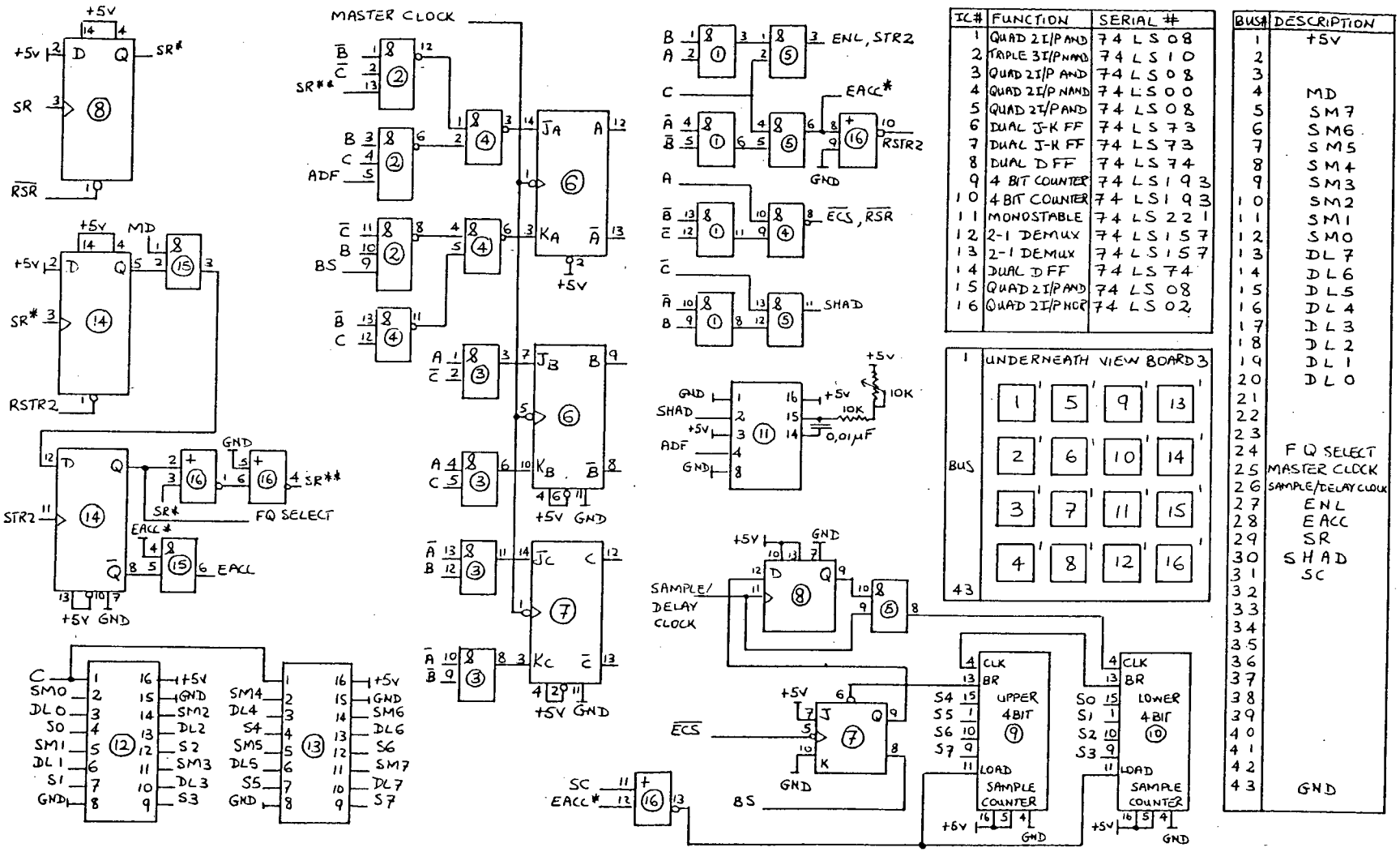

IC#	FUNCTION	SERIAL #
1	QUAD 2I/P AND	74 LS 08
2	TRIPLE 3I/P NAND	74 LS 10
3	QUAD 2I/P AND	74 LS 08
4	QUAD 2I/P NAND	74 LS 00
5	QUAD 2I/P AND	74 LS 08
6	DUAL J-K FF	74 LS 73
7	DUAL J-K FF	74 LS 73
8	DUAL D FF	74 LS 74
9	4 BIT COUNTER	74 LS 193
10	4 BIT COUNTER	74 LS 193
11	MONOSTABLE	74 LS 221
12	2-1 DEMUX	74 LS 157
13	2-1 DEMUX	74 LS 157
14	DUAL D FF	74 LS 74
15	QUAD 2I/P AND	74 LS 08
16	QUAD 2I/P NOR	74 LS 02

BUS#	DESCRIPTION
1	+5V
2	
3	
4	MD
5	SM7
6	SM6
7	SM5
8	SM4
9	SM3
10	SM2
11	SM1
12	SM0
13	DL7
14	DL6
15	DL5
16	DL4
17	DL3
18	DL2
19	DL1
20	DL0
21	
22	
23	
24	FQ SELECT
25	MASTER CLOCK
26	SAMPLE/DELAY CLOCK
27	ENL
28	EACC
29	SR
30	SHAD
31	SC
32	
33	
34	
35	
36	
37	
38	
39	
40	
41	
42	
43	GND

Board 3

FIGURE B-22

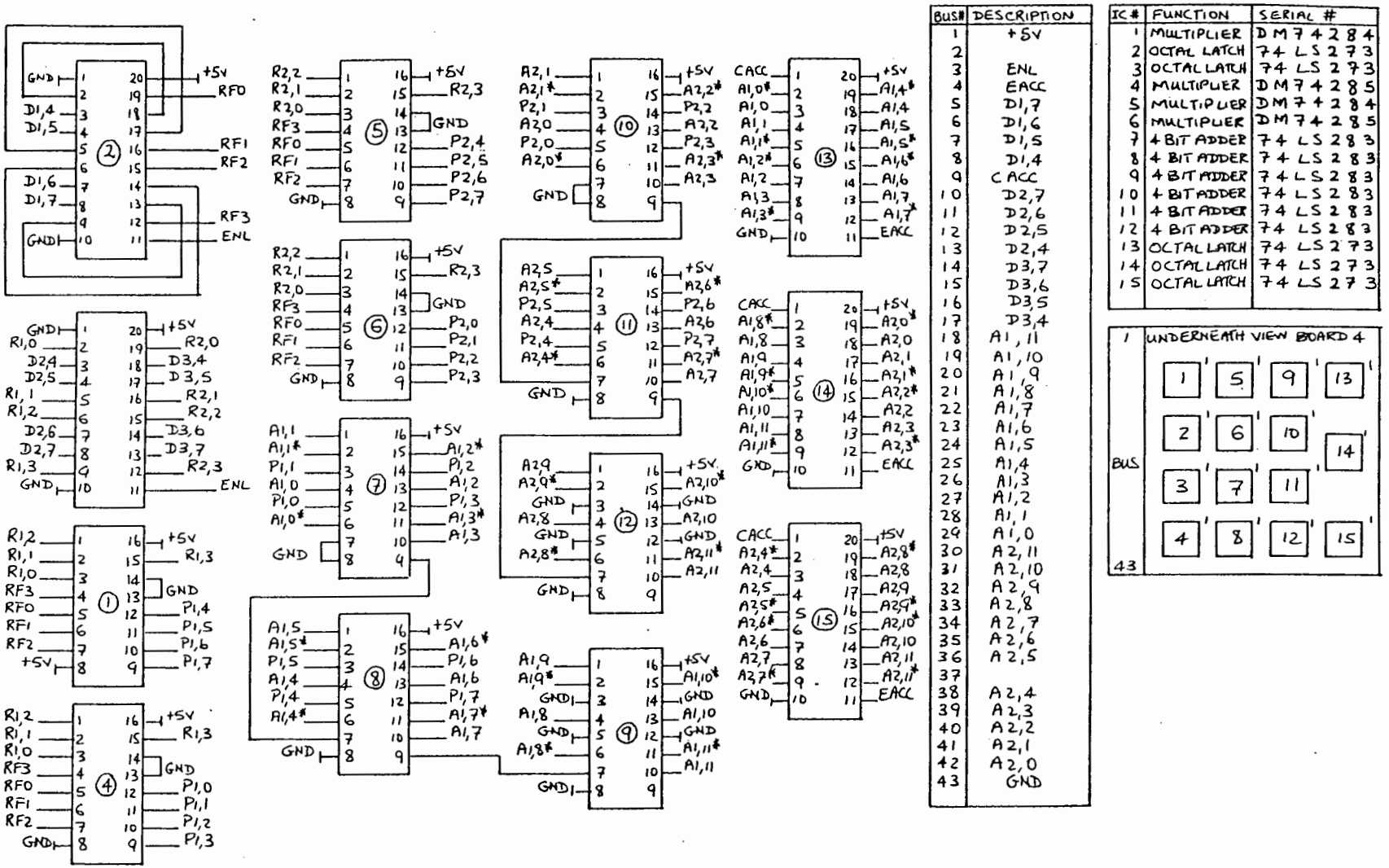

BUS#	DESCRIPTION
1	+5V
2	
3	ENL
4	EACC
5	D1,7
6	D1,6
7	D1,5
8	D1,4
9	CACC
10	D2,7
11	D2,6
12	D2,5
13	D2,4
14	D3,7
15	D3,6
16	D3,5
17	D3,4
18	A1,11
19	A1,10
20	A1,9
21	A1,8
22	A1,7
23	A1,6
24	A1,5
25	A1,4
26	A1,3
27	A1,2
28	A1,1
29	A1,0
30	A2,11
31	A2,10
32	A2,9
33	A2,8
34	A2,7
35	A2,6
36	A2,5
37	
38	A2,4
39	A2,3
40	A2,2
41	A2,1
42	A2,0
43	GND

IC #	FUNCTION	SERIAL #
1	MULTIPLIER	DM74284
2	OCTAL LATCH	74LS273
3	OCTAL LATCH	74LS273
4	MULTIPLIER	DM74285
5	MULTIPLIER	DM74284
6	MULTIPLIER	DM74285
7	4 BIT ADDER	74LS283
8	4 BIT ADDER	74LS283
9	4 BIT ADDER	74LS283
10	4 BIT ADDER	74LS283
11	4 BIT ADDER	74LS283
12	4 BIT ADDER	74LS283
13	OCTAL LATCH	74LS273
14	OCTAL LATCH	74LS273
15	OCTAL LATCH	74LS273

Board 4

FIGURE B-23

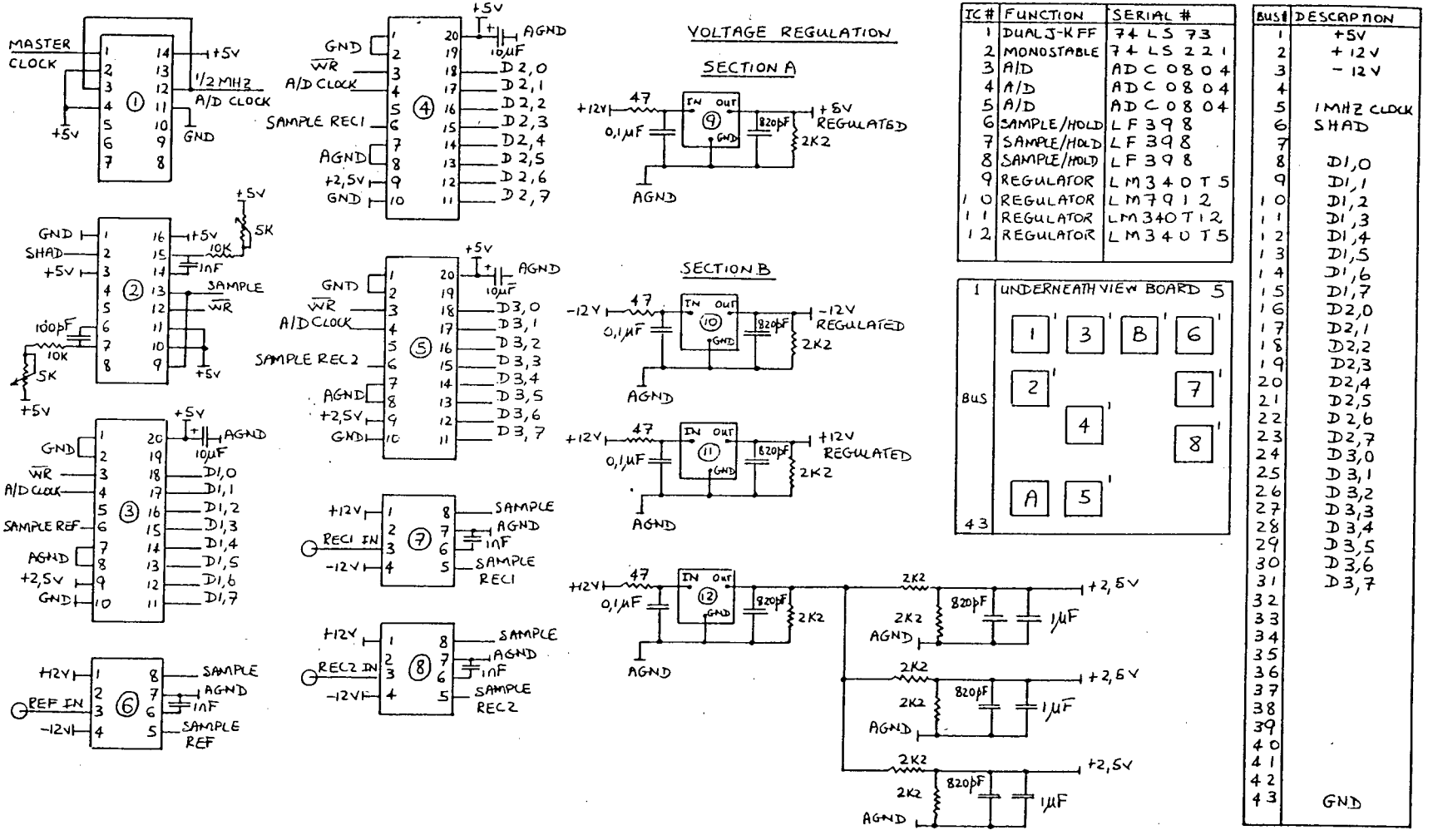

IC #	FUNCTION	SERIAL #
1	DUAL J-K FF	74 LS 73
2	MONOSTABLE	74 LS 221
3	A/D	ADC 0804
4	A/D	ADC 0804
5	A/D	ADC 0804
6	SAMPLE/HOLD	LF 398
7	SAMPLE/HOLD	LF 398
8	SAMPLE/HOLD	LF 398
9	REGULATOR	LM340T5
10	REGULATOR	LM7912
11	REGULATOR	LM340T12
12	REGULATOR	LM340T5

BUS #	DESCRIPTION
1	+5V
2	+12V
3	-12V
4	
5	1MHZ CLOCK
6	SHAD
7	
8	D1,0
9	D1,1
10	D1,2
11	D1,3
12	D1,4
13	D1,5
14	D1,6
15	D1,7
16	D2,0
17	D2,1
18	D2,2
19	D2,3
20	D2,4
21	D2,5
22	D2,6
23	D2,7
24	D3,0
25	D3,1
26	D3,2
27	D3,3
28	D3,4
29	D3,5
30	D3,6
31	D3,7
32	
33	
34	
35	
36	
37	
38	
39	
40	
41	
42	
43	GND

Board 5

FIGURE B-24

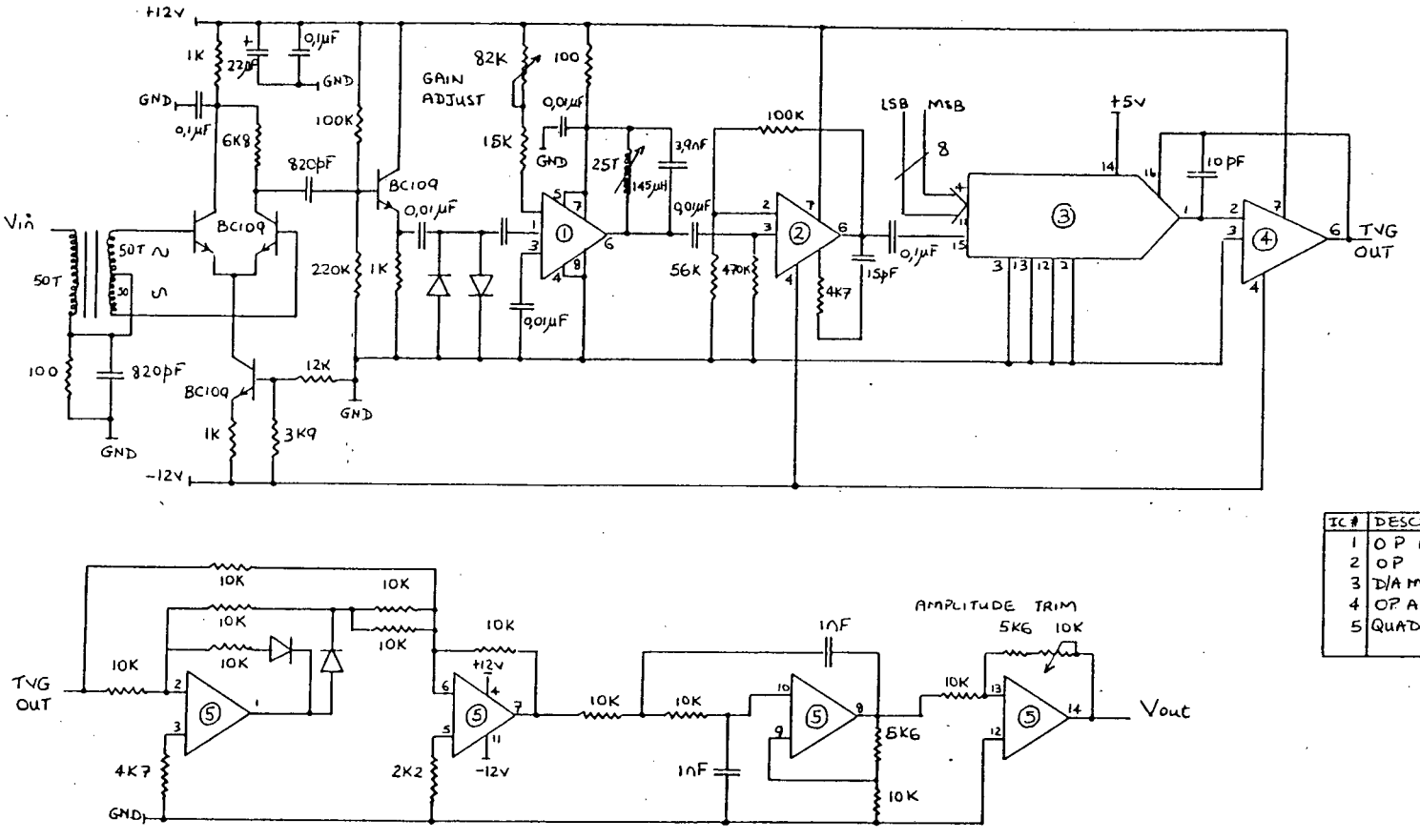

IC #	DESCRIPTION	SERIAL #
1	OP AMP	MC1590
2	OP AMP	LM318
3	D/A MULTIPLIER	AD7523
4	OP AMP	LM318
5	QUAD OP AMP	LF347

Board 6 and 7

FIGURE B-25

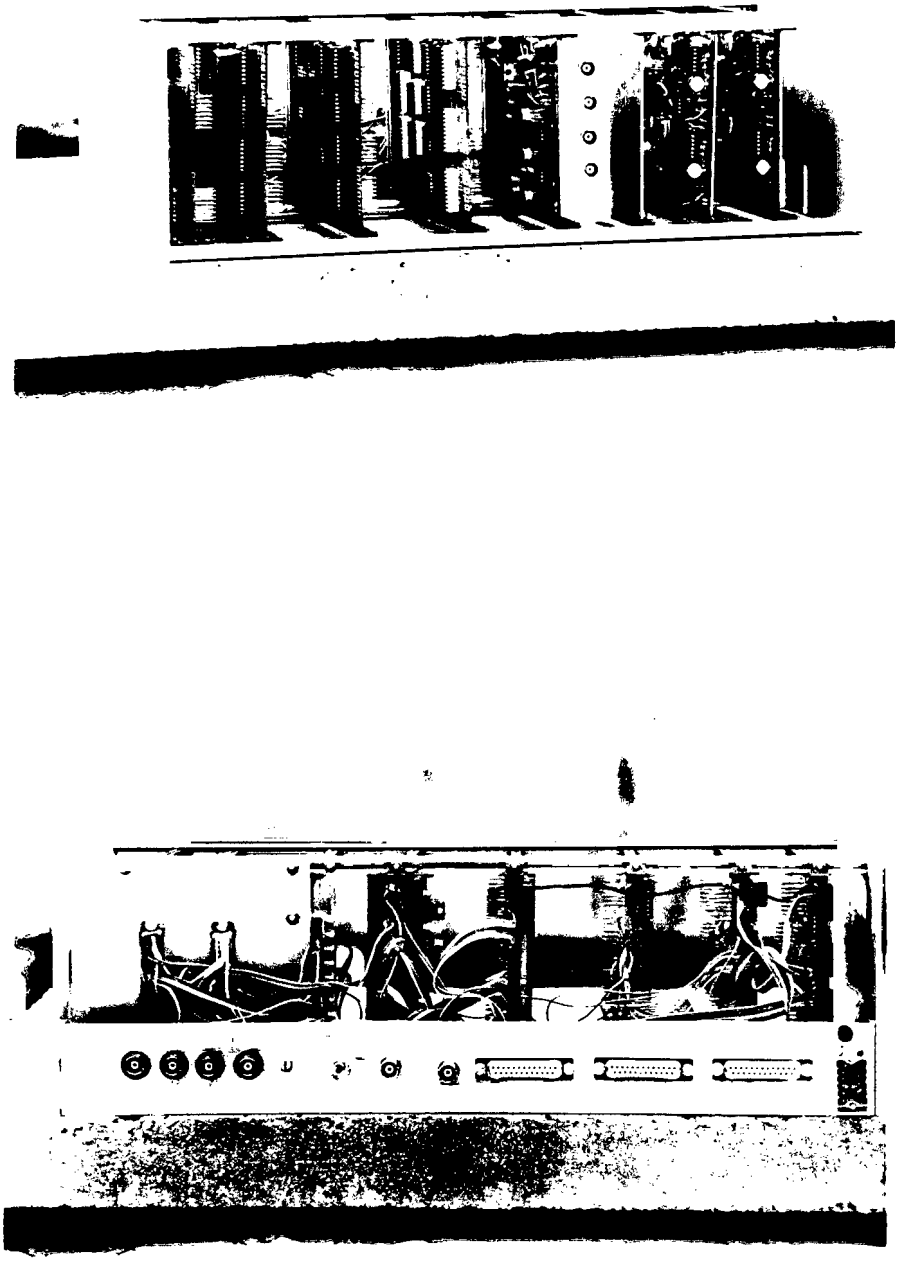

Correlator System

FIGURE B-26

10.3 POWER SUPPLY

A dedicated switch mode power supply is provided for the correlator system. The voltages available are +5V, +12V and -12V. The +5V is used for the digital system and the ±12V is used for the receivers.

10.4 EXTERNAL CONNECTIONS, MONITORING POINTS AND ADJUSTMENT POINTS

10.4.1 EXTERNAL CONNECTIONS

The following external connections are made.

MNEMONIC	DESCRIPTION
REF1 IN REF2 IN REC1 IN REC2 IN	The outputs of the 4 transducers are connected to their respective receiver front ends via these inputs.
CONNECTOR 1 CONNECTOR 2 CONNECTOR 3	The correlator system is connected to the HP85/86 computer interface via these three 25-way Delta connectors and ribbons.
POWER	The various voltages needed by the correlator system are brought from the switch mode power supply by a provided cable and locking socket system.
TRANSMITTER GATE	The correlator system's transmitter gating pulse is connected to the depth sounder's CORLOG gate via this output.

10.4.2 MONITORING POINTS

The following monitoring points are provided.

MNEMONIC	DESCRIPTION
SAMPLE SIGNAL	The time of sampling can be monitored via this BNC connector.
REF1 OUT REF2 OUT REC1 OUT REC2 OUT	The outputs of the 4 receivers are monitored via these BNC connectors. These outputs are the envelope detected versions of the amplified receive signals.

10.4.3 ADJUSTMENT POINTS

The following adjustment points are provided.

MNEMONIC	DESCRIPTION
REF1 GAIN REF2 GAIN REC1 GAIN REC2 GAIN	Four trimpots are provided so that the individual gains of the four receivers can be matched.
# OF PULSES	A set of eight digital switches are provided so that the number of pulses sent can be set with an 8 bit word. MSB corresponds to switch 7.

MNEMONIC	DESCRIPTION
A/D WINDOW	A trimpot is provided so that the monostable that generates the 200 s ADF false pulse can be set.
SAMPLE TRACKING LENGTH	A trimpot is provided so that the monostable that generates the 10 s SAMPLE tracking pulse can be set.
DELAY A/D START LENGTH	A trimpot is provided so that the monostable that generates the 1 s delay before $\overline{WR}$ goes true to start A/D can be set.

APPENDIX C

CONTENTS

1. DEPTH SOUNDER BLOCK DIAGRAM

The block diagram of the system is as follows.

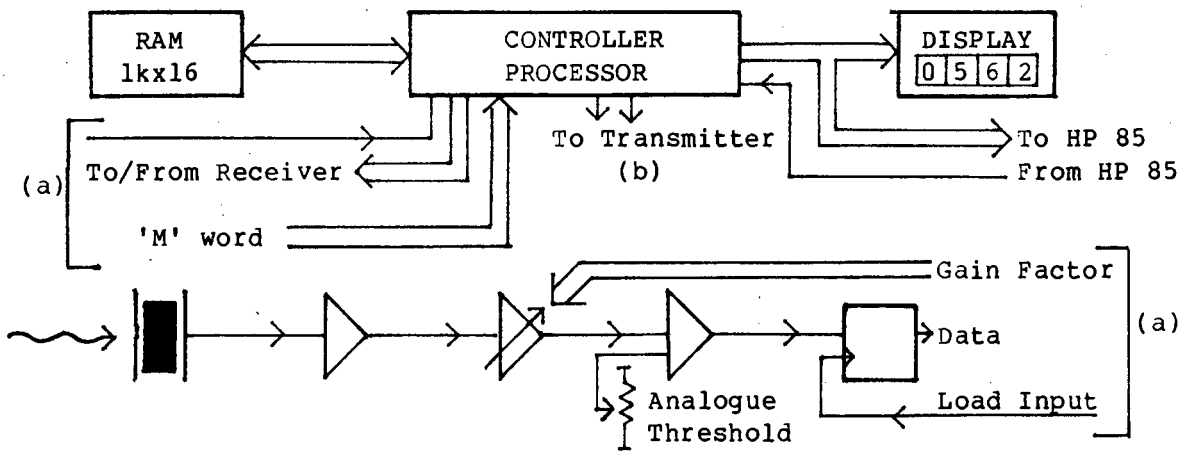

RECEIVER

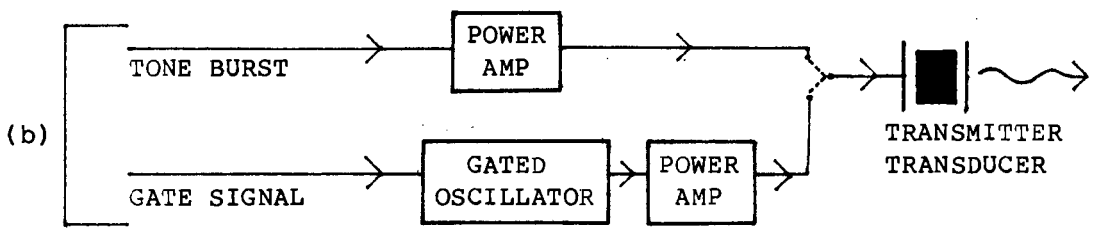

TRANSMITTER

Block Diagram

FIGURE C-1

2. MEMORY

2.1 MEMORY ELEMENTS

The memory can be thought of as a two-dimensional array, (n x k). It is made up a standard readily available, 4 bit by 1K RAM blocks. For simplicity of design, only 1 bit of the 4 bit by 1K blocks is used. The value of k = 1024 and n = 16. Hence 16, 4 bit by 1K blocks are used.

2.2 WRITING TO RAM / READING FROM RAM

Each element of RAM is accessed via a unique co-ordinate address system.

Writing to RAM is via two addresses, (ping ; depth). These addresses, (ping ; depth) are generated by 4 bit and 10 bit counters respectively.

Reading from RAM is via two addresses, (sum ; depth). The sum address is generated by a 4 bit counter.

After a range cell has been written to in RAM, the m out of n detector, reads and sums all 16 range cells of that depth. It does this by interchanging the ping address for the sum address, while leaving the depth address unchanged. The sum address is incremented after each of the 16 read and sum operations.

The memory map of RAM is found in Figure C-2(a).

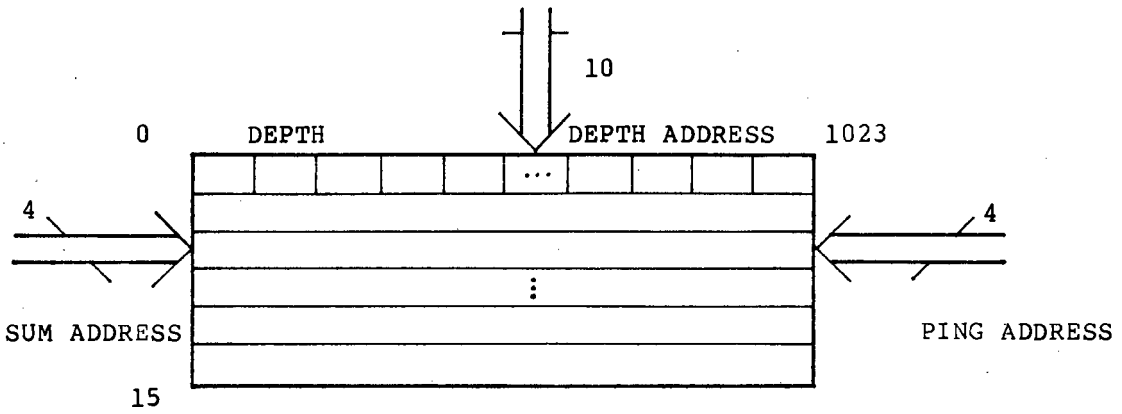

Memory Map

FIGURE C-2(a)

2.3 TIMING DIAGRAMS

The 4 bit by 1K RAM blocks (serial # M2114), are operated as follows. Figure C-2(b) shows one of the 16 blocks.

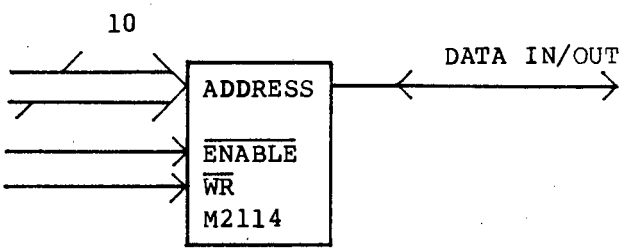

RAM Block

FIGURE C-2(b)

To write to RAM, Figure C-2(c) illustrates the procedure.

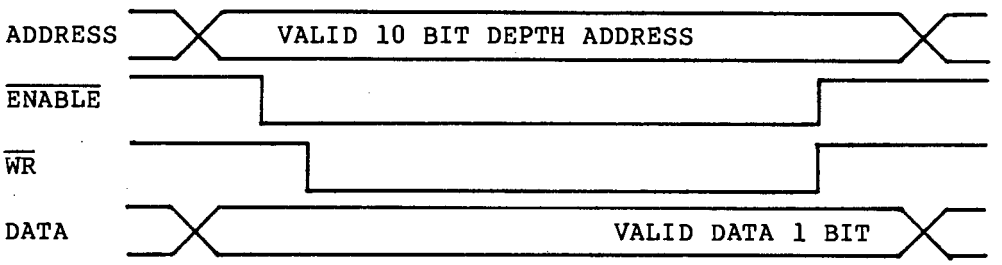

Write Cycle

FIGURE C-2(c)

To read from RAM, Figure C-2(d) illustrates the procedure.

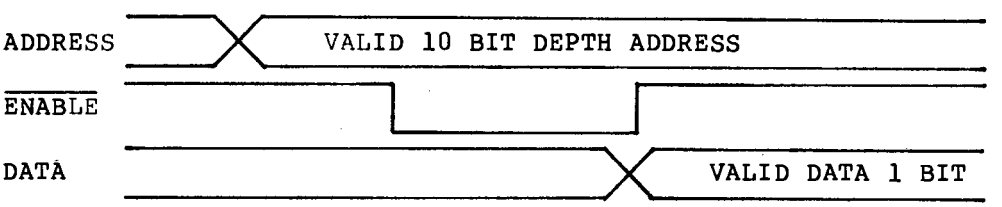

Read Cycle

FIGURE C-2(d)

2.4 READ/WRITE SEQUENCE

As mentioned previously, after writing to RAM with the ping address, RAM is read via the sum address. The depth address is the same in both cases.

The input data bus must be put into a high impedence mode when reading from RAM to avoid bus conflict. This is achieved by placing the quantiser (D flipflop) in tri-state during the read cycle.

This is illustrated in Figure C-2(e) and 2(f).

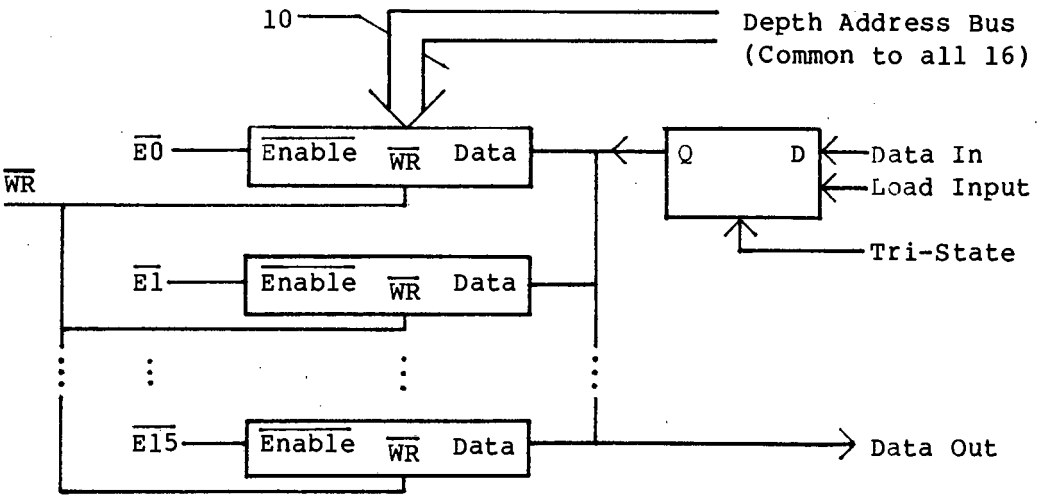

RAM Connection

FIGURE C-2(e)

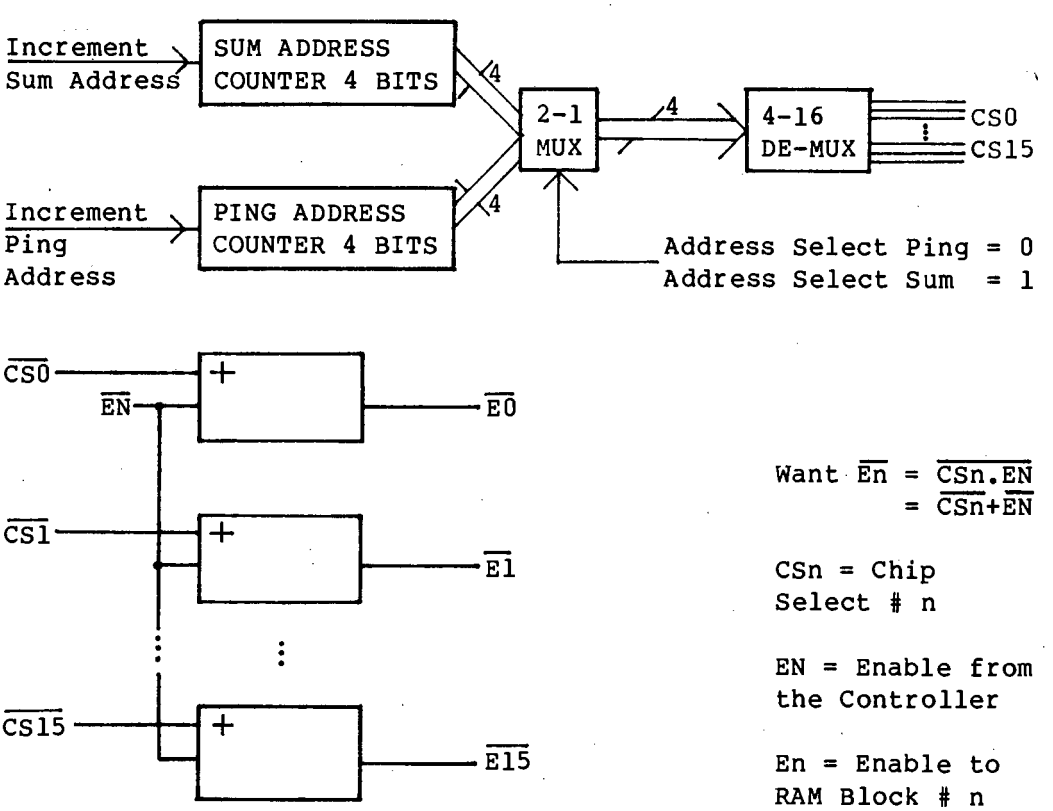

Address Select

FIGURE C-2(f)

3. TIMING

The system is synchronised to a 1MHz square wave crystal oscillator. Two events are timed, that of a ping and a range cell. This oscillator is called the master clock.

3.1 PING TIME

Let the maximum depth be Z max. The two-way propagation time for Z max is:

$$T_{TWP}\ \text{max} = \frac{2\ Z\ \text{max}}{c} \qquad c = \text{speed of sound in water.}$$

Let Z max = 100m, then T_{TWP} max = 133ms.

A guard time must be left between pings so that:

(1) the processor can display depth;

(2) the false targets (fish) are given time to change orientation, which decreases the possibility of false alarms.

Let the ping time Tp = 12 T_{TWP} max

= 1.6 seconds.

A ping clock is generated by dividing the master clock by 1638400. The ping clock is shown in Figure C-3.

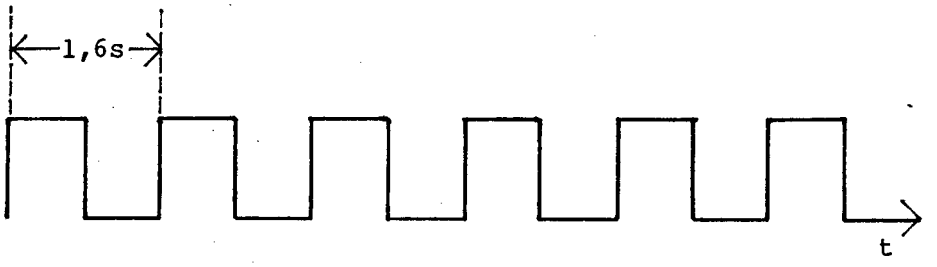

Ping Clock

FIGURE C-3

3.2 RANGE CELL TIME

A range cell period is achieved by counting a pre-set number of master clock periods. The maximum and minimum number of periods are 255 and 1 respectively, set by an 8 bit word.

PARAMETER	MIN	TYPICAL	MAX
RANGE CELL TIME [µs]	1	133	255
RANGE CELL LENGTH [mm]	0,75	100	191

With the typical value of 100mm for a range cell, the maximum depth than can be read is 102,4m.

4. PROCESSOR

4.1 ALGORITHM

The processor has an algorithm controlling it. The algorithm is first written step-wise and then symbol-wise for implementation in an algorithm state machine (ASM) design. The algorithm is broken up into a main routine and a read/write subroutine.

4.1.1 GENERAL ALGORITHM

Main Routine

(1) Proceed to next step on rising edge of ping clock or ping command from HP 85/86.

(2) Set depth address to zero.

(3) Start range cell counter. If already started, ignore.

(4) Proceed to next step on range cell counter borrow.

(5) Strobe read/write subroutine.

(6) Proceed to next step on return from subroutine.

(7) Increment depth address by one.

(8) If depth address $\neq$ zero, proceed to (3).
Proceed to next step if depth address = zero.

(9) Increment ping address.

(10) Proceed to (1).

Read/Write Subroutine

(1) Write value of analogue comparator to RAM in co-ordinates (depth; ping). Start range cell counter.*

(2) Set sum address to zero. Clear summer.

(3) Read value from RAM in address co-ordinates (depth; sum).

(4) Enable summer.

(5) Increment sum address by one.

(6) If sum address ≠ zero, proceed to (3). Proceed to next step if sum address = zero.

(7) If summer preset 'm' threshold, store display address, inhibit display address counter clock.

(8) Return to main routine.

* The timing of the range cell is restarted so as to avoid an accumulative timing error that would result if the timing was started after the read/write subroutine.

4.1.2 ASM TRANSLATABLE ALGORITHM

MAIN ROUTINE

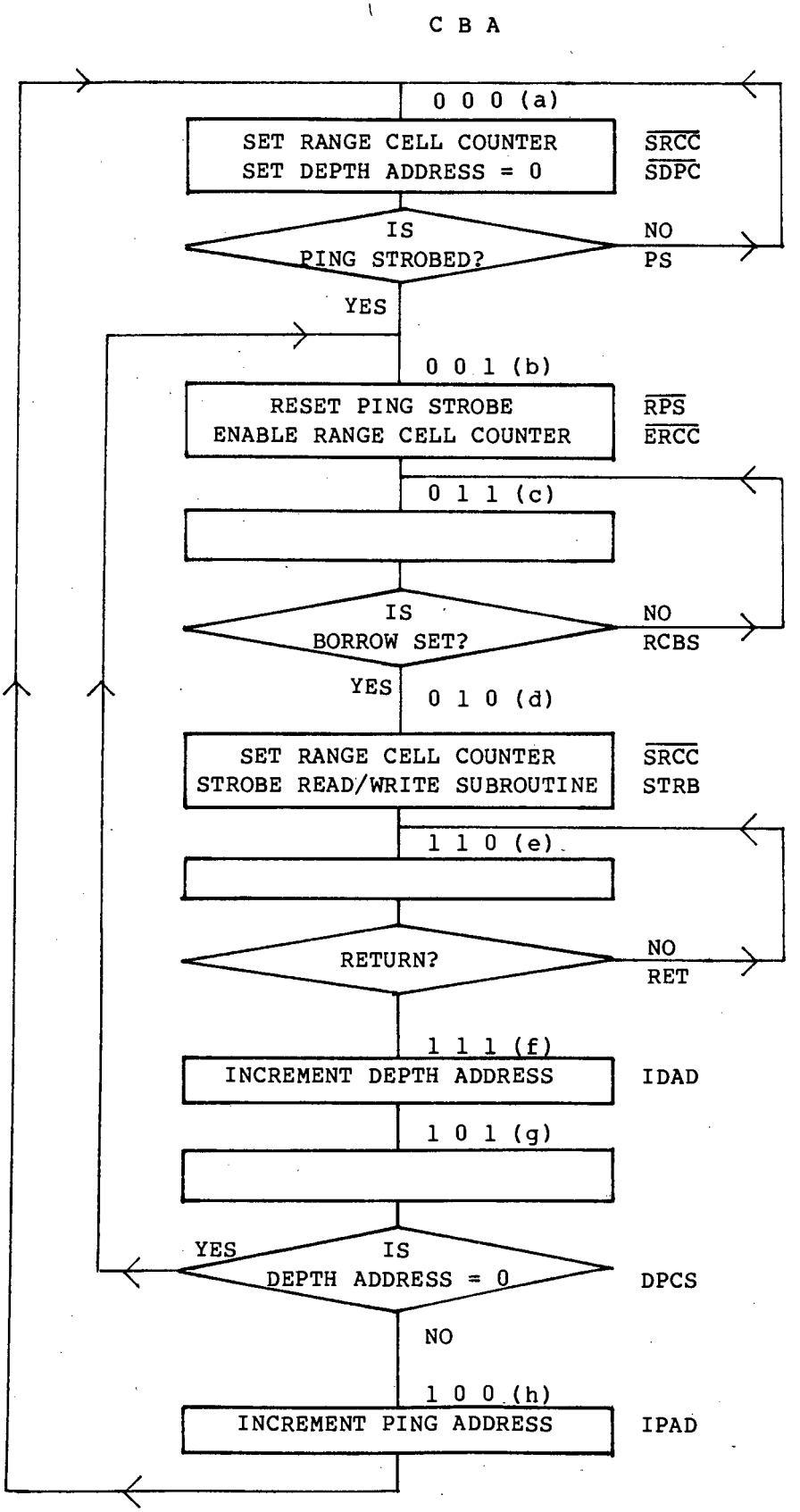

READ/WRITE SUBROUTINE

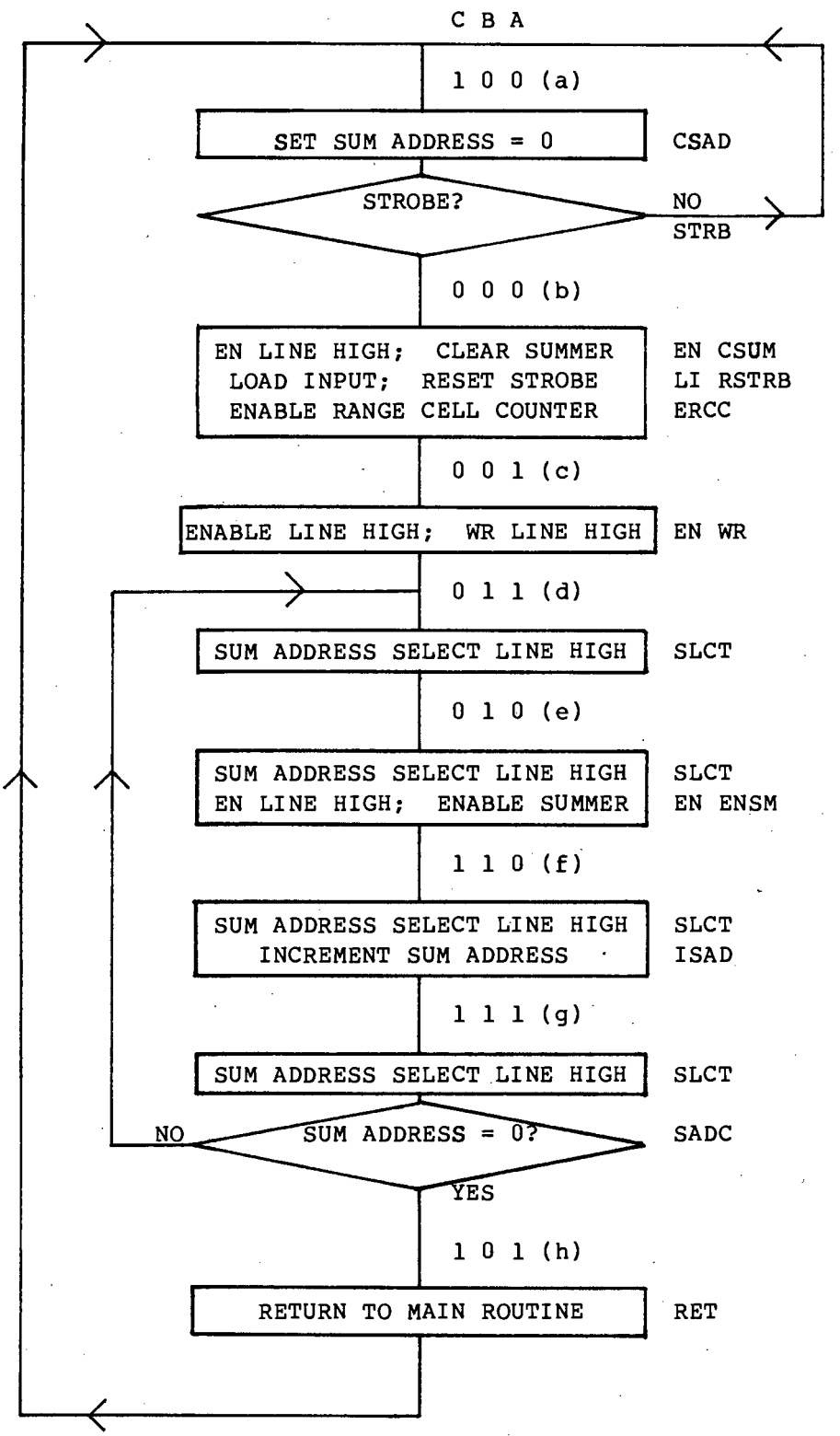

4.2 ASM DESIGN

Following the ASM design procedure, the algorithms were implemented in J-K flip-flop logic.

4.2.1 MAIN ROUTINE

State Assignments

C \ BA	00	01	11	10
0	a	b	c	d
1	h	g	f	e

State Variables

C \ BA	00	01	11	10
0	PS	-	-	0
1		-	-	RET

C \ BA	00	01	11	10
0	-		RCBS	-
1	-	DPCS		-

$J_A = PS.B.C+RET.B.C$

$= \overline{(PS.\bar{B}.\bar{C}).(RET.B.C)}$

$K_A = DPCS.B.C+RCBS.B.C$

$= \overline{(\overline{DPCS}.\bar{B}.C)+(\overline{RCBS}+\bar{B}+C)}$

C \ BA	00	01	11	10
0	0	1	-	-
1			-	-

C \ BA	00	01	11	10
0	-	-		
1	-	-	1	

$J_B = A.\bar{C}$

$= \overline{\bar{A} + C}$

$K_B = A.C$

$= \overline{\overline{A.C}}$

C \ BA	00	01	11	10
0				1
1	-	-	-	-

$J_C = \bar{A}.B$

$= \overline{A + \bar{B}}$

C \ BA	00	01	11	10
0	-	-		
1	1	DPCS		

$K_C = \bar{A}.\bar{B}.C+DPCS.\bar{B}$

$= \overline{\overline{(A+B+\bar{C})}+\overline{(DPCS+B)}}$

Decoded States

C \ BA	00	01	11	10
0	$\overline{SRCC}$ $\overline{SDPC}$	ERCC		$\overline{SRCC}$ STRB
1	IPAD		IDAD	

$\overline{SRCC} = \bar{A}.\bar{C}$ $\quad SRCC = \overline{\bar{A}.\bar{C}}$

$\overline{SDPC} = \bar{A}.\bar{B}.\bar{C}$ $\quad SDPC = \overline{\bar{A}.\bar{B}.\bar{C}}$

$STRB = \bar{A}.B.\bar{C} = \overline{A + \bar{B} + C}$

$IPAD = \bar{A}.\bar{B}.C = \overline{A + B + \bar{C}}$

$IDAD = A.B.C = \overline{\bar{A} + \bar{B} + \bar{C}}$

$ERCC = A.\bar{B}.\bar{C} = \overline{\bar{A} + B + C}$ $\quad \overline{ERCC} = \overline{\overline{\bar{A} + B + C}}$

4.2.2 READ/WRITE SUBROUTINE

State Assignments

C \ BA	00	01	11	10
0	b	c	d	e
1	a	h	g	f

State Variables

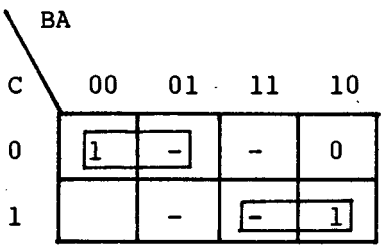

$J_A = \overline{B}.\overline{C}+B.C$

$= \overline{(\overline{B}.\overline{C}).(B.C)}$

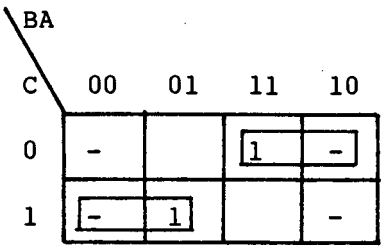

$K_A = \overline{B}.C+B.\overline{C}$

$= \overline{(\overline{B}.C).(B.\overline{C})}$

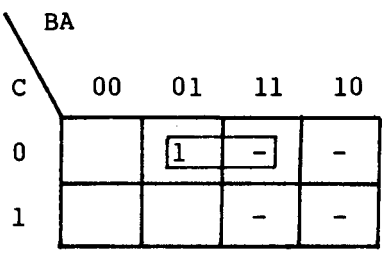

$J_B = A.\overline{C}$

$= \overline{\overline{A}+C}$

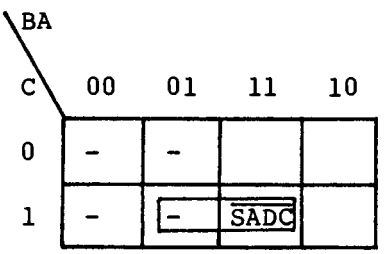

$K_B = \overline{SADC}.A.C$

$= SADC+(\overline{A.C})$

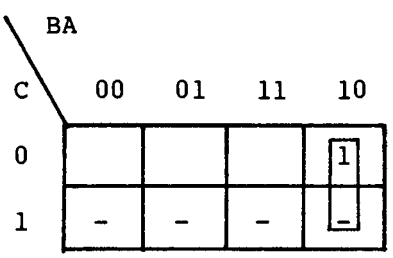

$J_C = \overline{A}.B$

$= \overline{A+\overline{B}}$

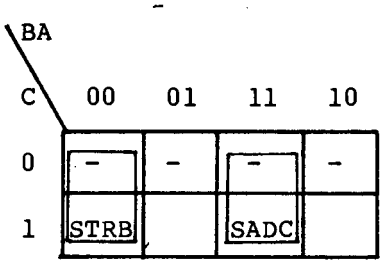

$K_C = STRB.\overline{A}.\overline{B}+SADC.A.B$

$= STRB.\overline{(\overline{A}.\overline{B})+(\overline{SADC.A.B})}$

Decoded States

C \ BA	00	01	11	10
0	EN LI CSUM	EN WR	SLCT	SLCT EN ENSUM
1	CSAD	CLSL RET	SLCT	ISAD SLCT

$$CSAD = \bar{A}.\bar{B}.C = \overline{A + B + \bar{C}} \qquad EN = \bar{B}.\bar{C} + \bar{A}.B.\bar{C}$$

$$LI = CSUM = ERCC = \bar{A}.\bar{B}.\bar{C} \qquad = (\overline{\bar{B}.\bar{C}}).(\overline{\bar{A}.B.\bar{C}})$$

$$= \overline{A + B + C} \qquad ISAD = \bar{A}.B.C$$

$$WR = A.B.C = \overline{\bar{A} + B + C} \qquad = \overline{A + \bar{B} + \bar{C}}$$

$$ENSUM = \bar{A}.B.\bar{C} = \overline{A + \bar{B} + C} \qquad SLCT = B$$

$$CLSL = RET = A.\bar{B}.C = \overline{\bar{A} + B + \bar{C}}$$

5. M OUT OF N DETECTOR AND DISPLAY

For a given depth the 16 range cells are read from RAM. This data is summed and the resultant compared with a preset value 'm'. If the resultant is greater than 'm', then the m out of n line goes high. The display is a 4 digit, 7 segment display, driven from a 16 bit BCD counter and BCD to 7 segment driver. The counter is incremented at the same time as the depth address and inhibited when the m out of n line goes high. A block diagram is found in Figure C-4.

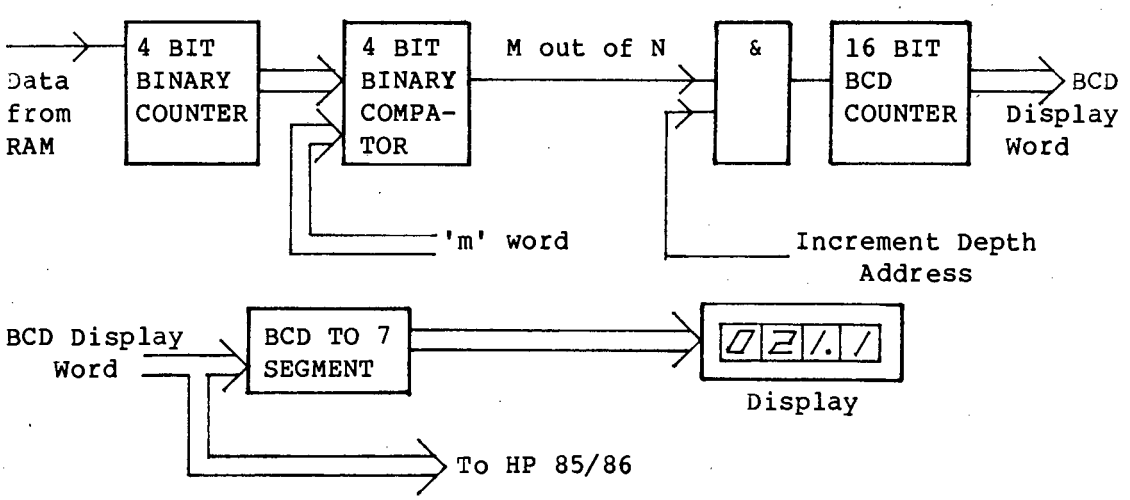

M out of N Detector and Display

FIGURE C-4

6. INTERFACING TO THE HP 85/86

As mentioned previously, the depth sounder can either stand alone or be interfaced to the HP 85/86. For the interfacing information, refer to Appendix A.

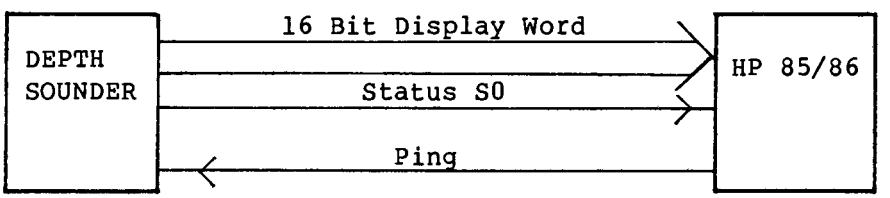

Interfacing Depth Sounder

FIGURE C-5

The HP 85/86 strobes the ping line. It then waits for the status line to go high, indicating processor has valid depth, whereupon it reads the depth via the 16 bit display word. The timing is as follows:

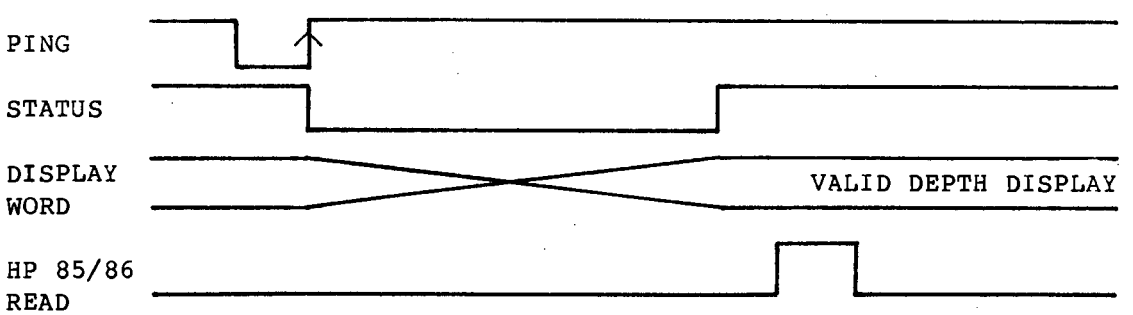

Interface Timing

FIGURE C-6

The status line is the means the depth sounder uses to indicate that it is waiting for the next rising edge of the ping clock (i.e. the depth reading is valid). This is the decoded state 000 = CBA (see 4.1.2 Main Routine) and is equivalent to SDPC.

7. TRANSMITTER/TRANSDUCER

7.1 TIMING

Tone bursts of 194kHz (resonant frequency of receiver transducer) are transmitted vertically towards the seabed. They are generated as follows: On the rising edge of each ping clock, a gating signal is triggered, which has variable length. This signal is available:

(1) to gate an external oscillator which feeds a power amp and transducer. The reason for this is that another projector and receiver transducer at a different frequency to the 194kHz of the correlation log system, may then be used;

(2) to be 'ored' with the correlator's gating signal. The resultant gating signal is used to gate an internal square wave oscillator of 194kHz. This tone burst is fed to an external power amp and transducer. (See Figure C-7 overleaf.)

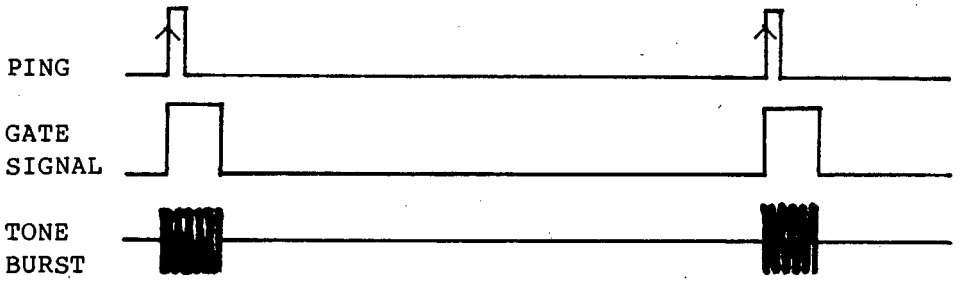

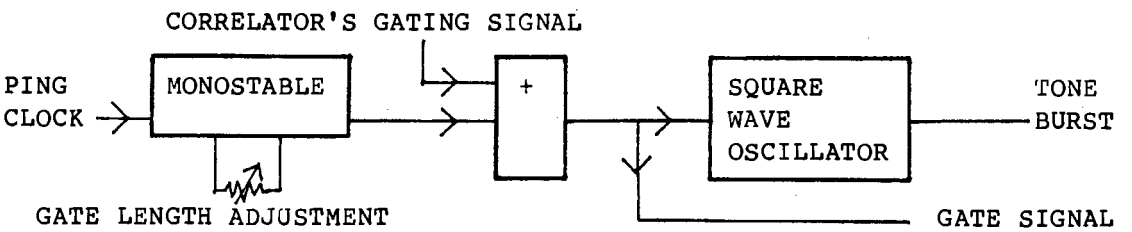

Transmitter

FIGURE C-7

The length of the transmit pulse must:

(1) be long enough so that enough power is transmitted for the receive signal to be above the noise;

(2) not be too long so that the reverberation and back-scatter interference makes the minimum readable depth unacceptable.

A typical transmit pulse length is 0,35ms.

7.2 POWER AMP

The commercial power amp used has the following information:

COMPANY	EIN ROCHESTER
MODEL	240L
SERIAL #	661
BANDWIDTH	20kHz to 10MHz
OUTPUT	50dB into 50Ω load
INPUT IMPEDENCE	50Ω

The internal 194kHz square wave oscillator is buffered and matched to the 50Ω input impedence of the power amp. The maximum input voltage to the power amp is 1 volt. An amplitude adjustment is provided on the buffer so that the amplitude of the square wave can vary between 0 and 0,9 volts. This provides an adjustable transmit power to cope with different sea bottoms.

8. TIME VARYING GAIN (TVG) RECEIVERS

8.1 TVG CONCEPT AND REALISATION

Consider an acoustic beam, transmitted vertically downward from the sea surface, reflecting off the sea bed at a depth of Z metres and returning to the sea surface again. (See Figure C-8 overleaf.)

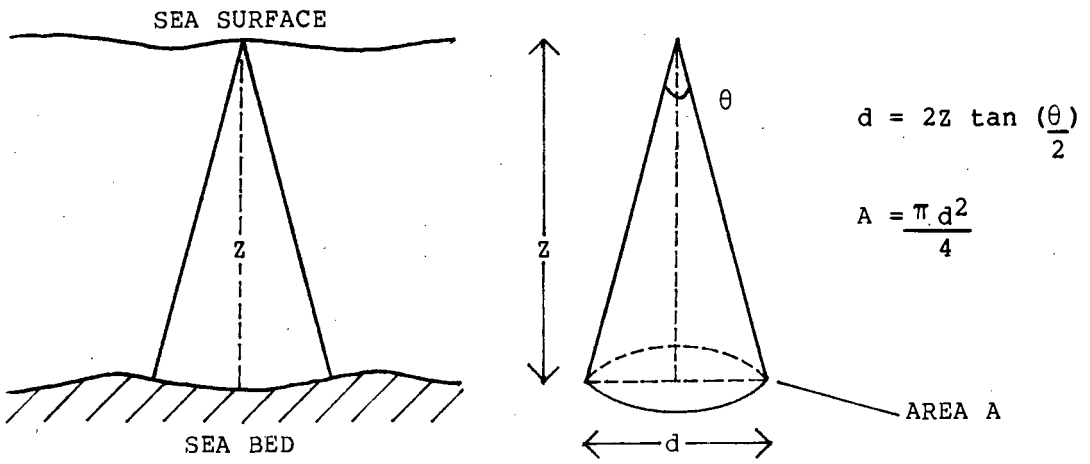

Insonifying Beam

FIGURE C-8

The sonar equation states

$$S = SL + TS - 2TL \quad [\text{in dB}]$$

where S = echo intensity back at sonar

SL = source level

TS = target strength

TL = transmission loss

The diameter of the incident insonifying beam is proportional to z. Hence the area of the beam is proportional to z^2.

As TS is proportional to incident area,

so TS is proportional to z^2.

Now $TL = 10 \log_{10} z^2 + \alpha z$.

Where α is the absorption coefficient in dB/km,

α is approximately 60dB per km. [URICK[1]].

Therefore absorption at 100m is 6dB.

Now spherical spreading loss at 100m is 40dB,

Hence the αZ term can be ignored in the TL equation.

So TL is proportional to Z^2,

Hence S is proportional to Z^{-2}.

As the amplitude A of the return echo is proportional to $S^{0,5}$, it follows that:

A is proportional to Z^{-1}.

To cancel out the effect of the return amplitudes inverse proportionality to depth, the gain of the receiver must be proportional to depth.

i.e. GAIN $G \propto Z$

Depth $Z = \frac{T_{TWP} \times C}{2}$ where C = speed of sound

T_{TWP} = two-way propagation time

So let $G \propto T_{TWP}$

The gain-time law that is used is shown in Figure C-9.

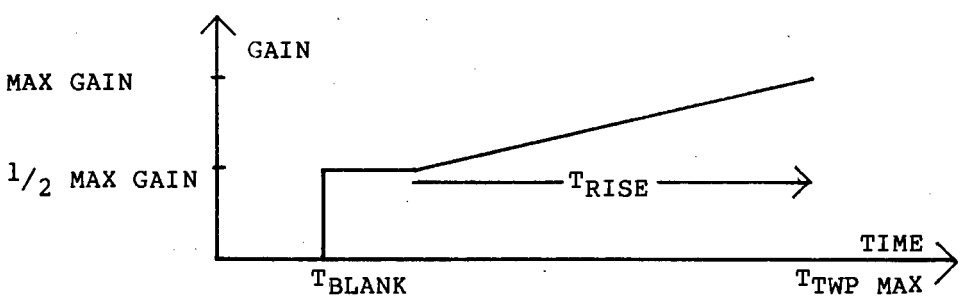

Gain Time Law

Figure C-9

The TVG is realised by using a multiplying D/A as in Figure C-10.

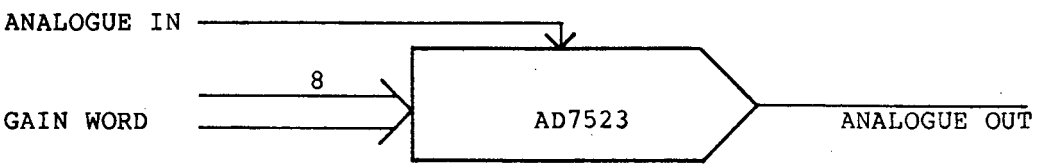

Multiplying D/A

FIGURE C-10

Analogue Out = Analogue In x $\frac{\text{Gain Word}}{255}$

The gain word is made up as follows:

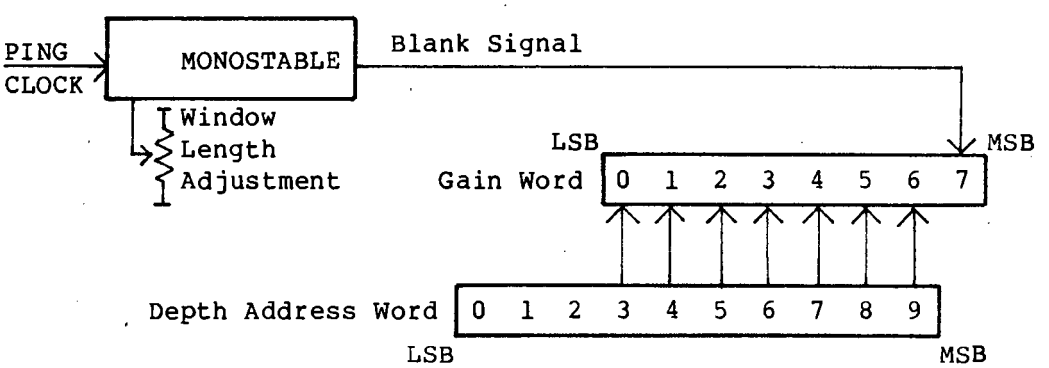

Gain Word

FIGURE C-11

On the rising edge of the ping clock a monostable is triggered so that its output is low for a preset time. This output is the MSB of the gain word. The other 7 bits of the gain word are derived from the most significant 7 bits of the depth address word.

The reason for the time, T_{Blank}, of no gain (Figure C-9), is so that reverberation and transmitter break-through can be gated out. T_{Blank} is set up after the transmit pulse length has been set. This is illustrated in Figure C-12.

The depth address is incremented after each range cell. The time, T_{Rise}, when the gain increases from half maximum value to maximum value is:

$$T_{Rise} = \text{Range cell time} \times (1023-7)$$

$$= \text{Range cell time} \times 1016$$

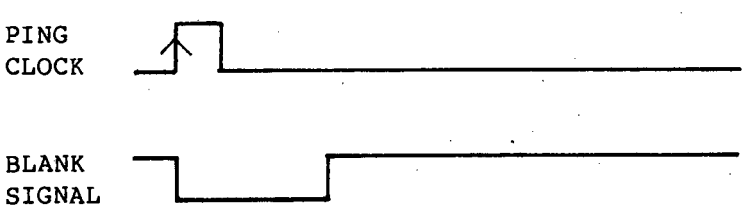

Blank Time

FIGURE C-12

8.2 GAIN STAGES

The receiver consists of 4 stages, namely:

(1) a low noise long tail pair front end with gain of approximately 46dB;

(2) a wideband amplifier, the MC1590 with an LM318 op-amp as buffer. The gain of this stage can be varied by changing the AGC bias point on the 1590;

(3) a TVG amplifier using the AD7523 8 bit D/A with LM318 op-amp as buffer;

(4) an envelope detector and LM311 analogue comparator followed by a D type flipflop with tri-state output. The comparator threshold is adjustable with a potential divider. A typical value of 2,5V was found adequate.

The receiver is a broadband design and is tuned to the carrier frequency of the return echo by a parallel LC circuit at the output of the 1590.

f resonant = 194kHz.

The L was chosen to be 165 µH with 15 µH variability wound with 25 turns of Litz wire on a 3H1 A315 core.

Now $f = \frac{1}{2\pi\sqrt{LC}}$ for a parallel LC circuit

Therefore

$$C = \frac{1}{L(2\pi f)^2} = \frac{1}{180\mu H \times (2\pi \times 194kHz)^2}$$

C = 3,7 nF for 180µH

and C = 4,5 nF for 150µH

Choose C = 3,9 nF

9. RACK SYSTEM

9.1 MOTHERBOARD

The rack is designed to hold 100mm wide, plug-in boards. The boards which plug in to a motherboard interconnect the various boards with power, bus facilities and control lines. A layout of the motherboard is given in Figure C-13.

9.2 BOARD LAYOUTS

Eight boards are needed to realise the depth sounder and their various functions are tabulated below.

BOARD #	FUNCTION
1	Read/Write Controller
2	Main Routine Controller
3	Address Counters
4 & 5	RAM
6	M out of N Detector and Display Counters
7	Ping Clock Generator and Transmit Pulse Generator
8	Receiver

The circuit diagrams of each board are shown in Figures C-14 through C-20.

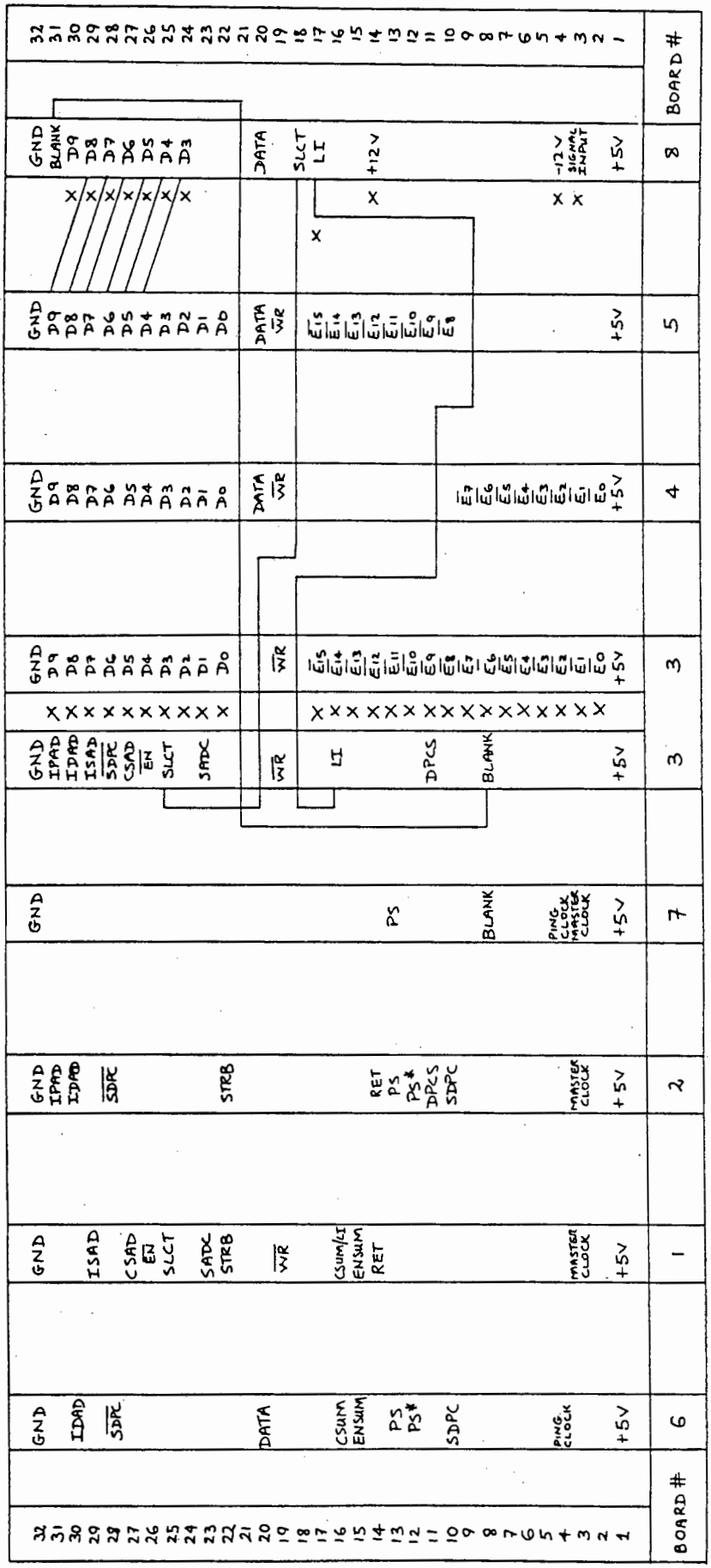

Mother Board

FIGURE C-13

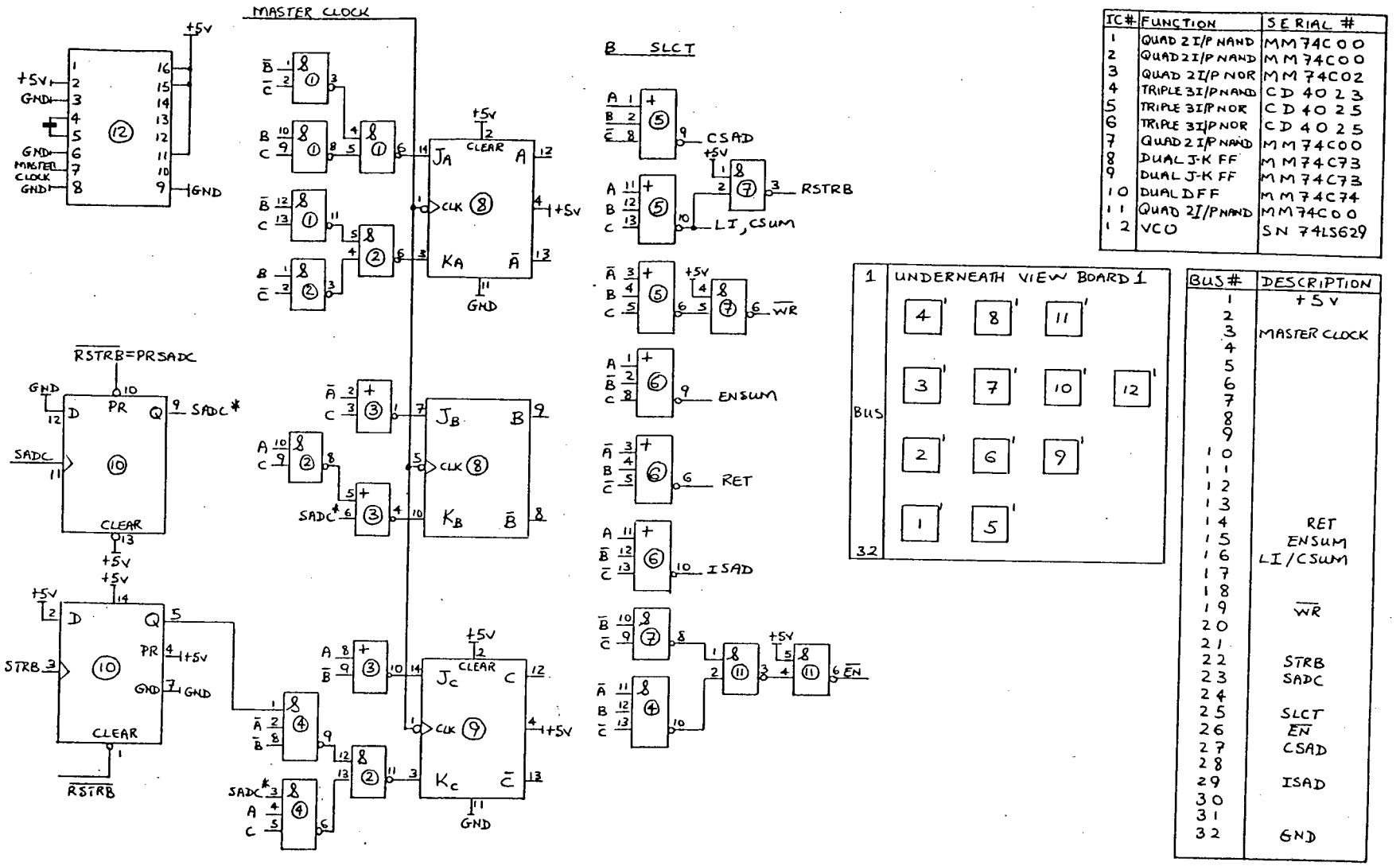

IC#	FUNCTION	SERIAL #
1	QUAD 2 I/P NAND	MM74C00
2	QUAD 2 I/P NAND	MM74C00
3	QUAD 2 I/P NOR	MM74C02
4	TRIPLE 3 I/P NAND	CD4023
5	TRIPLE 3 I/P NOR	CD4025
6	TRIPLE 3 I/P NOR	CD4025
7	QUAD 2 I/P NAND	MM74C00
8	DUAL J-K FF	MM74C73
9	DUAL J-K FF	MM74C73
10	DUAL D FF	MM74C74
11	QUAD 2 I/P NAND	MM74C00
12	VCO	SN 74LS629

BUS #	DESCRIPTION
1	+5V
2	
3	MASTER CLOCK
4	
5	
6	
7	
8	
9	
10	
11	
12	
13	
14	RET
15	ENSUM
16	LI/CSUM
17	
18	
19	$\overline{WR}$
20	
21	
22	STRB
23	SADC
24	
25	SLCT
26	$\overline{EN}$
27	CSAD
28	
29	ISAD
30	
31	
32	GND

Board 1

FIGURE C-14

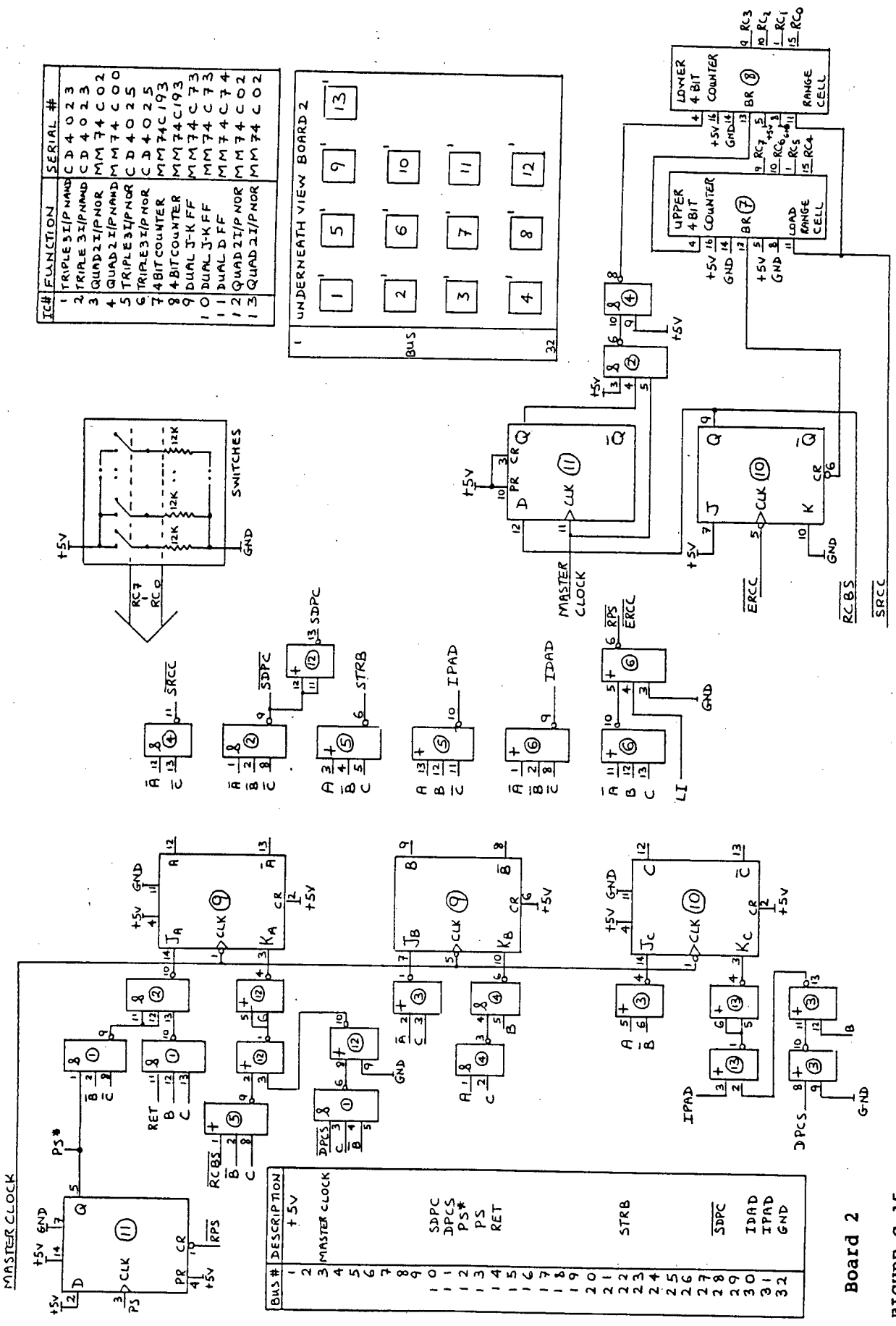

Board 2

FIGURE C-15

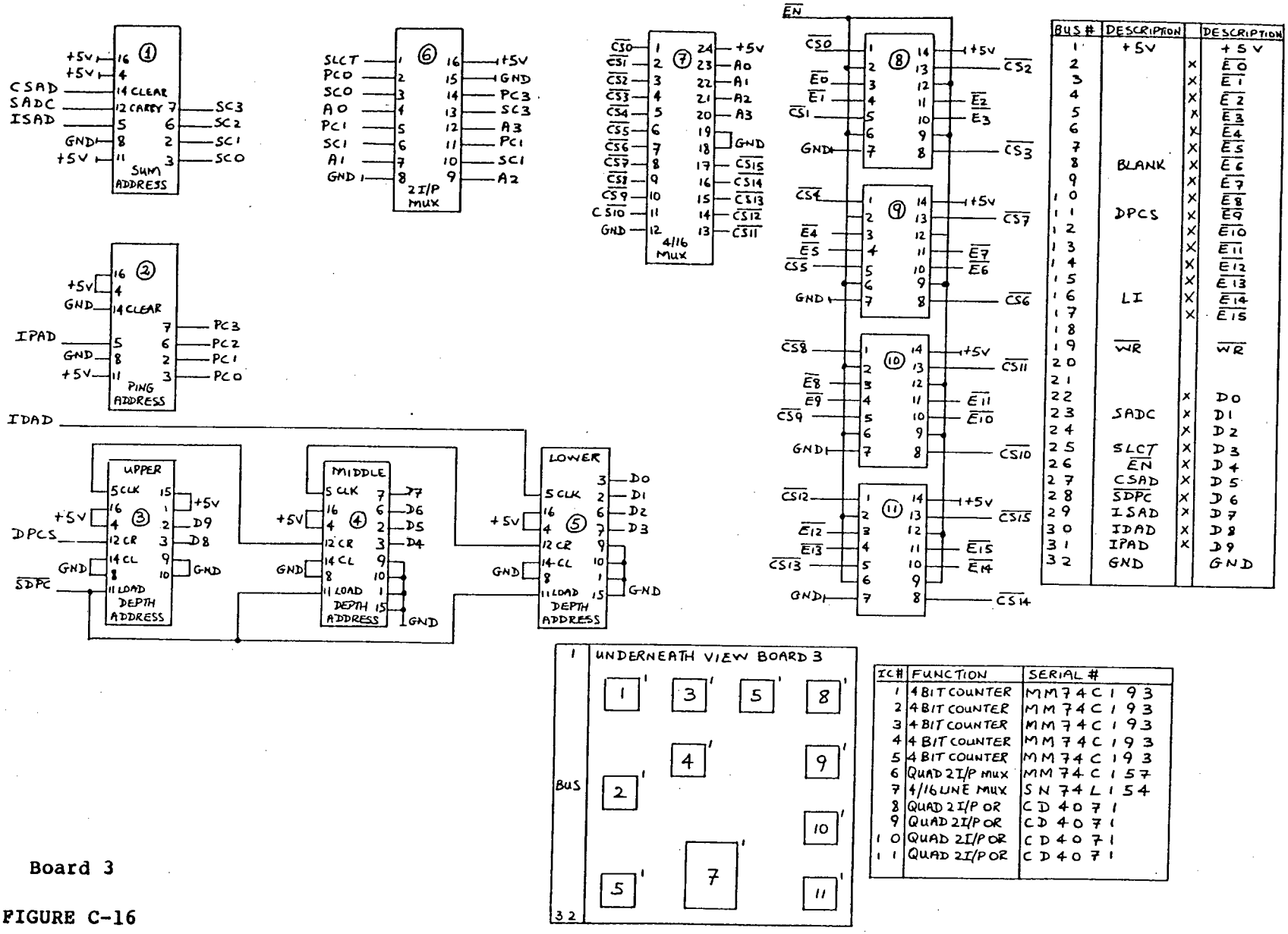

BUS #	DESCRIPTION		DESCRIPTION
1	+5V		+5V
2		X	$\overline{E0}$
3		X	$\overline{E1}$
4		X	$\overline{E2}$
5		X	$\overline{E3}$
6		X	$\overline{E4}$
7		X	$\overline{E5}$
8	BLANK	X	$\overline{E6}$
9		X	$\overline{E7}$
10		X	$\overline{E8}$
11	DPCS	X	$\overline{E9}$
12		X	$\overline{E10}$
13		X	$\overline{E11}$
14		X	$\overline{E12}$
15		X	$\overline{E13}$
16	LI	X	$\overline{E14}$
17		X	$\overline{E15}$
18			
19	$\overline{WR}$		$\overline{WR}$
20			
21			
22		X	D0
23	SADC	X	D1
24		X	D2
25	SLCT	X	D3
26	$\overline{EN}$	X	D4
27	CSAD	X	D5
28	$\overline{SDPC}$	X	D6
29	ISAD	X	D7
30	IDAD	X	D8
31	IPAD	X	D9
32	GND		GND

IC #	FUNCTION	SERIAL #
1	4 BIT COUNTER	MM74C193
2	4 BIT COUNTER	MM74C193
3	4 BIT COUNTER	MM74C193
4	4 BIT COUNTER	MM74C193
5	4 BIT COUNTER	MM74C193
6	QUAD 2I/P MUX	MM74C157
7	4/16 LINE MUX	SN74L154
8	QUAD 2I/P OR	CD4071
9	QUAD 2I/P OR	CD4071
10	QUAD 2I/P OR	CD4071
11	QUAD 2I/P OR	CD4071

Board 3

FIGURE C-16

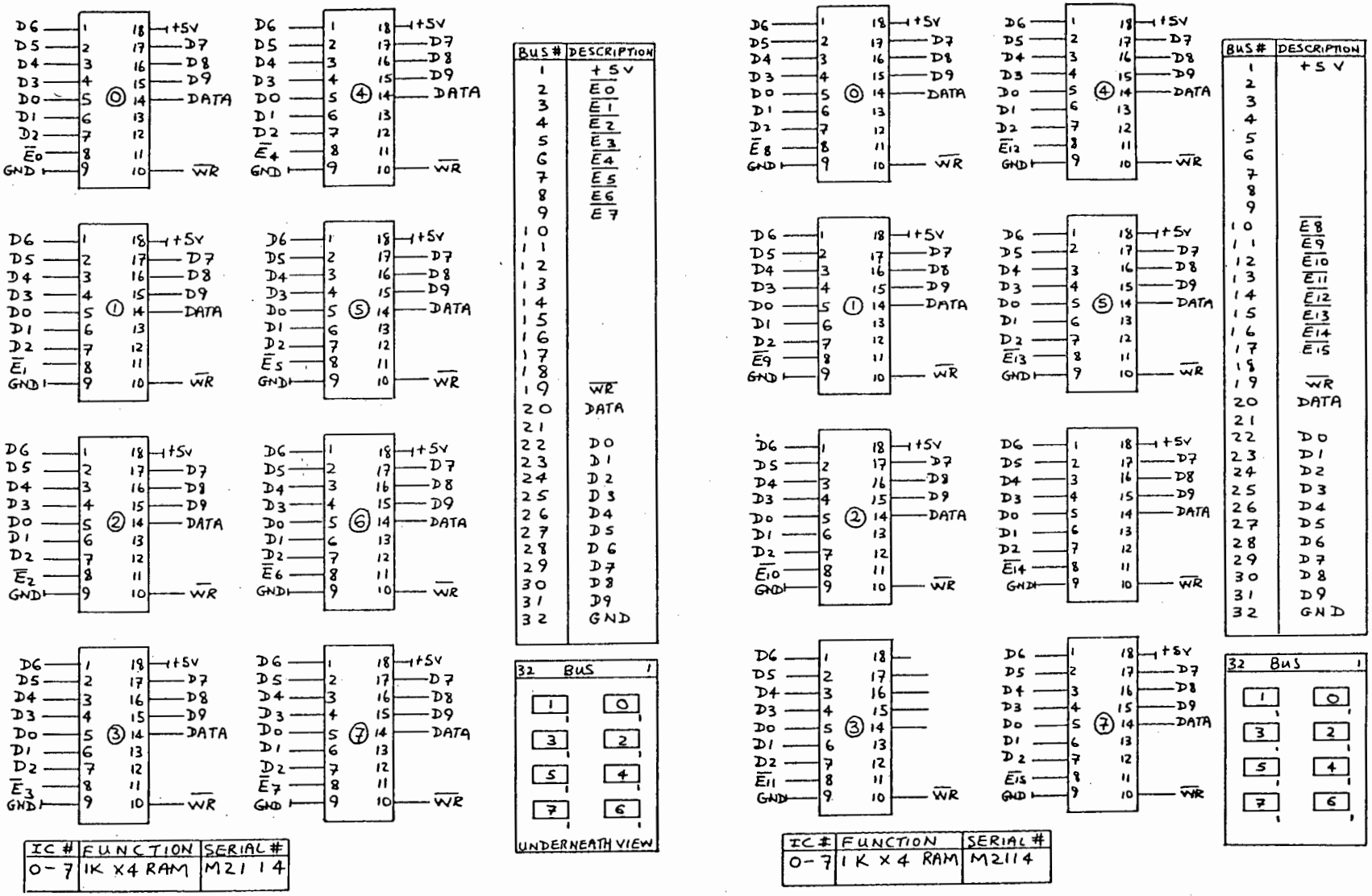

IC #	FUNCTION	SERIAL #
0-7	1K X4 RAM	M2114

Board 4 & 5

FIGURE C-17

IC #	FUNCTION	SERIAL #
0-7	1K X4 RAM	M2114

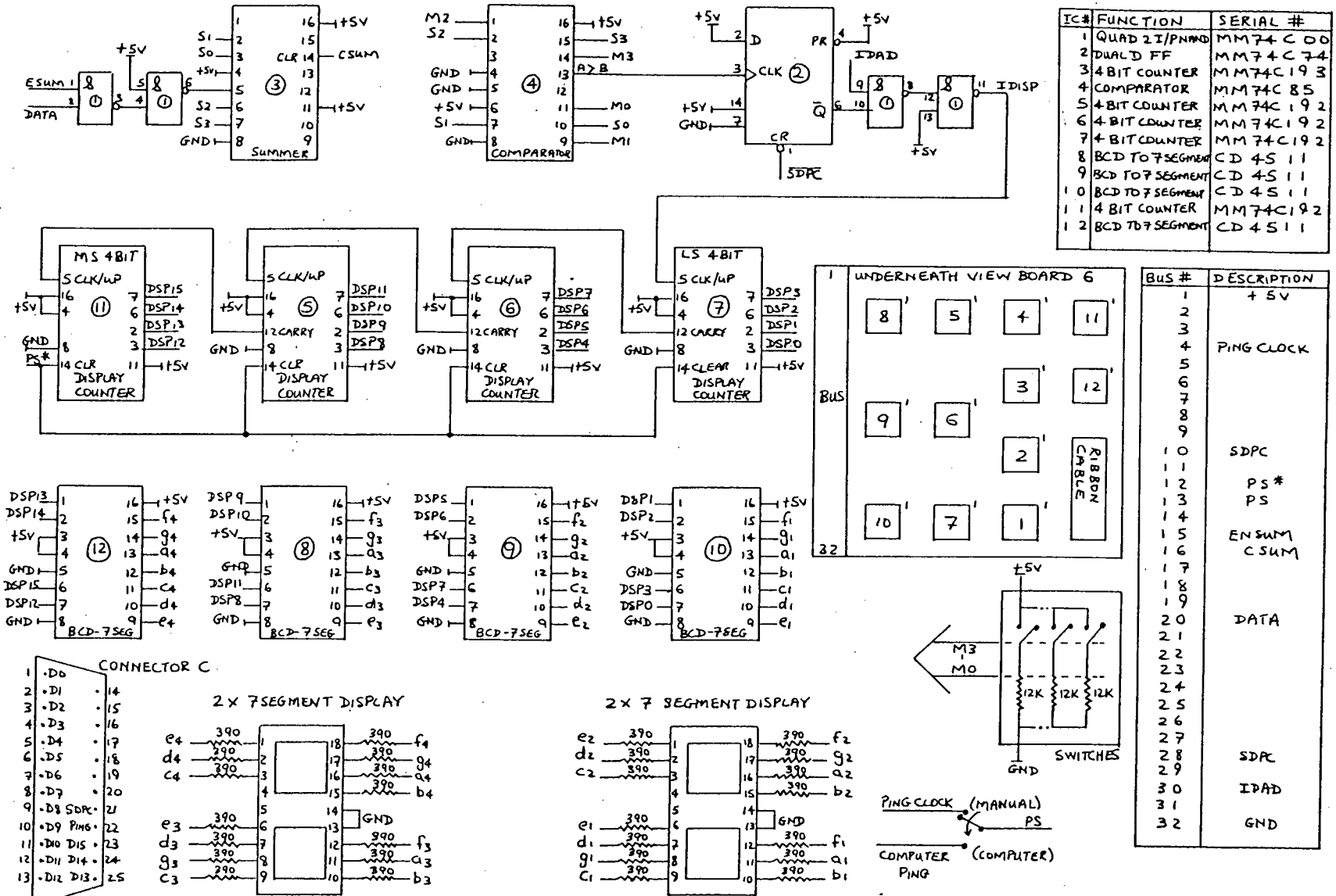

IC#	FUNCTION	SERIAL #
1	QUAD 2 I/P NAND	MM74C00
2	DUAL D FF	MM74C74
3	4 BIT COUNTER	MM74C193
4	COMPARATOR	MM74C85
5	4 BIT COUNTER	MM74C192
6	4 BIT COUNTER	MM74C192
7	4 BIT COUNTER	MM74C192
8	BCD TO 7 SEGMENT	CD4511
9	BCD TO 7 SEGMENT	CD4511
10	BCD TO 7 SEGMENT	CD4511
11	4 BIT COUNTER	MM74C192
12	BCD TO 7 SEGMENT	CD4511

BUS #	DESCRIPTION
1	+5V
2	
3	
4	PING CLOCK
5	
6	
7	
8	
9	
10	SDPC
11	
12	PS*
13	PS
14	
15	ENSUM
16	CSUM
17	
18	
19	
20	DATA
21	
22	
23	
24	
25	
26	
27	
28	SDPC
29	
30	IDAD
31	
32	GND

FIGURE C-18

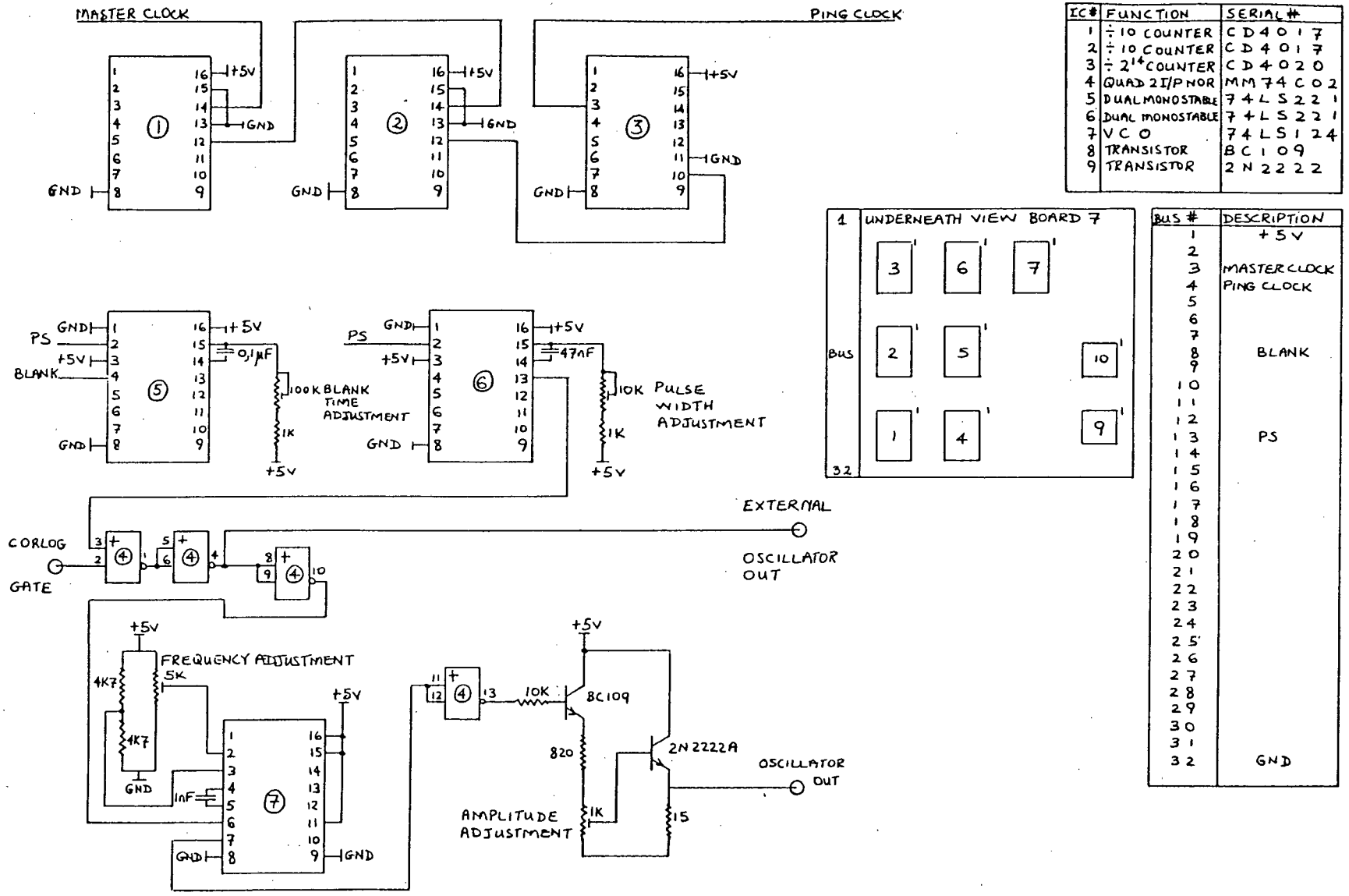

IC#	FUNCTION	SERIAL #
1	÷10 COUNTER	CD4017
2	÷10 COUNTER	CD4017
3	÷ 2^{14} COUNTER	CD4020
4	QUAD 2I/P NOR	MM74C02
5	DUAL MONOSTABLE	74LS221
6	DUAL MONOSTABLE	74LS221
7	VCO	74LS124
8	TRANSISTOR	BC109
9	TRANSISTOR	2N2222

BUS #	DESCRIPTION
1	+5V
2	
3	MASTER CLOCK
4	PING CLOCK
5	
6	
7	
8	BLANK
9	
10	
11	
12	
13	PS
14	
15	
16	
17	
18	
19	
20	
21	
22	
23	
24	
25	
26	
27	
28	
29	
30	
31	
32	GND

Board 7

FIGURE C-19

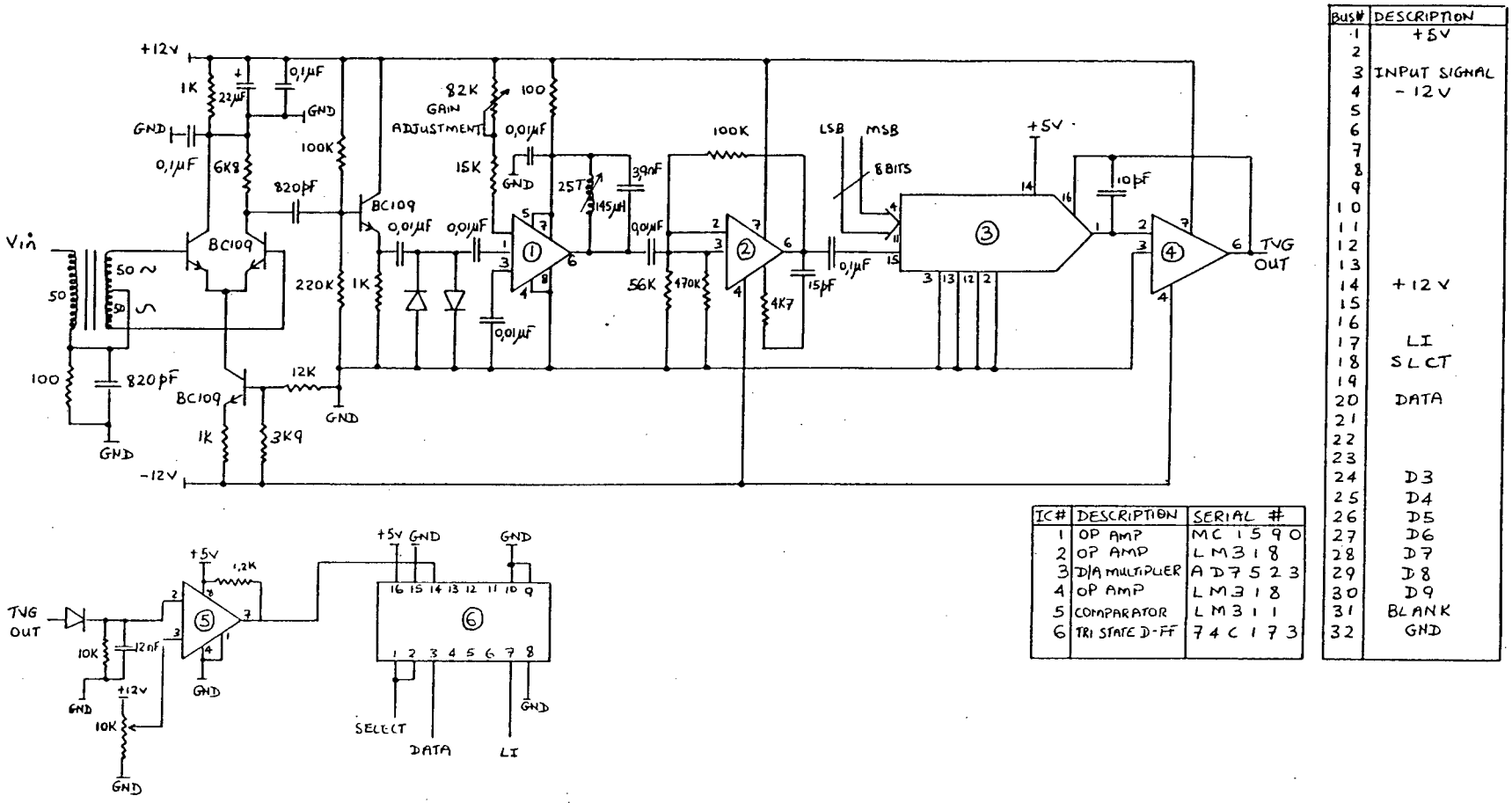

IC#	DESCRIPTION	SERIAL #
1	OP AMP	MC 1590
2	OP AMP	LM318
3	D/A MULTIPLIER	AD7523
4	OP AMP	LM318
5	COMPARATOR	LM311
6	TRI STATE D-FF	74C173

Bus#	DESCRIPTION
1	+5V
2	
3	INPUT SIGNAL
4	-12V
5	
6	
7	
8	
9	
10	
11	
12	
13	
14	+12V
15	
16	
17	LI
18	SLCT
19	
20	DATA
21	
22	
23	
24	D3
25	D4
26	D5
27	D6
28	D7
29	D8
30	D9
31	BLANK
32	GND

Board 8

FIGURE C-20

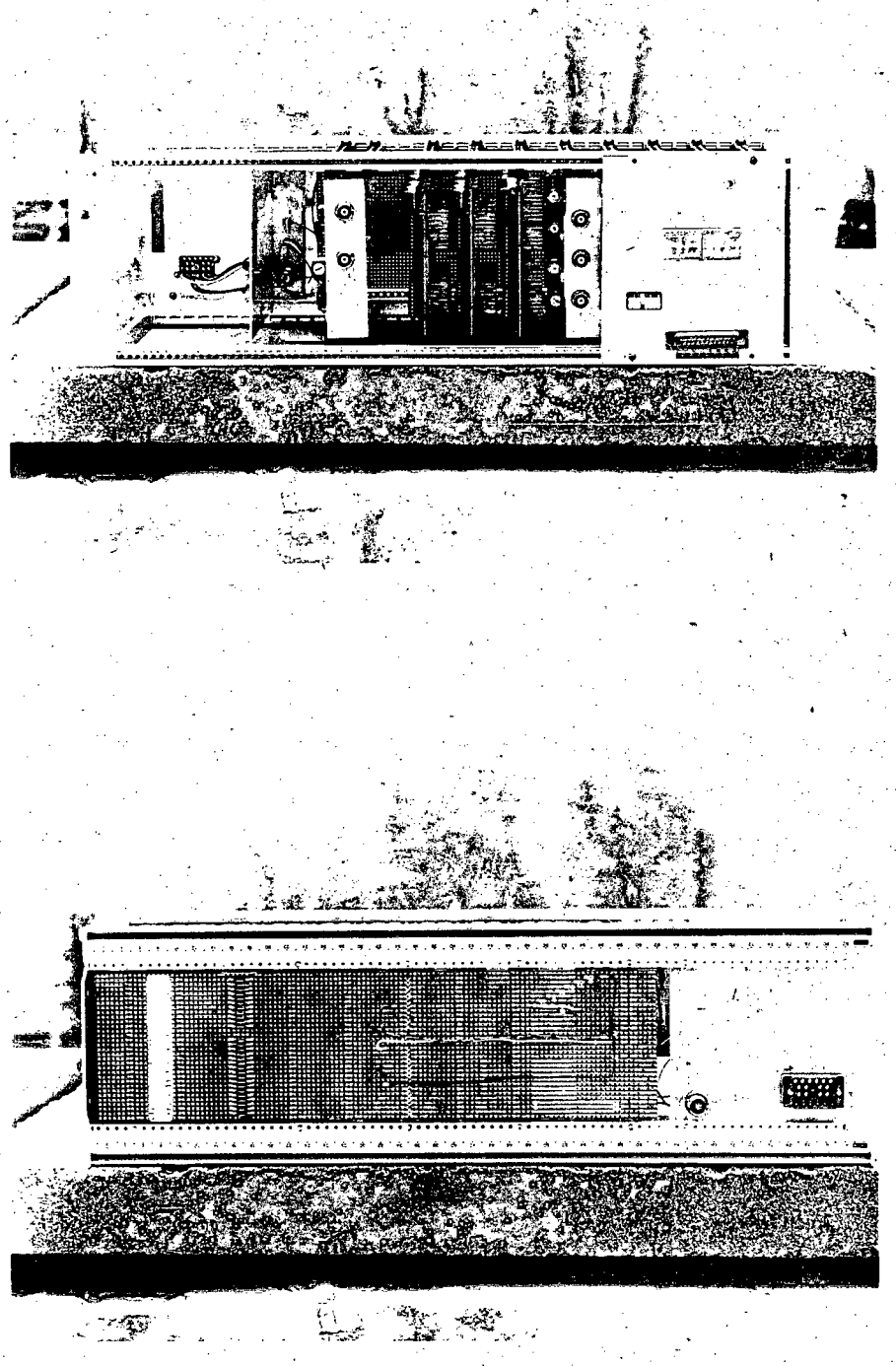

Depth Sounder

FIGURE C-21

9.3 POWER SUPPLY

A dedicated switch mode power supply is provided for the depth sounder. The voltages available are: +5V, +12V, -12V and +24V. The +5V is used for the digital system, the ±12V is used for the receiver and the +24V is to be used for the envisaged transmitter power amplifier.

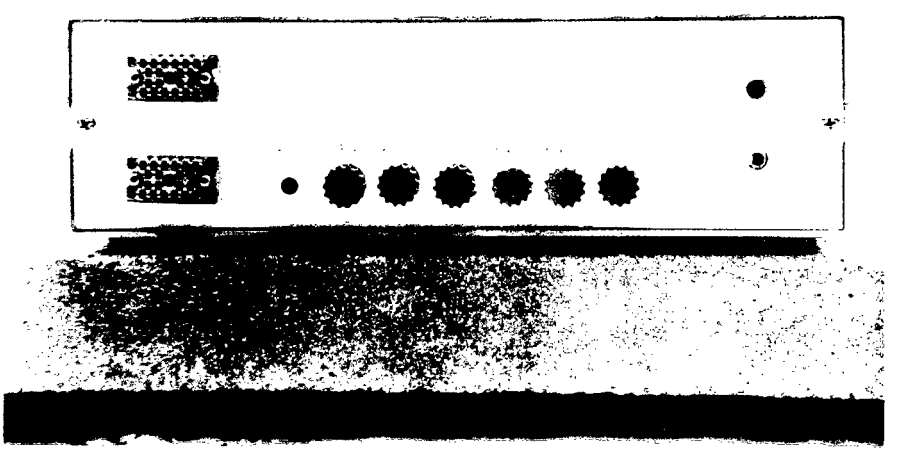

Power Supply

FIGURE C-22

9.4 EXTERNAL CONNECTIONS, MONITORING AND ADJUSTMENT POINTS

9.4.1 EXTERNAL CONNECTIONS

The following external connections are listed:

MNEMONIC	DESCRIPTION
REC IN	The output of the depth sounder transducer is connected to receiver input (REC IN)
CABLE C	The depth sounder is connected to the computer interface via this 25 way Delta connector and ribbon
CORLOG GATE	The transmitter gating pulse from the correlation log is connected to the depth sounder via CORLOG gate
OSC OUT	The transmitter tone burst generator is connected to the Power amp's input via OSC OUT
EXT OSC OUT	The combined transmitter gating signals of the correlation log and depth sounder are connected to an external gateable oscillator via this output
MANUAL/COM-PUTER SWITCH	To operate depth sounder in stand alone mode this switch must be in manual position. If depth sounder is to be under computer control, the switch must be in the computer position
POWER	The various voltages needed by the depth sounder are brought from the switch mode power supply by a provided cable and locking socket system

9.4.2 MONITORING POINTS

The following monitoring points are provided:

MNEMONIC	DESCRIPTION
1590 OUT	The (constant gain) amplified version of the return echo can be monitored from this point
DAC OUT	The (TVG) amplified version of the return echo can be monitored from this point

9.4.3 ADJUSTMENT POINTS

The following adjustment points are provided:

MNEMONIC	DESCRIPTION
M/N	The 'm' out of 'n' threshold is set via this set of 4 binary switches. White numbers imply high setting. #1 is LSB and #4 is MSB
PULSE WIDTH	Adjustment of the transmitter gating pulse width can be made via this pot
BLANK	Adjustment of the blanking time of the TVG amp can be made via this pot
VOLTAGE	Adjustment of the amplitude of the transmitter tone burst and hence the transmitter power can be made via this pot

FREQUENCY	Adjustment of the frequency of transmission can be made via this pot
THRESHOLD	The analogue threshold of the detector can be set via this pot
GAIN	The gain of the 1590 stage of the receiver is varied by this pot
RANGE CELL	An 8 bit binary word set up length with switches corresponds to the range cell in microseconds. #1 is LSB and #8 is MSB

REFERENCE

1. Urick R.J., "Principles of underwater sound", 3rd Edition, McGraw-Hill Book Company (1983) pp 102-111.

APPENDIX D

SPATIAL CORRELOGRAM

CONTENTS

1. INTRODUCTION

In Chapter 2 the ideal spatial correlogram was described. The aim of this appendix is to describe a series of experimental correlograms that were produced in the Central Acoustics Laboratory's tank at UCT.

2. EXPERIMENTAL PROCEDURE

The tank in which the experiments were performed has a gantry on which the transducer assembly was mounted. The gantry can be moved the length of the tank and in this way a fairly constant velocity can be obtained.

The correlation log depends on variation of return signal amplitude as different parts of the sea bed are insonified. It was found that this was not the case when using the steel tank bottom as a sea bed. The return echoes were of constant amplitude regardless of position. By using a sea bed constructed of foam strips glued to a large metal sheet, the amplitude of the return echoes were found to change sufficiently with transducer motion for the correlation log to function.

The transducer assembly is drawn to scale in Figure D-1. It has a set of six receive transducers, mounted 12mm apart, and a block of 3 x 3 transmit transducers making up a square 33mm long.

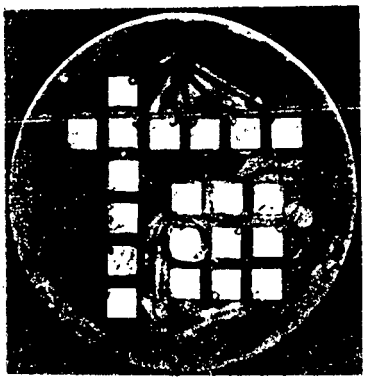

Transducer Assembly

FIGURE D-1

The return pulse from the constructed sea bed was received on all six receive transducers. Each receiver was taken in turn as a reference. The return pulses on the reference transducer were correlated with the subsequent pulse received on each of the other receivers. A delay of one interpulse period was thus imposed.

A number of correlation coefficients result from the above procedure, each one corresponding to a particular receiver spacing. For correlation coefficients corresponding to the same spacings, the average coefficient was taken.

The amplitude of 11 return pulses received by the 6 receivers was recorded.

Six sets of 11 samples resulted:

$\{\text{Rec } W_i\}$ W = 1 to 6 and i = 1 to 11.

The correlation of the reference receiver signal with a second receiver signal results in a correlation coefficient that is calculated as follows:

Let the reference receiver be Rec x x = 1 to 6

and the second receiver be Rec y y = 1 to 6

Then the correlation coefficient for the spacing of (y-x) receive transducers is:

$$\rho(y-x) = \frac{\sum_{1}^{10} [\text{Rec } x_i - \overline{\text{Rec } x}]\,[\text{Rec } y_{i+1} - \overline{\text{Rec } y}]}{\{\sum_{1}^{10} [\text{Rec } x_i - \overline{\text{Rec } x}]^2 \sum_{1}^{10} [\text{Rec } y_{i+1} - \overline{\text{Rec } y}]^2\}^{0.5}}$$

$$\overline{\text{Rec } x} = \frac{1}{10} \sum_{1}^{10} \text{Rec } x_i \qquad \overline{\text{Rec } y} = \frac{1}{10} \sum_{1}^{10} \text{Rec } y_{i+1}$$

Half the correlation coefficients will correspond to negative spacing which implies that the second receiver is ahead of the reference with respect to the direction of motion.

3. RESULTS

A computer program was written that implemented the correlation coefficient equation and plotted the spatial correlogram. Figures D-2 and D-3 are examples of these.

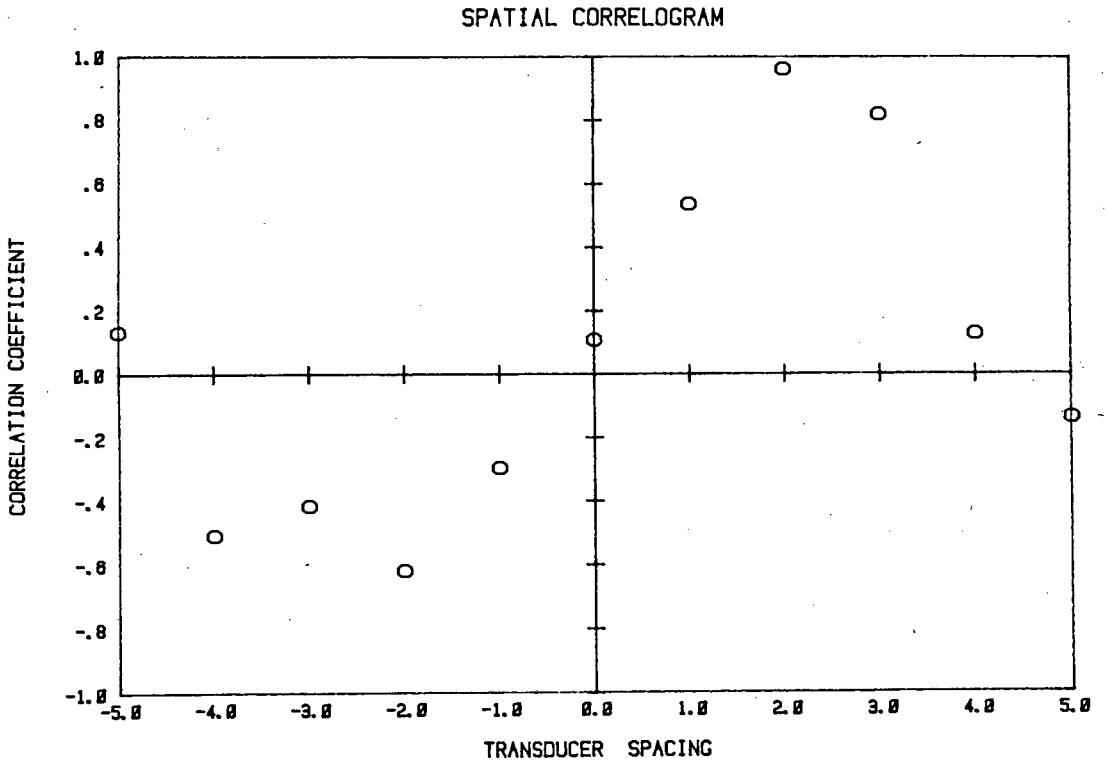

FIGURE D-2(a)

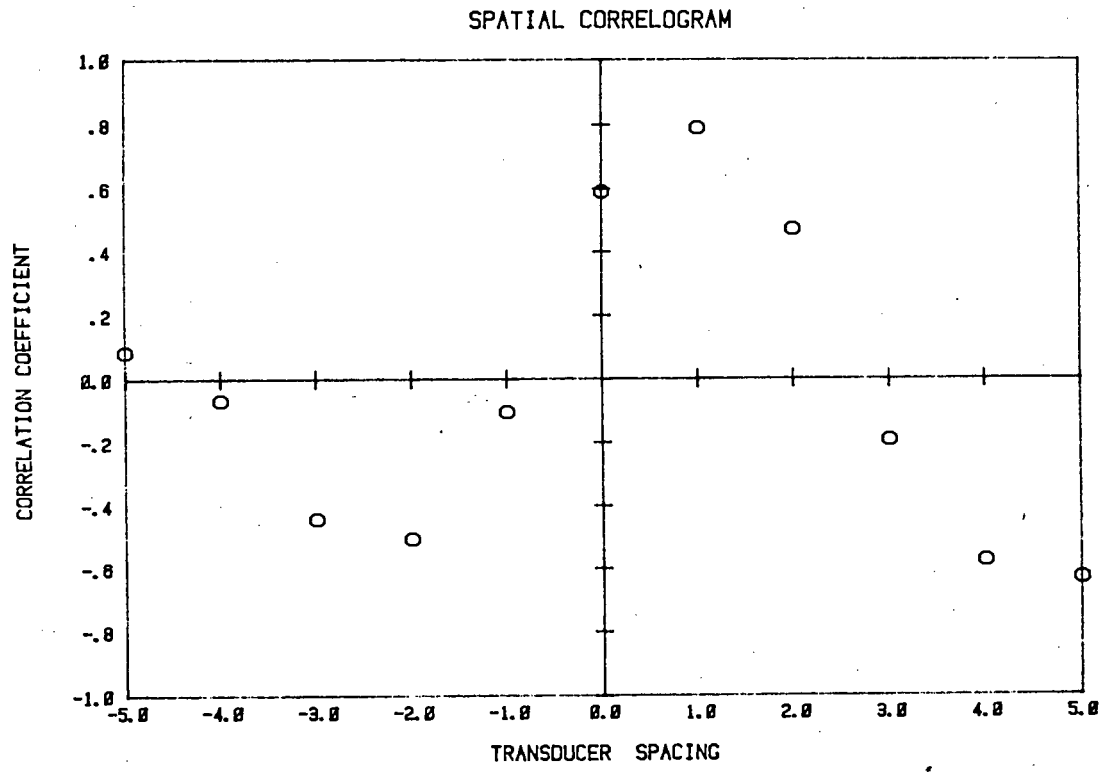

FIGURE D-2(b)

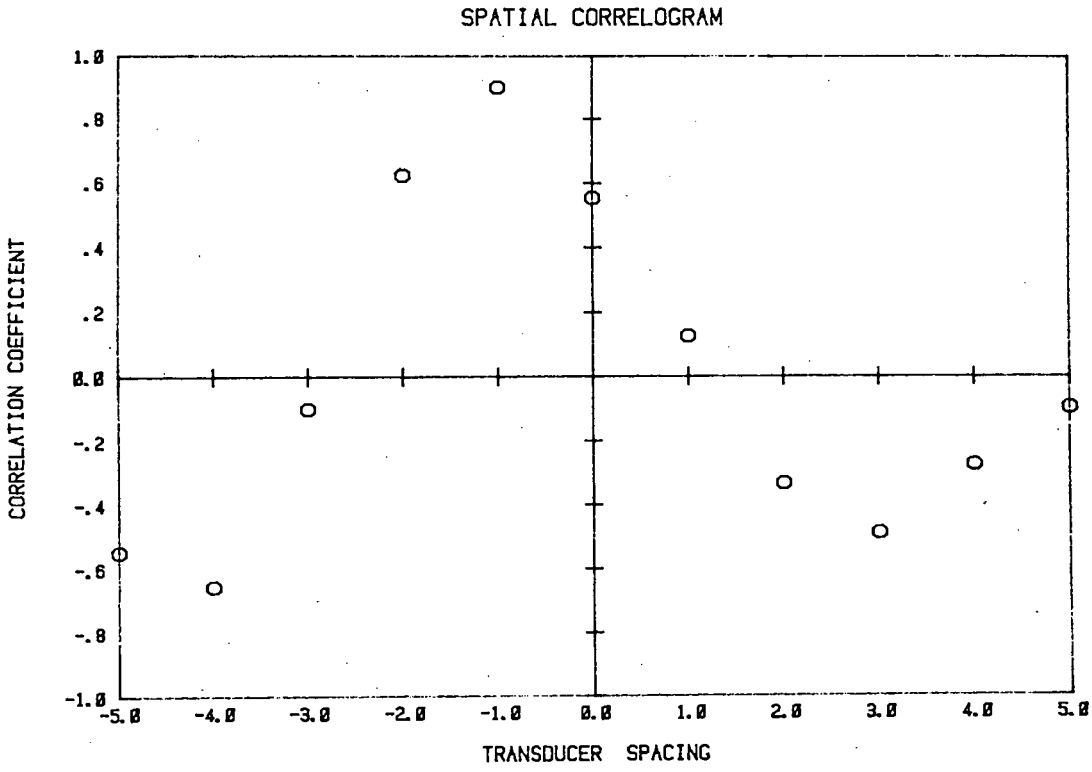

FIGURE D-3(a)

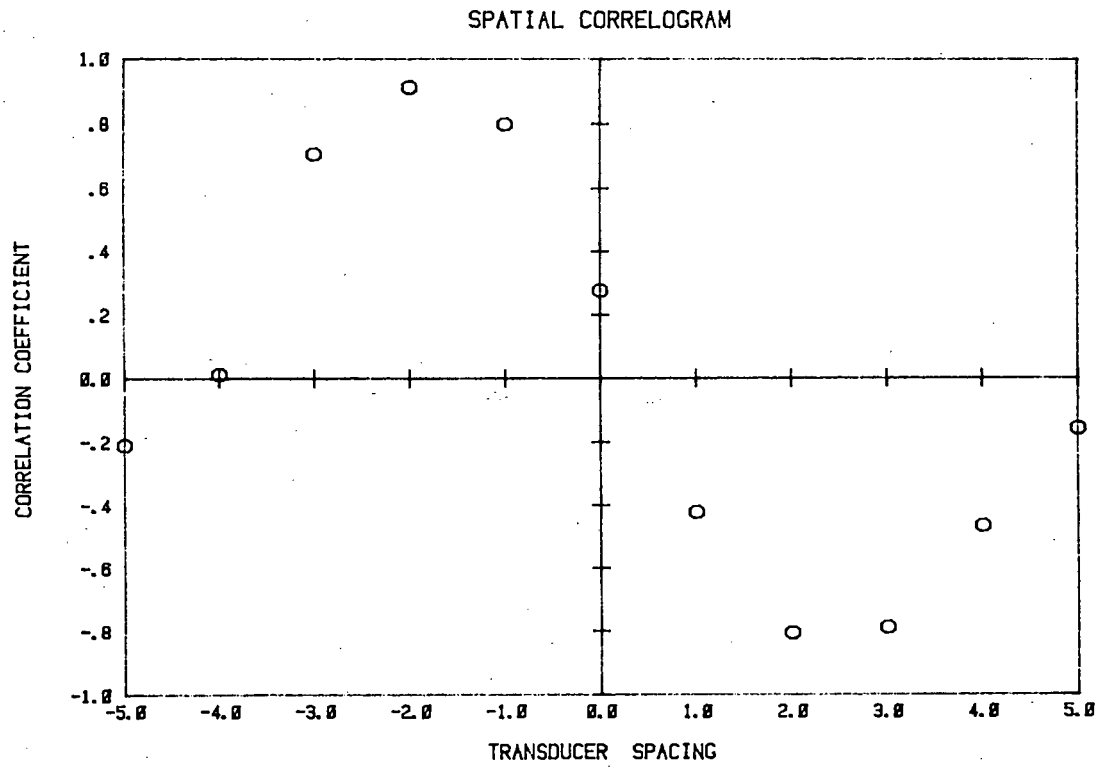

FIGURE D-3(b)

4. ANALYSIS AND CONCLUSIONS

Consider the two correlograms in Figures D-2(a) and (b). The velocity of the gantry was the same in both cases but the interpulse period and hence the delay T was halved in Figure D-2(b). The effect on the correlogram is that it is shifted to the left. The amount of shift can be determined by considering that the separation d = 2VT for maximum correlation. With a constant velocity, d is a linear function of T. Hence if T is halved, so is d.
This is experimentally verified, since the correlogram peak in Figure D-2(b) has shifted to the left by about half the peak displacement of Figure D-2(a).

Figure D-3 shows two correlograms resulting from the gantry moving in the opposite direction. The velocity is thus negative. The peak position of the correlogram is seen to be negative. The velocity was held constant when the correlograms in Figure D-3(a) and (b) were calculated. The interpulse period in Figure D-3(a) was half that of Figure D-3(b). The resulting shift in the correlogram peak is evident.

It was found that a close agreement existed between the predicted and actual position of the spatial correlogram. For example consider Figure D-2(a). The average gantry speed was about 1m/s and the interpulse period used was 12ms. This means that a delay of 12ms was imposed. The predicted peak position is d = 2VT = 2.1.12 = 24mm. The actual peak position is about 24mm.

It becomes evident on examining the correlograms that to determine the exact position of the peak using interpolation techniques will result in large inaccuracies. This is discussed further in Section 3.4.

Denbigh[1] predicted that the width of the spatial correlogram would be similar to the width of the transmit transducer. The width of the transmit transducer is about 33mm and the width of the spatial correlogram is about 3 transducer spacings which is about 36mm. A close agreement thus exists between the predicted and actual width of the correlogram.

The large negative correlation coefficients found in all the correlograms are a result of the small number of points used for correlation. Their number was limited due to the small capacity of the data storage device used. If a larger number of points could be used then the negative correlation coefficients would tend to be zero. Also evident is a high degree of symmetry around the point of maximum correlation.

The main conclusions that should be drawn from the analysis of the experimental spatial correlograms is that by varying the delay T the position of the peak of the function can be changed to any desired position and that the function is symmetric around the point of maximum correlation. Both these characteristics are used in the inter-intrapulse correlation log.

REFERENCE

1. Denbigh P.N., " A design study for a correlation log to measure the speed at sea ", J. Navigation, (1982), 35, pp 160 - 184.